Journal of Materials Processing Technology 211 (2011) 787–829

Contents lists available at ScienceDirect

Journal of Materials Processing Technology

journal homepage: www.elsevier.com/locate/jmatprotec

Electromagnetic forming—A review

V. Psyk[a,*], D. Risch[a], B.L. Kinsey[b], A.E. Tekkaya[a], M. Kleiner[a]

[a] Institute of Forming Technology and Lightweight Construction, Technische Universität Dortmund, Baroper-Strasse 301, 44227 Dortmund, Germany
[b] University of New Hampshire, Kingsbury Hall, 33 Academic Way, Durham, NH, USA

ARTICLE INFO

Article history:
Received 10 September 2010
Received in revised form 7 December 2010
Accepted 15 December 2010
Available online 23 December 2010

Keywords:
Electromagnetic forming
Impulse forming
High-speed forming

ABSTRACT

Electromagnetic forming is an impulse or high-speed forming technology using pulsed magnetic field to apply Lorentz' forces to workpieces preferably made of a highly electrically conductive material without mechanical contact and without a working medium. Thus hollow profiles can be compressed or expanded and flat or three-dimensionally preformed sheet metal can be shaped and joined as well as cutting operations can be performed. Due to extremely high velocities and strain rates in comparison to conventional quasistatic processes, forming limits can be extended for several materials. In this article, the state of the art of electromagnetic forming is reviewed considering:

- basic research work regarding the process principle, significant parameters on the acting loads, the resulting workpiece deformation, and their interactions, and the energy transfer during the process;
- application-oriented research work and applications in the field of forming, joining, cutting, and process combinations including electromagnetic forming incorporated into conventional forming technologies.

Moreover, research on the material behavior at the process specific high strain rates and on the equipment applied for electromagnetic forming is regarded. On the basis of this survey it is described why electromagnetic forming has not been widely initiated in industrial manufacturing processes up to now. Fields and topics where further research is required are identified and prospects for future industrial implementation of the process are given.

1. Introduction

Electromagnetic forming is an impulse or high-speed forming technology, which uses pulsed magnetic fields to apply forces to tubular or sheet metal workpieces, made of a material of high electrical conductivity. The force application is contact free and no working medium is required. The principle is based on physical effects described by Maxwell (1873). Maxwell explained that a temporarily varying magnetic field induces electrical currents in nearby conductors and additionally exerts forces (the so-called Lorentz forces) to these conductors. Northrup (1907) reported accordingly that "in passing a relatively large alternating current through an non-electrolytic, liquid conductor contained on a trough, that the liquid contracted in cross-section and flowed up hill lengthwise of the trough, climbing up upon the electrodes" was observed. With increasing current a contraction of the cross-section and a depression in the liquid was found. The first one who generated magnetic field strengths which were sufficient to deform solid conductors was Kapitza (1924). Thus, he provided the foundation for the electromagnetic forming process. However, the earliest work on technologically exploiting this principle for a target-oriented forming of metals began in the 1950s with the patent of Harvey and Brower (1958). A more detailed description including examples of applications is given in Brower (1969).

Depending on the arrangement and the geometry of the coil and workpiece, different applications of electromagnetic forming are achieved: compression and expansion (also called bulging) of tubular components or hollow profiles as well as forming of initially flat or three-dimensional preformed sheet metals (see Fig. 1). According to these three different variants of the process, different types of coils for the electromagnetic forming process can be distinguished. During tube compression the coil encloses the workpiece, while in the setup for the expansion it is the other way around. According to Belyy et al. (1977) tubes with a diameter in the range of 3 mm up to 2 m and with thicknesses of up to 5 mm can be processed. For electromagnetic sheet metal forming flat coils are used. Here, the area of the formed workpiece can be in the range of 10^{-4} up to 0.02 m^2 and the sheet thickness can be up to 5 mm (Belyy et al., 1977). However, the charging energy depends on the area to be formed, so that a machine with higher maximum charging energy is required if large tubes or sheets shall be processed.

* Corresponding author.
E-mail address: verena.psyk@iul.tu-dortmund.de (V. Psyk).

0924-0136/$ – see front matter © 2010 Elsevier B.V. All rights reserved.
doi:10.1016/j.jmatprotec.2010.12.012

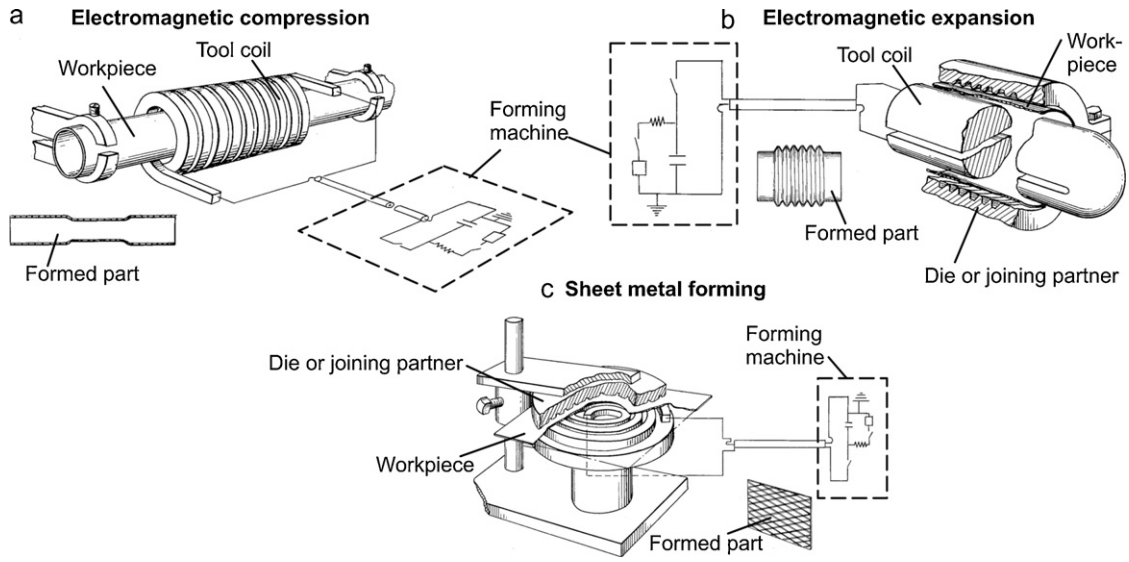

Fig. 1. Different coil types for the electromagnetic forming processes according to Harvey and Brower (1958).

Apart from these three major process variants, which are frequently discussed in the literature, some special variants are mentioned in Furth and Waniek (1962). These are electromagnetic forming with direct electrode contact. While in most cases a required current in the workpiece is realized via induction, Furth and Waniek (1962) suggest passing the current directly to the metal through electrodes. They claim this method to be more efficient than the conventional procedure and they recommend using electrodes with flexible extensions in order to prevent sparking or erosion. A second idea presented in Furth and Waniek (1962) deals with electromagnetic forming by pulling. While in typical applications the workpiece is always pushed away from the tool coil, here a special setup including two different coils is suggested in order to establish pulling forces, which allows forming bulges on hollow objects or large sheets, where a force application on the inner or reverse side is not possible.

Another special process variant is suggested in Brower (1966) for the first time. In this variant the electromagnetic forces act on the workpiece via an elastic medium. For this purpose the setup for electromagnetic sheet metal forming illustrated in Fig. 1 is supplemented by a pressure concentrator and an elastomeric punch, which is positioned between the tool coil and workpiece. In contrast to the more conventional electromagnetic forming variants, this process is not limited to workpieces made of an electrically conductive material. In Livshitz et al. (2004) a comparison between direct electromagnetic forming and electromagnetic forming through an elastic medium is given. It is pointed out that using the elastic medium the current oscillation frequency should be lower then in case of direct electromagnetic forming (a frequency of 5 kHz is advised, here). Furthermore, information about the suitability of elastomers of different modulus of elasticity are given. It is said that an elastomer of higher modulus of elasticity allows using an open die while in case of an elastomer of lower modulus of elasticity has to be applied in a closed system in order to achieve good efficiency.

Bühler and von Finckenstein (1971) claimed the joining of tubular workpieces to be the most widespread and economically promising field of application. Bauer (1980) even stated that only the process variant of the electromagnetic compression has advantages compared to conventional forming processes at all. However, according to Beerwald (2005) a kind of renaissance of the electromagnetic forming can be observed over the last years, which is related to the increasing trend of implementing lightweight construction concepts especially in the automotive industry. As recently stated by Schäfer and Pasquale (2010) as well as by Zittel (2010), at the moment joining operations are still the most relevant ones, but according to Löschmann et al. (2006), the significance of the electromagnetic sheet metal forming can be expected to increase within industry until 2012.

The electromagnetic forming process has several advantages in comparison to conventional, quasistatic forming processes. The major ones are summarized in the following:

- Due to the contact-free force application, it is possible to form covered semi-finished parts without destroying the layer as stated by Bertholdi and Daube (1966). No mechanical contact between the tool coil and workpiece exists, so that no impureness or imprint occurs on the workpiece surface.
- According to Erdösi and Meinel (1984) the process is environmentally friendly, because no lubricants are used. Additionally, this results in a simplification of the workpiece processing, because there is no need to clean the workpiece.
- A high repeatability can be achieved by adjusting the forming machine once. According to Daube et al. (1966) the adjustment of the applied forces via the charging energy and the voltage, respectively is very accurate. Belyy et al. (1977) quantify that the forming energy can be dosed precisely up to 1%. According to Bertholdi and Daube (1966) reworking operations are usually not necessary.
- Joining of dissimilar materials including material combinations of metals and glass, polymers, composites or different metals is possible. This is shown in Al-Hassani et al. (1967) on the example of a metallic cap joined to a glass bottle and in Rafailoff and Schmidt (1975) for the example of a joint between a metallic tube and a porcelain component.
- In contrast to the conventional sheet metal forming the electromagnetic sheet metal forming process uses only one form defining tool. Hence, the tool costs can be decreased significantly (Plum, 1988).
- Springback is significantly reduced in comparison to conventional quasistatic forming operations. This simplifies the die design significantly.
- According to Saha (2005) high production rates can be achieved. In the case of manual feeding the production rate is limited by the time required for loading and unloading of the part. As mentioned in Brower (1969) production rates of 350–400 parts per hour can

be achieved if closing a coil cover directly initiates the charge-and-fire cycle. In a more recent publication a charging time of approximately 8 s is reported for modern pulse generators. Belyy et al. (1977) state that the process can be easily automated and mechanized and mention an output capacity of 3600 operations per hour or even more.

- Due to the fact that the magnetic forces penetrate low-conductive materials like glass, ceramics and polymers, applications within a vacuum, an inert gas atmosphere or under clean room conditions are possible as predicated by Belyy et al. (1977) as well as by Dengler and Glomski (1991). So the forming of sensitive materials can be realized.
- The process can be operated by remote control and the pulsed power generator need not physically be in the same room as the tool coil. According to Zittel (1976) this can be exploited, e.g. in order to close nuclear fuel waste containers in a radioactive environment.
- Due to the high workpiece velocities (about 250 m/s) and the high strain rates in the range of $10^4\,s^{-1}$ the mechanical properties of the workpiece material can be improved compared to the quasistatic ones. Details about investigations on the material behavior are presented in Section 4.
- Belyy et al. (1977) also pronounce that the process offers a high technological flexibility, because the same coil can be used to form workpieces of different configurations. Moreover, they claim that it is possible to perform EMF in hard-to-reach areas, because the coil can be connected to the capacitor by a flexible bus bar.

Nevertheless, there are some disadvantages of the electromagnetic forming process:

- The process is most suitable for materials with a high electrical conductivity and low flow stress. Wilson (1964) as well as later on Bertholdi and Daube (1966) specified that the maximum specific resistance should not be lower than 15 μΩ cm. This corresponds to a specific electrical conductivity of about 6.7 MS/m. In a recent publication, Schäfer and Pasquale (2009) refer to the conductivity of mild steel, as a limiting value which conforms to the earlier statements. However, according to Belyy et al. (1977) lower conductive materials can be formed successfully if EMF machines with high discharge frequency (60–100 kHz) or a so-called driver foil is used. They claim that well-annealed copper is the best material for a driver. However, Dengler and Glomski (1991) recommend the application of aluminum foil for this purpose.
- Only a small part of the charging energy is used for the plastic deformation resulting in a comparable bad efficiency (Weimar, 1963). Bertholdi and Daube (1966) found that the ratio of deformation energy and capacitor charging energy is not higher than 20%. In Bauer (1969) an efficiency of only 2% is reported.
- Significant requirements regarding safety aspects are necessary, because high currents and high voltages resulting in strong magnetic fields can occur (Plum, 1988).
- As mentioned already in Boulger and Wagner (1960) the main limitation for the process is the mechanical and the thermal loading of the tool coil. Up to now efforts have been made to build coils which can withstand this load long-term. A promising concept of a durable flat coil is presented in Golovashchenko et al. (2006a) and some results of lifetime tests on a realized coil are shown in Golovashchenko et al. (2006b).
- Belyy et al. (1977) state that it is difficult to realize a deep drawing state by electromagnetic forming. They explain that in order to reach this strain state it is necessary to form the workpiece by various coils which must fit to the shape of the workpiece.

In the following a review about electromagnetic forming is presented. After a description of the process principle and process variants mentioned in the literature (see Section 2), information about basic research considering the process analysis is given in Section 3. Thereby especially:

- the determination of the transient process parameters, i.e. the magnetic pressure and the workpiece deformation,
- the interactions in-between these process parameters,
- the energy transfer during the process, and
- the influence of the electrical conductivity.

are considered. Differentiations according to the process variants are made wherever this was appropriate.

Subsequently, the material behavior at the process specific high strain rates is regarded in Section 4. Information about the equipment necessary for electromagnetic forming is summarized in Section 5. A comprehensive overview regarding application-oriented research work as well as some industrial application examples is presented in Section 6. Thereby, special focus is set on applications in the field of:

- forming,
- joining,
- cutting, and
- process combinations as well as process chains including electromagnetic forming operations.

The review is completed by a brief summary and some recommendations for future work in Section 7. A list of the symbols used in this article and the according meanings is composed in Table 1.

2. Principle of the electromagnetic forming process

The typical setup of an electromagnetic forming configuration corresponds to a resonant circuit. The high magnetic fields, which are necessary to form metals with a high electrical conductivity, are achieved via a pulse generator. According to Ertelt (1982), the tool coil-workpiece-unit characterizes a transformer. Equivalent circuit diagrams of different degrees of simplification have been used in literature to represent this setup, but with regard to the direct transferability of the typical components the design suggested by Bauer (1967) is the most descriptive one. Here, the forming machine is represented by a serial circuit consisting of a capacitor C, an inductance L_i as well as a resistor R_i. The tool coil is represented by its resistance R_{coil} and its inductance L_{coil}, both connected in series to the pulse power generator (see Fig. 2).

Within this high speed forming process, pulsed magnetic fields are used to form metals with a high electrical conductivity. Thereby, the stored charging energy of a capacitor battery $E_C(t)$, which according to Eq. (1) can be calculated from the capacity C and the charging voltage $U(t)$, is suddenly discharged by closing the high current switch:

$$E_C(t) = \frac{1}{2}CU(t)^2, \tag{1}$$

The resulting current $I(t)$, which is a highly damped sinusoidal oscillation, is determined by the electrical properties of the resonant circuit. For the calculation the different inductances and resistances can be summarized and represented by an equivalent inductance L_{rc} and an equivalent resistance R_{rc}. If the capacitance C, the inductance L_{rc} and the resistance R_{rc} of the resonant circuit are known the differential equation for the description of damped

Table 1
List of symbols.

Symbol	Unit	Meaning	Symbol	Unit	Meaning
a	mm	Gap width between tool coil and workpiece	r	mm	Radius, radial coordinate
B	G	Magnetic flux density	s	mm	Tube's wall thickness
b	mm	Sheet thickness	t	s	Time
C	F	Capacitance	T	K	Temperature
C	MPa	Strength coefficient	U	V	Voltage
E	J	Energy	u	mm	Displacement
f	s^{-1}	Frequency	v	mm/s	Velocity
F	N	Force	z	mm	Axial coordinate
H	A/mm	Magnetic field strength	ΔG	J	Activation free enthalpy
I	A	Current	Δt_{rise}	s	Rise time
J	A/mm^2	Current density	β	s^{-1}	Damping coefficient
k	–	Distribution coefficient	δ	mm	Skin depth
L	H	Inductance	ε	–	Strain
l	mm	Length	$\dot{\varepsilon}$	s^{-1}	Strain rate
m	–	Strain rate sensitivity	κ	Ω^{-1}	Conductivity
n	–	Number of turns	π	–	Ludolph's number (3.141...)
N	mm^{-1}	Number of turns per length	μ	Vs/Am	Permeability
n	–	Strain hardening exponent	ρ	kg/mm^3	Density
p	MPa	Pressure	σ	N/mm^2	Flow stress
R	Ω	Resistance	ω	rad/s	Angular frequency

oscillations (Eq. (2)) can be applied:

$$L_{rc}\frac{dI(t)}{dt} + R_{rc}I(t) + \frac{1}{C}\int I(t)\,dt = 0 \tag{2}$$

Assuming a capacitor voltage U_0 and no current at the beginning of the process (i.e. $U(t=0)=U_0$ and $I(t=0)=0$) as initial conditions, the differential equation leads to the following solution:

$$I(t) = \frac{U_0}{\omega L}\,e^{-\beta t}\sin\omega t \tag{3}$$

with the damping coefficient β:

$$\beta = \frac{R_{rc}}{2L_{rc}} \tag{4}$$

and the frequency of the current ω:

$$\omega = \sqrt{\omega_0^2 - \beta^2} \quad \text{with} \tag{5}$$

$$\omega_0 = \frac{1}{\sqrt{L_{RC}C_{RC}}} \tag{6}$$

The current is related to the corresponding magnetic field, which is concentrated between the workpiece and the tool coil. This magnetic field creates eddy currents that flow in the opposite direction in the workpiece. These are located close to the surface of the workpiece due to the skin effect. This effect was first described in Lamb (1883) for the case of spherical conductors and was generalized to conductors of any shape in Heaviside (1951). The depth of penetration of the current into the workpiece called skin depth δ mainly depends on the specific electrical conductivity κ of the workpiece and the frequency f of the closed electrical circuit:

$$\delta = \frac{1}{\sqrt{\pi f \kappa \mu_0 \mu_r}} \tag{7}$$

where μ_0 represents the magnetic permeability in a vacuum and μ_r is the relative permeability of the material with eddy currents induced.

A magnetic pressure, also called Maxwell pressure, acts nearly orthogonal onto the workpiece surface. The applied magnetic pressure acts only in areas close to the winding of the coil so that the deformation of the workpiece starts in these pressurized areas. This pressure causes a plastic deformation of the workpiece by exceeding the flow stress (see Fig. 3). Thereby, workpiece velocities in the magnitude of 10^2 m/s are achievable. Several approaches to estimate the acting magnetic pressure are known from literature and will be described in Section 3.1.1. The different directions of the current, the magnetic field lines and the pressure are illustrated in Fig. 3 for the setups of the electromagnetic compression and expansion of tubes as well as for the setup of electromagnetic sheet metal forming.

In tube compression processes the setup described above is frequently complemented by an additional component, which is positioned between the tool coil and workpiece. This tool is commonly referred to as a fieldshaper (also field-shaper or field shaper), but there are also some publications, in which it is called field concentrator (e.g. the patent by Khimenko et al., 1979) or flux concentrator (e.g. in Kim and Platner, 1959; Brower and Hayward, 1966). A fieldshaper is a usually axis-symmetric component made of an electrically high conductive material, which features one or more axial slots as shown in Fig. 4. In this process variant again

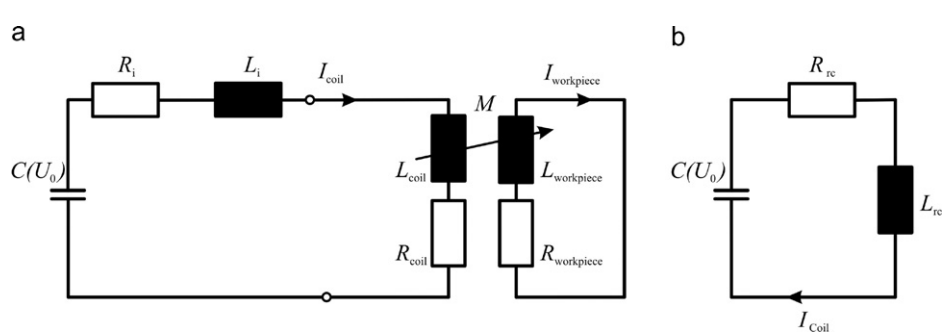

Fig. 2. Equivalent circuit diagrams: a) detailed version (Bauer, 1967); b) reduced version (Jablonski, 1976).

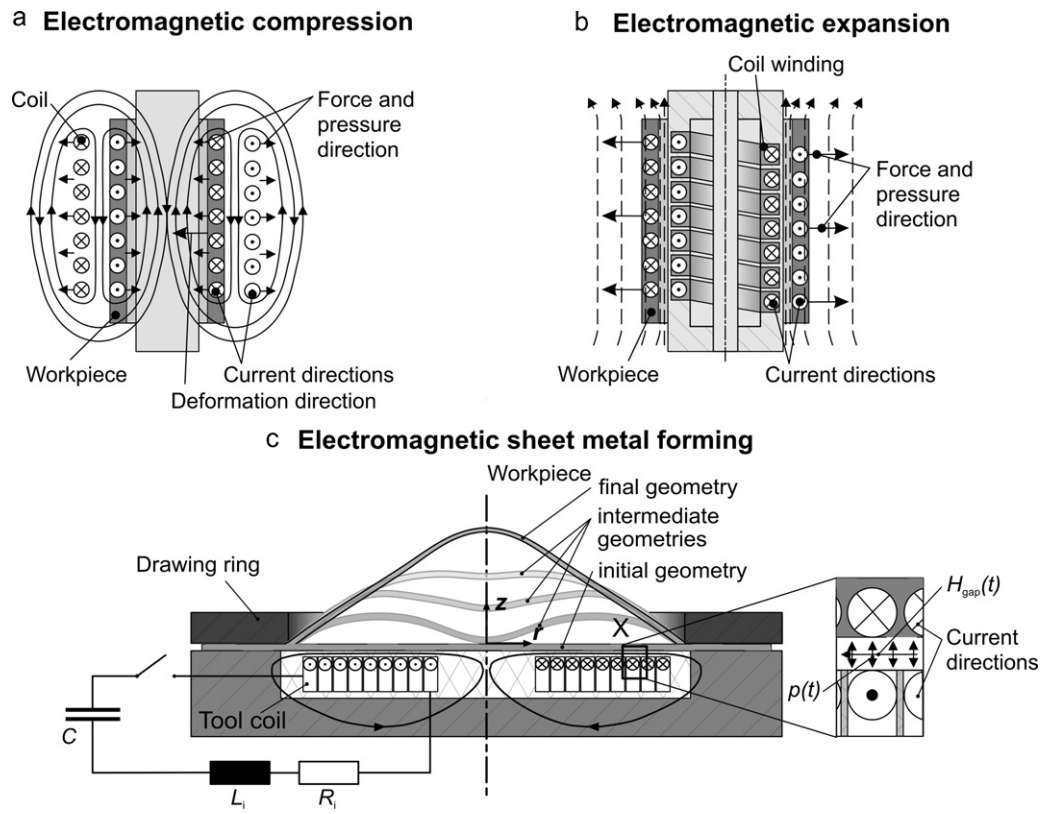

Fig. 3. Directions of the current, the magnetic field lines and the pressure during a) electromagnetic compression (von Finckenstein, 1967); b) electromagnetic expansion (Bauer, 1967); c) electromagnetic sheet metal forming (Beerwald et al., 2003).

the sudden discharge of the capacitor causes a damped sinusoidal current flowing through the tool coil which induces a related electromagnetic field according to the first Maxwell equation. Baines et al. (1965) indicates that the electrically conductive parts of the fieldshaper can be regarded as a short circuited second winding of a current transformer. According to the second Maxwell equation a current is induced here. Due to the skin effect and Lenz' law this induced current flows opposed to the coil current at the outer surface of the fieldshaper. At the axial slots the current is directed to the inner surface of the fieldshaper (the so-called concentration area). Here the current direction is the same as in the tool coil. Initially the magnetic field is shielded by the induced current and therefore limited to the gap volume.

Compared to the outer surface of the fieldshaper the concentration area is typically much smaller, resulting in a higher current density and higher field strength, here. Due to this magnetic field another current is induced in the workpiece in the region of the concentration area, which in turn shields the magnetic field. However, the tool coil, the fieldshaper and the workpiece are electrical conductors in a magnetic field, so that by Lorentz (1895) forces are acting on all components as soon as the currents are flowing. These so-called Lorentz forces initiate a plastic deformation of the workpiece as soon as the resulting stresses in the workpiece reach the flow stress.

Babat and Losinsky (1940) were the first ones making use of a fieldshaper in order to inductively heat a workpiece. One of the most important advantages of the use of a fieldshaper in an electromagnetic forming operation identified by Kim and Platner (1959) is that the mechanical loading of the tool coil can be significantly reduced in comparison to a direct acting coil (i.e. without a fieldshaper) resulting in a higher coil lifetime. The background of this correlation is that, in the case of a sophisticated choice of the size ratio of the fieldshaper surface in the concentration area and the outer fieldshaper surface, the forces between the fieldshaper and

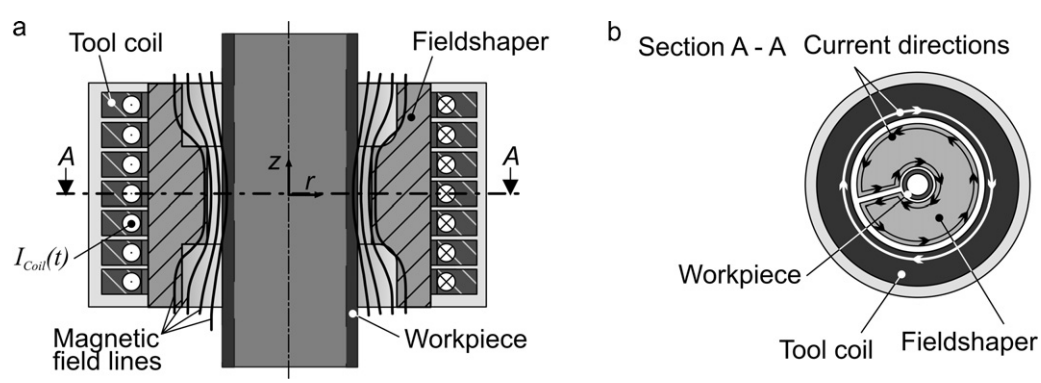

Fig. 4. a) Sketch of the magnetic field distribution for a fieldshaper featuring a step, Dietz et al. (1967b); b) current directions in tool coil fieldshaper and workpiece, Dietz et al. (1967a).

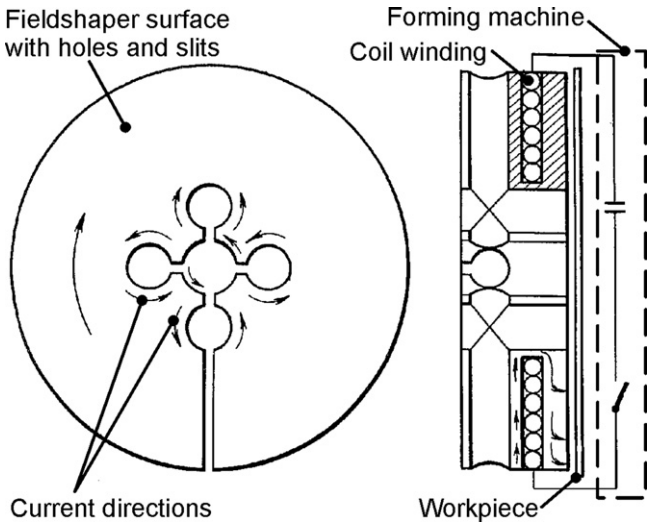

Fig. 5. Fieldshaper applied for sheet metal forming according to Bely et al. (1975).

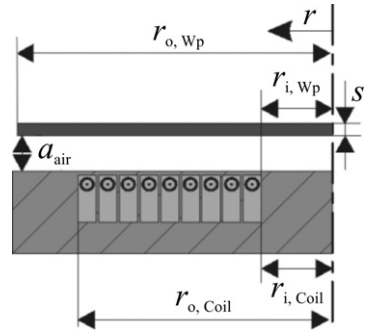

Fig. 6. Schematic of a spiral, flat coil for sheet metal forming (Risch, 2009).

workpiece are significantly higher than the forces between the tool coil and fieldshaper. Moreover, Rowland (1967) shows that fieldshapers can be used in order to adjust the diameter and length of an existing tool coil to different workpieces and forming tasks, respectively, so that the flexibility of the process is increased significantly. This flexibility can be increased by the detailed design of the fieldshaper. As described in Beerwald (2005) the field and force distribution significantly depends on the gap width between the fieldshaper and workpiece. Thus, the force distribution and the resulting workpiece contour can be adjusted by a target-oriented contouring especially of the fieldshaper's concentration area. As another important advantage Rowland (1967) points out that separable fieldshapers (i.e. fieldshapers featuring at least two axial slots) can be applied if the overall workpiece geometry requires coil diameters which are significantly larger than the workpiece geometry in the forming zone. This is, e.g. the case if a tube features locally strong curvatures or if it needs to be connected to relatively large fittings at both ends. As stated in Bauer (1980), the inner side of the fieldshaper need not be rotationally symmetric, but it can also be of a triangular, rectangular or polyangular cross-section geometry in order to form or join accordingly shaped workpieces.

More recently Uhlmann and Hahn (2003) used fieldshapers for the joining by electromagnetic compression of inductively heated magnesium tubes. Since the requirements on coils for inductive heating and coils for electromagnetic forming, respectively, vary significantly, two different tool coils are applied which are connected via one and the same fieldshaper. Thus, the forming can be realized directly after the heating process without time and temperature losses.

On the other hand, the use of a fieldshaper entails the disadvantage of an inhomogeneity in the magnetic field and consequently in the force distribution along the circumference of the workpiece. Both, the magnetic field and the force feature a local minimum in the area of the axial gap(s) in the fieldshaper which is more significant the higher the gap width is. Moreover, according to Furth et al. (1957) the process efficiency is reduced if a fieldshaper is applied. Reasons for this effect are additional resistive losses in the fieldshaper and losses of inductive energy due to inefficient inductive coupling of the tool coil, fieldshaper, and workpiece and due to additional gap volumes. However, these losses can be reduced and thus the process efficiency can be increased if the fieldshaper material is of high electrical conductivity as shown in Wilson and Srivastava (1965) (Fig. 5).

In principle the application of fieldshapers is not limited to electromagnetic compression. As suggested in Neubauer et al. (1988) the use in electromagnetic expansion is also possible, but there are only very few publications, dealing with this topic. Some basic investigations regarding the correlations between the charging energy, fieldshaper geometry and resulting workpiece geometry are presented in Suzuki et al. (1987). Another special application of fieldshapers is suggested in Bely et al. (1975). Here a specially shaped fieldshaper is used in order to adapt a cylindrical compression coil to the forming of a sheet metal workpiece. Thereby, a higher efficiency and a more uniform distribution of the forces is realized via holes which are made in the fieldshaper face facing the workpiece and connected to the nearest end surface by means of slits (compare Fig. 5).

In Jurgasch and Damavandi (2006) this idea is seized for the combined inductive heating and electromagnetic forming of magnesium sheets. The influence of the surface shape on the temperature distribution and the achievable workpiece deformation is demonstrated exemplarily. Similarly, Kamal and Daehn (2007) used a fieldshaper to produce a more uniform magnetic/pressure field for sheet metal forming.

Moreover, a form defining tool (a so-called mandrel) can be positioned inside the workpiece during electromagnetic tube compression. In this process variant the mandrel supports the workpiece during the compression process and the workpiece aligns to the mandrel and adopts the shape.

3. Process analysis

For a target-oriented dimensioning of electromagnetic forming processes, knowledge about the relevant process parameters as well as their influences and dependencies is essential and has therefore been a topic of intensive research since the 1960s up to now. Within this work especially the determination of the acting loads and the resulting deformation of the workpiece is an important aspect. The acting loads depend on many different parameters which can be classified as machine parameters, tool parameters and workpiece parameters. Important machine parameters are the capacity, the inner inductance, the inner resistance, the ringing frequency and the charging energy. Tool parameters are properties as, e.g. the geometry, the inductance, and the material of the coil, the fieldshaper properties, and the die/mandrel. Important workpiece parameters are the geometry, the material, the electrical conductivity, and the mechanical properties (e.g. flow stress and strain at failure). This means that for one and the same charging energy of the capacitor, depending on the machine, the coil, and the workpiece properties completely different loads can occur and consequently significantly different forming results can be achieved. Thus, the charging energy which is a frequently declared process parameter, alone is not sufficient to describe the loads.

In order to enable a comparison between experimental studies in which different equipment is applied, the course of the coil current (i.e. frequency and maximum current) and the temporary course as well as the local distribution of the magnetic field strength and the magnetic pressure can be used to give a more detailed description of the acting loads.

For the characterization of a sinusoidal oscillation the frequency and amplitude can be used. However, since the current is a damped sinusoidal oscillation, there is a wide spectrum of different frequencies included which depend on the resistance, the capacitance and the inductance of the equivalent circuit. To simplify the description, frequencies which make up a significant part of the oscillation can be identified by means of Fourier analysis as suggested in Brosius (2005) or alternatively a significant frequency f_{sig} can be calculated from the current rise time Δt_{rise} using Eq. (8) as done in Bühler and Bauer (1968b):

$$f_{sig} = \frac{1}{4\,\Delta t_{rise}} \tag{8}$$

Similarly, the pressure course can also be characterized by its amplitude and rise time.

Due to the acting loads the workpiece deformation results. However, the acting loads also depend on workpiece parameters (e.g. electrical conductivity) and on the gap width between the tool coil and workpiece. Consequently, the variation of these properties due to the workpiece deformation affects the magnetic pressure. These interdependencies complicate the process analysis. The significance of this interaction depends on the process variant and on the course of the magnetic pressure itself. Due to the typically higher deformations it is usually more distinctive during sheet metal forming than during tube compression or expansion and it is more important the slower the pressure pulse is as shown in Beerwald et al. (2003). Depending on the specific loading case significantly nonlinear deformation paths can occur as reported in Badelt et al. (2003). Therefore, in order to give a detailed description of the deformation process knowledge about the time-dependent displacement curve of the workpiece surface is required. To simplify this, typically characteristic points are identified and regarded.

3.1. Determination of transient process parameters

3.1.1. Determination of the acting loads

By Lorentz (1895) the volume forces $\vec{F}$ acting on the workpiece can be determined on the basis of the current density $\vec{J}$ and the magnetic flux density $\vec{B}$:

$$\vec{F} = \vec{J} \times \vec{B} \tag{9}$$

Disregarding the component of the magnetic field strength that is oriented in the direction of the workpiece thickness – i.e. the radial component in the case of tube forming and the z-component in the case of sheet metal forming – the current density equals the negative derivative of the magnetic field strength H with respect to the radius r as shown in Eq. (10) and the with respect to the z-coordinate, respectively, as shown in Eq. (11):

$$\vec{J} = -\frac{\partial H}{\partial r} \tag{10}$$

$$\vec{J} = -\frac{\partial H}{\partial z} \tag{11}$$

The magnetic flux density is the result of the product of the permeability μ and the magnetic field strength. Thus, according to Bauer (1967) the radial forces acting on a tubular workpiece F_r can be calculated using Eq. (12):

$$F_r = -\mu H \frac{\partial H}{\partial r} = -\frac{1}{2}\mu \frac{\partial (H^2)}{\partial r} \tag{12}$$

Similarly, the forces acting on a sheet metal workpiece can be calculated by Eq. (13):

$$F_z = -\mu H \frac{\partial H}{\partial z} = -\frac{1}{2}\mu \frac{\partial (H^2)}{\partial z} \tag{13}$$

These volume forces acting on the workpiece can be transformed mathematically to virtual surface forces, the so-called magnetic pressure p. According to Bühler and Bauer (1968b) the pressure difference between two points in the wall of the workpiece can be determined by integrating the acting forces over the distance and thus, the overall pressure acting on a tubular workpiece can be calculated by using the inner radius r_i and the outer radius r_o of the tube as integration limits (see Eq. (14)):

$$p(r,t) = \int_{r_o}^{r_i} F(r,t)dr = \frac{1}{2}\mu \left(H_{gap}^2(t) - H_{pen}^2(t)\right) \tag{14}$$

Similarly in the case of sheet metal forming, the lower and the upper surface of the workpiece can be used as integration limits. In both cases – tube and sheet forming – the magnetic pressure depends only on the magnetic field strength in the gap between the tool coil and workpiece H_{gap} and on the penetrated magnetic field H_{pen}.

As described in Bauer (1965) on the example of a tube compression process, these field strengths can be measured using suitable measuring loops which are positioned inside the tubular workpiece and in the gap outside the workpiece and orientated orthogonal to the magnetic field lines. Due to the temporary change of the magnetic flux density, a voltage is induced in the measuring loop. If the area of the probe is known the integral of the voltage can directly be used in order to calculate the flux density. A procedure for the calibration of measuring loops with unknown areas is given in Bauer (1967).

If the skin depth is small in comparison to the thickness of the workpiece, the penetrated magnetic field is frequently neglected and so the magnetic pressure can be calculated by the simplified Eq. (15):

$$p(t) = \frac{1}{2}\mu H_{gap}^2(t) \tag{15}$$

According to experimental investigations and analytical calculations considering the tube compression processes performed by Mühlbauer and von Finckenstein (1967) this simplification is allowable, if the ratio of skin depth and inner radius of the workpiece is less than 0.2 and the ratio of wall thickness and skin depth is at least two. Dietz et al. (1967a) declared on the basis of analytical estimations that this simplification is acceptable if the wall thickness equals at least 1.5 times the skin depth.

3.1.1.1. Tube compression process. In the case of direct acting compression coils, the magnetic pressure can be estimated analytically as shown in Dietz et al. (1967a). Here, initially an undamped sinusoidal current is assumed and the magnetic field, the eddy-current density, the magnetic field energy and the joule losses are calculated. Thus, the equivalent inductance and resistance for a setup without workpiece deformation are determined and it was shown that these equivalent parameters are only slightly influenced by the workpiece deformation. Therefore, the authors conclude that a sufficiently accurate approximation of the maximum achievable magnetic pressure of the damped coil current can be deduced from the energy balance setup for the undamped sinusoidal current.

In order to calculate the axial distribution of the magnetic field strength in the gap H_{gap} for a setup with a direct acting compression coil, Beerwald (2005) used a relationship based on the number of turns of the tool coil n, the coil current $I(t)$, the coil length l and a

so-called distribution coefficient k_H:

$$H_{gap}(t) = \frac{nI(t)}{l} k_H \text{ with} \tag{16}$$

$$k_H = \frac{1}{\pi}\left(\arctan\frac{2z+l}{a} - \arctan\frac{2z-l}{a}\right) \tag{17}$$

The mentioned distribution coefficient depends on the effective gap a between the tool coil and workpiece, which includes the width of the air gap a_{Air} and half of the skin depth of the workpiece δ_{Wp} and of the coil δ_{Coil} as shown in Eq. (18):

$$a = a_{air} + \frac{1}{2}(\delta_{Wp} + \delta_{Coil}) \tag{18}$$

The current course can either be measured as in Beerwald (2005) or calculated analytically by analyzing the resonant circuit (see Eqs. (2)–(6)).

If a fieldshaper is applied it influences the inductance and resistance and thus the current course in the resonant circuit. Equations for the analytical estimation of these parameters for a simple non-staggered fieldshaper (i.e. the length of the concentration area equals the outer length of the fieldshaper) are given in Dietz et al. (1967a). If the fieldshaper features a staggered geometry (i.e. the length of the concentration area is shorter than the outer length of the fieldshaper), the distribution of the magnetic field outside of the concentration area is inhomogeneous. Dietz et al. (1967b) approximates this inhomogeneous distribution by a cone. Assuming a sinusoidal coil current the authors determine the magnetic field energy and the Joule heating in order to approximate the maximum magnetic pressure in the first half wave of a damped coil current on the basis of an energy balance. A verification of the analytically predicted values with measurements show a good agreement.

A simpler analytical approximation of the magnetic pressure for the application of a staggered fieldshaper is suggested in Beerwald et al. (2001). Here, the authors define a concentration coefficient c_H, which equals the ratio of the magnetic field strength in the operating gap between the fieldshaper's concentration area and the workpiece and the magnetic field strength in the leak gap between the tool coil and the outer surface of the fieldshaper. It is proportional to the ratio of the length of the tool coil and the length of the fieldshaper's concentration area and depends on the magnetic resistances of the operating gap and of the areas next to the concentration area as well as on the magnetic resistance of the inner surface of the fieldshaper to the skin depth. A comparison to results of finite-element (FE) simulations shows that the analytically determined values slightly overestimate the magnetic field in the concentration area.

Yu et al. (2005) also used FE simulations in order to analyze the influence of the fieldshaper with trapezoidal cross-section on the pressure distribution. Simplifying the setup as rotationally symmetric, the authors use a two-dimensional model of coil, fieldshaper, workpiece and surrounding air in order to show that, compared to a direct acting tool coil, a fieldshaper leads to a more homogeneous pressure distribution. In a parameter study they show how the magnetic pressure increases with decreasing length of the concentration area if a constant charging energy is applied. As a qualitative verification the workpiece geometry is compared to experimental results.

Finally, a three-dimensional FE simulation is presented in Bahmani et al. (2008). The authors determine the distribution of the magnetic field considering the deformation of the workpiece but disregard the axial gap in the fieldshaper. A comparison to results of a two-dimensional simulation showed the same qualitative distribution but different quantitative values. An experimental verification is not presented here.

3.1.1.2. Tube expansion process. In electromagnetic tube expansion, the magnetic field strength in the gap between the workpiece and tool coil depends on the current induced in the workpiece. In contrast to the tube compression, this induced current is not as high as the coil current and therefore, the magnetic field strength cannot be calculated from the coil current as easily as in the case of tube compression. However, Bauer (1967) measured the magnetic field between the workpiece and tool coil in order to determine the force acting on the workpiece. Building on Gourdin (1989) the principle of virtual work is used in order to determine the acting loads on the basis of a measured coil current and the measured current in the workpiece. In contrast Al-Hassani et al. have been working on analytical approaches for calculating the workpiece current and in a second step the magnetic pressure from the measured coil current. In their earlier work Al-Hassani et al. (1967) neglected the time dependency of the gap width between the tool coil and workpiece and thus the variation of the parameters of the equivalent circuit diagram (inductance and resistance) during the forming process. Those parameters were assumed constant and values for a mean gap width determined on the basis of the average tube radius before and after deformation were used for the analysis. An improved strategy for the pressure calculation taking the varying geometry of the workpiece into account is presented in Al-Hassani et al. (1974). Due to the interdependencies of the electrical and the geometrical parameters in the system and the acting loads and the workpiece deformation respectively, a solution cannot be found directly but only by iteration so that a numerical approach is chosen, here. A comparison of the calculated coil current and workpiece deformation to measured values shows satisfactory results.

3.1.1.3. Sheet metal forming. In contrast to the electromagnetic tube compression, there are only a few scientific papers addressing the estimation of the magnetic pressure in an electromagnetic sheet metal forming process. The reason for this is that the electromagnetic forming of sheet metal is the most complex process variant and only a few physically reasonable assumptions can be made.

Göbl (1969) claims that the process cannot be described mathematically in a closed form. The major reason is that the deformation of the workpiece and the according increase of the gap volume between the workpiece and tool coil influence the acting magnetic pressure and in sheet metal forming this effect is much more relevant than in the case of tube compression or expansion. Hence, also Fischer (1983) concludes that a closed analytical solution is not possible. Nevertheless, there are some possibilities to estimate the magnetic pressure, but in these cases the temporal course and the local distribution are approximated in a coarse manner.

Al-Hassani (1975) presents an analytical derivation to estimate the pressure distribution of a spirally wound, flat tool coil, which is based on the geometrical dimension of the tool coil (see Fig. 6) and the maximum current I.

Regarding the magnetic field H_r in the radial direction as well as the magnetic pressure p_r, Al-Hassani (1975) indicates following equations:

$$H_r = \frac{In}{\pi l}\left[\tan^{-1}\left(\frac{-2a_{air}r}{a_{air}^2 + r_{o,Coil}^2 - r^2}\right) + \tan^{-1}\left(\frac{-2a_{air}r}{a_{air}^2 + r_{i,Coil}^2 - r^2}\right)\right] \tag{19}$$

$$p_r = \frac{\mu_0 I^2 n^2}{2\pi^2 l^2}\left[\tan^{-1}\left(\frac{-2a_{air}r}{a_{air}^2 + r_{o,Coil}^2 - r^2}\right) + \tan^{-1}\left(\frac{-2a_{air}r}{a_{air}^2 + r_{i,Coil}^2 - r^2}\right)\right]^2 \tag{20}$$

here n represents the number of turns and l represents the width of the winding, a_{air} indicates the gap width between the tool coil and workpiece and $r_{i,\,Coil}$ and $r_{o,\,Coil}$ respectively represent the inner and the outer radii of the tool coil. The radial position is indicated by

the value of r. The experimental verification of this approximation formula is satisfactory according to Al-Hassani (1975).

In contrast, Beerwald (2005) uses a harmonic field simulation to determine the pressure distribution. Thereby, the ratio of the numerical result of the field strength $H_{gap}(t_{max},r)$ when the current reaches the maximum and maximum possible field strength $H_0(t_{max})$ determines a factor of pressure distribution $k_H(r)$, analogous to the distribution coefficient for the tube compression process introduced in Eq. (17):

$$k_H(r) = \frac{H_{gap}(t_{max}, r)}{H_0(t_{max})} \quad \text{with } H_0 = \frac{nI(t_{max})}{l_{coil}} \tag{21}$$

However, not only the local field distribution and pressure distribution but also the temporal field and pressure course are of interest. So, the process itself can be characterized temporally as well as locally. In Ertelt (1982), a method is described to approximate the temporal course of the magnetic pressure. This approach is based on the key values of the pulse generator and the geometrical as well as electrical properties of the tool coil. The magnetic pressure is determined by Eq. (22):

$$p(t) = \frac{E_{Sp}(t)}{V_{eff}} \tag{22}$$

here V_{eff} defines the effective volume with the assumption, that this volume contains the complete magnetic energy, which is responsible for the retroactivity between the electrical and magnetic values. $E_{Sp}(t)$ is the energy, which is transferred into the coil energy and can be calculated on the basis of the specific values of the peak current, see Eq. (23):

$$E_{Sp}(t) = \frac{1}{2} L_A I(t)^2 \tag{23}$$

The inductance L_A of the workpiece-tool coil unit can be determined using a commercial inductance measurement instrument or estimated analytically by applying the correlations described in Timpl et al. (1981). The transient current response $I(t)$ can be identified using Eqs. (2)–(6) or determined from measurements. The effective volume V_{eff} can be calculated by Eq. (24) (geometrical dimensions of tool coil the setup according to Fig. 6):

$$V_{eff} = \frac{\pi}{4}((r_{o,Coil}+r_{o,Wp})^2 - (r_{i,Coil}+r_{i,Wp})^2)\left(a_{air} + \frac{1}{2}\delta_{Coil} + \frac{1}{2}\delta_{Wp}\right) \tag{24}$$

Thereby, $r_{o,Coil}$ and $r_{o,Wp}$ represent the outer radii of the tool coil and the workpiece, respectively. The gap width between the workpiece and tool coil is symbolized by a_{air} and δ_{Coil} and δ_{Wp} represent the skin depth within the tool coil and the workpiece, respectively.

It has to be mentioned that the described approaches to determine the acting load are developed on stationary workpieces. Thereby, the retroactivity of the deformation on the magnetic pressure was neglected despite Brosius et al. (2003) claims that this interaction is required for a correct analysis of the forming process.

3.1.2. Determination of the workpiece deformation

As mentioned above, the second important aspect with regard to the process analysis is the determination of the workpiece deformation. In order to determine this parameter, measurement techniques as well as analytical and numerical approaches have been used. Considering the measurement techniques, three major variants have been introduced already in the 1960s, which are still being used and refined in current investigations.

3.1.2.1. Measurement techniques. For a metrological determination of the workpiece deformation during electromagnetic tube expansion processes, Kegg and Haverbeck (1962) used high speed cameras. A visualization of a free electromagnetic sheet metal forming process is presented in Bach et al. (2003) and can be seen in Fig. 7 while first pictures showing the course of an electromagnetic sheet metal forming process into a (transparent) die made of acryl glass is presented in Risch (2009).

A tactile measurement approach is presented in Lippmann and Schreiner (1964) for the example of a tube compression process (see Fig. 8). They used cylindrical mandrels each allowing a specific radial deformation of the tube and applied a voltage between tube and mandrel which was monitored by an oscilloscope. As soon as the workpiece hits the mandrel a voltage drop can be recognized. Thus, for each distinct radial displacement a corresponding contact moment can be determined and the course of the complete workpiece deformation can be assembled from different measurements.

A further development allowing a determination of the axial distribution of the deformation and the forming velocity in a tube expansion process[1] is presented in Poynton et al. (1967). In order to do so, several contact pins are used instead of a mandrel. These pins are positioned at a specific axial location and at a specific radial distance to the tubular workpiece. They feature different series resistors, so that the voltage steps measured at the moment of contact are different and can be reassigned to the different contact pins. This principle was adapted to the electromagnetic sheet metal forming process in Badelt et al. (2003) for the use of one contact pin while in Risch (2009) multiple contact pins were used in order to measure the radial displacement and velocity distribution of the sheet.

An alternative optical measurement technique for detecting the trajectory of the middle cross-section during an electromagnetic tube compression process is presented in Bauer (1965). It is based on the shadowing principle A parallel ray of light is sent axially through the workpiece so that the tube's complete cross-section is illuminated. At the other side the light is gathered by a lens and directed to the cathode of a vacuum photocell. The generated current causes a voltage at the resistance which is proportional to the received light. With increasing workpiece deformation more and more light is shadowed by the workpiece and the measured voltage decreases. Thus, the compression of the workpiece can directly be measured after calibrating the system in order to determine the correlation between the workpiece diameter and the measured voltage. A variant of this measuring principle in which not the complete cross-section is illuminated but only a narrow light beam is sent through the tube is presented in Bauer (1969). The application of the same shadowing principle for measuring the workpiece's bulging during an electromagnetic expansion process is described in Bauer (1967). In more recent publications, as, e.g. in Beerwald et al. (1999), the shadowing principle is still being applied for tube compression and expansion processes but in this setup modern semi-conductor components (so-called position sensitive devices – PSD) are used. In Badelt et al. (2003) the principle is adapted to the electromagnetic sheet metal forming process.

While the measurement techniques described above are suitable for measuring the displacement of the workpiece surface and the velocity and the acceleration can be determined by differentiating the measured curves with respect to the time, Barker and Hollenbach (1972) developed a measurement technique that can be used for the direct measurement of the surface velocity. This velocity interferometer system for any reflector (VISAR), according to Daehn et al. (2008), has become a standard for high speed velocity measurements. The principle of velocity interferometry goes back to the 1960s. It is based on the relativistic Doppler-effect and wave superposition, which may be constructive or destructive. For the measurement, coherent light is directed towards the surface point to be measured and the reflected radiation is collected. Due

[1] In Poynton et al. (1967) the tube expansion is initiated by a gas detonation and not by electromagnetic forming.

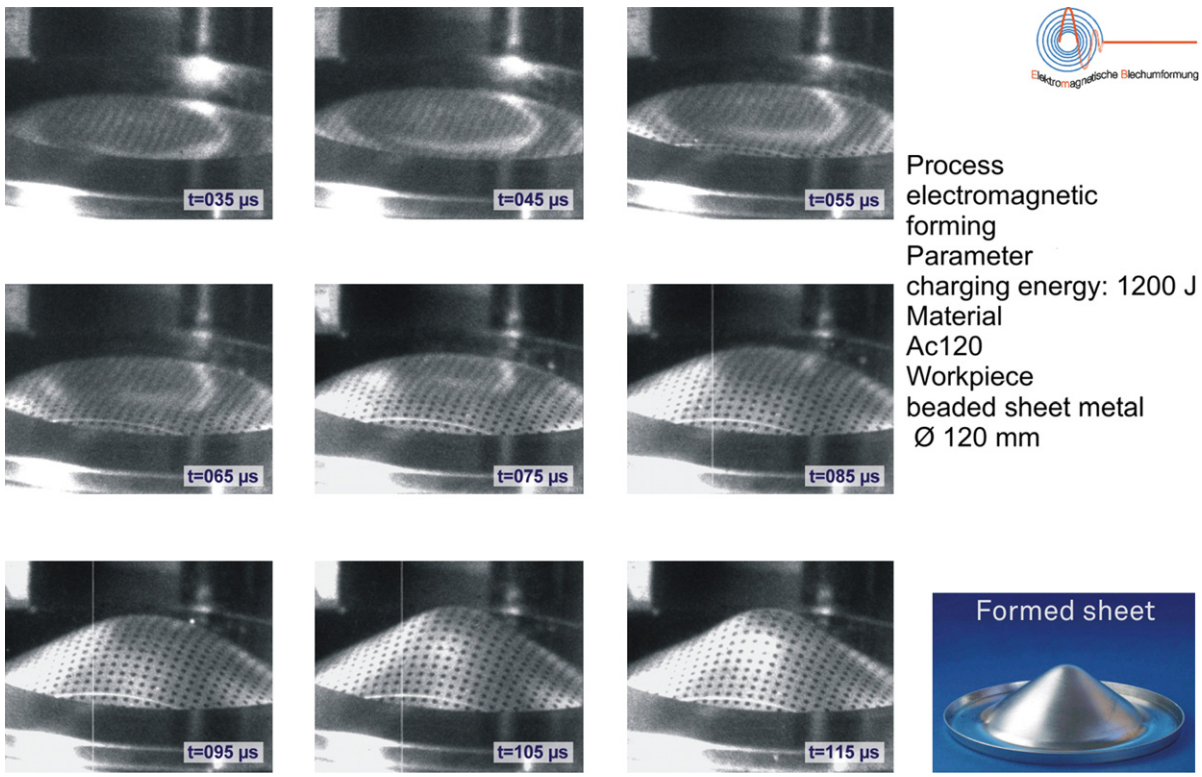

Fig. 7. Sequence of an electromagnetic sheet metal forming process into a die (Bach et al., 2003).

to the velocity of the reflecting surface, the wavelength of the light is changed. The reflected radiation is sent to an interferometer, producing an output containing the input signal and a time delayed version of the input signal. On the basis of the reflected wavelength, or more precisely the reflected optical phase, object motion and velocity can be detected. A detailed description of different well established as well as recently deployed VISAR systems is given in Dolan (2006). However, according to Daehn et al. (2008), the analysis of the data gathered by a VISAR system is difficult, the technique is expensive and the system is not suitable for the application in any manufacturing facility. Considering these aspects, the Photon Doppler Velocimetry (PDV) which was developed by Strand et al. (2005) offers significant advantages. In this system newly available fiber optic lasers and components as well as higher speed oscilloscopes are applied and Daehn et al. (2008) considers this as a breakthrough in robust and inexpensive velocimetry. A schematic of the PDV-system is shown in Fig. 9.

3.1.2.2. Analytic and numerical approaches. The theoretical basis to describe the physical effects for the production and usage of high transient magnetic fields were established in the 1950s and 1960s by Furth and Waniek (1956) as well as Lal and Hiller (1968). This work was followed up by the development of analytical approaches in order to calculate the deformation of the workpiece. These approaches are exclusively focusing on tube forming processes, because this is the simplest process variant. Nevertheless, also in these attempts significant simplifications are made in order to be able to predict the deformation of the workpiece. For example, it is assumed that the tube is thin-walled and both the tube and tool coil are of infinite length. Thus, the displacement u depends only on the time while the dependencies on the radius and the axial position can be neglected (Lippmann and Schreiner, 1964). In many publications including Birdsall et al. (1961), the basic equation that is setup is the pressure equilibrium. Lippmann and Schreiner (1964) equalize the magnetic pressure and the inertia force of the tube, which depends on the density ρ, the wall thickness s and the acceleration (d^2u/dt^2) and solve the equation for the workpiece acceleration. This leads to Eq. (25) in which B_z represents the axial component

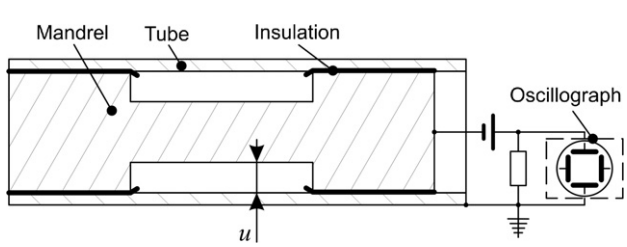

Fig. 8. Setup and principle of the tactile displacement measurement according to Lippmann and Schreiner (1964).

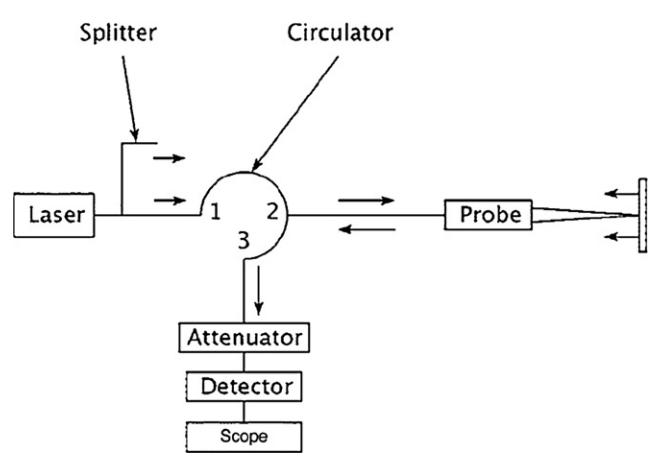

Fig. 9. Schematic diagram for Photon Doppler Velocimetry (PDV) (Daehn et al., 2008).

of the magnetic flux density.

$$\frac{d^2u}{dt^2} = \frac{1}{2\mu_0\rho s}B_z^2 \tag{25}$$

A subsequent integration of the acceleration allows calculating the velocity υ according to Eq. (26) and the displacement u of the workpiece according to Eq. (27). In both equations B_m represents the maximum occurring magnetic flux density during the deformation process.

$$\upsilon = \frac{du}{dt} = \frac{B_m^2}{2\mu_0\rho s}t \tag{26}$$

$$u = \frac{B_m^2}{4\mu_0\rho s}t^2 \tag{27}$$

A similar approach for calculating the workpiece deformation is presented in Dietz et al. (1968). The authors again setup the equation for the movement of the workpiece on the basis of Newton's second law of motion by equalizing the difference between the magnetic forces and a "contra-force" of the workpiece, both referring to the volume that is accelerated, with the product of the workpiece density and acceleration. The mentioned "contra-force" of the workpiece is calculated by Barlow's Formula. Considering the flow stress of the material experimental data determined via quasistatic compression tests is used. Regarding the magnetic pressure a simplified description of the course using piecewise linear functions is applied. On this basis Dietz et al. (1968) solve the equation of motion differentiating between two different cases depending on whether the deformation of the workpiece is completed during the first pressure pulse or not. The results are compared to experiments considering the electromagnetic compression of copper tubes.

A method for calculating the minimum required field strength for the electromagnetic compression of rotationally symmetric tubes is suggested in Bühler and Bauer (1968b). In order to do so the authors assume the workpiece to be made of a homogeneous, isotropic, and incompressible material, so that the Tresca yield criterion can be applied. Further assuming that the magnetic field is completely shielded by the induced current, the simplified Eq. (15) can be used to determine the magnetic pressure. The minimum field strength required depends only on the geometric workpiece characteristics, i.e. wall thickness s and outer radius r_o, and the flow stress k_f and it can be calculated using Eq. (28).

$$H_{\min} \approx \sqrt{-\frac{2}{\mu_0}k_f \ln\left(1 - \frac{s}{r_a}\right)} \tag{28}$$

However, Fenton and Daehn (1998) state that the deformation behavior has a significant influence on the current course and consequently on the acting magnetic pressure. Due to the deformation of the workpiece, the inductance course of the workpiece-tool coil – unit is influenced. One possibility to consider this interdependency and to generate a realistic and sufficiently accurate process model is to realize a coupled finite element analysis. Takatsu et al. (1988) presented the first completely numerical solution including the deformation course of the workpiece. He coupled the electromagnetic fields and the structure mechanical simulation in defined time steps considering a rate-dependent material model. The numerical results were verified with photos taken from a high speed camera. Despite several assumptions, the comparison of the numerical and the experimental results agree well. The experimental data from Takatsu et al. (1988) is used in Fenton and Daehn (1998) to verify their two-dimensional simulations. These simulations are based on a C-program bibliotheca, which is not freely accessible. The authors use a Arbitrary Lagrangian Eulerian (ALE) method for solving the coupled system. This means that for small mesh distortion the Lagrangian form of the field equations is applied while in case of more distinctive mesh distortion the Eulerian form is used.

Oliveira and Worswick (2003) combine the commercial codes ANSYS/EMAG for the electromagnetic simulation and LS-DYNA for the structural simulation in order to represent the electromagnetic forming process. The required information about the acting forces respective of the resulting geometry is exchanged by means of an interface. While in Oliveira and Worswick (2003) the results of the electromagnetic sheet metal forming for a free operation are presented, the expansion regarding the forming into a die is described in Oliveira et al. (2005). In both papers the aluminum alloys AA5182 and AA5754 were investigated in experimental as well as numerical analyses. Furthermore, the possibility to model the process in a three-dimensional way is shown.

The implementation of a fracture model in the structural simulation is presented in Imbert et al. (2005) in order to investigate the interaction between the workpiece and the die. In doing so, a modified Gurson–Tveergaard–Needleman material model is integrated in the simulation. However, due to the computation time, no coupling strategy was applied, but the pressure estimation according to Al-Hassani (1975) was used to determine the acting forces.

Bessonov and Golovashchenko developed a fully coupled simulation considering:

- the electromagnetic field propagation, which is defined by quasi-stationary Maxwell equations transformed in Lagrangian form,
- a dynamic elastic–plastic deformation, which is modeled using the solid mechanics equation of motion, the modified theory of elastic plastic flow and the Von Mises yield criterion, and
- the heat transfer, which is considered via the energy conservation law.

In this simulation tool also the forming machine is modeled as a R–L–C circuit, so that the current course can be calculated on the basis of the electrical parameters of the machine and the charging energy. Exemplary results of 2D simulations are shown. However, only a qualitative verification by a comparison with experimental investigations is given.

Similarly, Karch and Roll (2005) present a fully transient electrodynamic structure mechanical coupled simulation in ANSYS for the tube compression process. Here, the current displacement, the temperature development in the tube and tool coil, the modeling of the RLC-equivalent circuit, and the retroactivity of the deformation on the electromagnetic fields were considered disregarding only the strain rate dependency of the flow curves. A qualitative and quantitative comparison with experimental tube compression processes shows a good agreement. In Kleiner and Brosius (2006) a two-dimensional fully transient strategy is described. Here, the coupling is realized between MSC. Mentat with a self-developed electromagnetic FE-Code.

One major problem considering the three-dimensional simulation of the electromagnetic forming process is the calculation time. The model size in finite element simulations is extremely high, because not only the tools and the workpiece but also the surrounding air has to be considered. Moreover, in order to be able to calculate the magnetic field distribution with sufficient accuracy, a dense meshing is required especially in the region of the coil and the workpiece. In order to realize a fast three-dimensional magnetomechanical problem Schinnerl et al. (2002) used an implicit multigrid method. However, in this work the modeling of the mechanical system is restricted to linear elasticity.

Stiemer et al. have been working on a fully transient coupled simulation of the electromagnetic forming process over several years. Temperature effects are neglected in this simulation. In Stiemer et al. (2006) the authors present a simulation strategy in which the electromagnetic field is calculated via a Eulerian formulation for a stationary grid. The mechanical structure is modeled by a Lagrangian formulation with a grid, which is free to move over the

stationary electromagnetic grid. By applying this modeling strategy a fast solving of the coupled system is possible and the displacements are calculated with high accuracy. However, regarding the acting forces oscillations occur. Later in Stiemer et al. (2009) an ALE formulation was used for the modeling of the magnetic system. Here, the electromagnetic grid is moved together with the mechanical structure. This strategy was also used for the modeling of three-dimensional problems. In order to be able to solve the electromagnetic equations efficiently in these cases, Nedelec-finite-elements have been applied.

Conraux et al. (2006) introduce a coupling method, in which the FE-code SYSMAGNA for the electrodynamical effects and PAM-STAMP for the structure–mechanical simulation are used. In this paper results regarding the electromagnetic tube compression as well as the electromagnetic sheet metal forming are discussed. The model description is based on finite elements.

Contrary, L'Eplattenier et al. (2008) present a new electromagnetic module, implemented in LS DYNA. This module should be very suitable regarding the mechanical, thermal, and electromagnetic coupled tasks. The electrical fields are determined by means of the finite element method, while the surrounding air is connected via the boundary element method on the electromagnetic finite element simulation. The verification experiments correspond well to the numerical results L'Eplattenier et al. (2009). Meanwhile, this tool has been used in several investigations. One example is the analysis of the force distribution and the rebound during electromagnetic forming of sheet metal workpieces into conical dies and into oblong dies with v-shaped cavities, which is presented in Imbert et al. (2010).

In Demir et al. (2010) the commercially available code ANSYS is used for a three-dimensional calculation of the magnetic field distribution and coupled with LS DYNA, which is applied for the calculation of the corresponding workpiece deformation and especially the resulting wrinkling effects in a free tube compression process. In the model, geometrical imperfections regarding the roundness as well as the wall thickness distribution of the tube are considered and their effect on the achievable forming result is calculated. Verification by comparing the results of the simulation to experimental data is given.

3.2. Acting loads and deformation during electromagnetic forming

The easiest possibility to influence the current and the magnetic pressure course is via an adjustment of the capacitor charging energy. If the parameters of the forming machine, the tool coil, and the workpiece are equal, an increase of the charging energy will lead to an increase of the current and the pressure maximum, while the rise time will remain approximately the same. The current and pressure rise time can be adjusted via the capacity of the forming machine and/or via the common inductance of the unit of tool coil and workpiece.

3.2.1. Tube compression process

The influence of the acting load on the workpiece deformation is illustrated exemplarily in Fig. 10 on the basis of measured current courses, the acting magnetic pressures and the corresponding diameter-related displacements of the smallest cross-section measured using the shadowing principle.[2] Considering the current course, two curves with significantly different frequencies but leading to the same deformation of the workpiece are being compared. These have been realized applying forming machines with different properties and especially different capacities (case 1: $C = 22\ \mu F$; case 2: $C = 1197\ \mu F$).

In the measured current with the high frequency (curves indicated as 1) the typical damped sinusoidal oscillation can be clearly identified. Here, the workpiece deformation starts immediately after the first rising of the current and the magnetic pressure and it continues for several oscillations of the current. The current of the lower discharging frequency (curves indicated as 2) is the more common case. Here, the current and consequently the magnetic pressure are rising at the beginning of the process but no workpiece deformation can be measured, yet. A plastic workpiece deformation can be identified by a rise of the displacement curve as soon as the inertial forces are exceeded and the yield strength of the workpiece material is reached. The deformation process is completed during the first half wave of the coil current and the first pressure pulse accordingly. Similar experiments performed in Beerwald (2005) show an elastic, radial oscillation of the tube that follows the plastic deformation, which cannot be recognized, here. This oscillation can be attributed to the fact that the high kinetic energy resulting from the high velocity cannot be dissipated spontaneously in a free forming operation. The frequency of this oscillation is correlated to the natural frequency of the tube and can be more or less distinctive. In Psyk et al. (2006b) the oscillation of aluminum and magnesium tubes are compared applying the same equipment and comparable process parameters. It is shown that in the case of aluminum a clear oscillation can be identified while this is not possible for the magnesium tubes.

The example in Fig. 10 clearly shows that different load conditions can lead to the same displacement. However, depending on the process parameters a much higher energy can be required. The physical background for this effect is explained by Mattke and Dehoff (1969): in the case of very high frequencies and the related short pressure application time, even high amplitudes are not sufficient to overcome the inertia of the workpiece. Here, the theoretical extreme is the Dirac-impulse. In contrast for very low frequencies – the extreme case, here is direct current – the induced magnetic field and current are extremely low so that no pressure difference is built up over the thickness of the workpiece.

Another experimental study considering not only the mean displacement but also the accuracy of the cross-section geometry considering the achievable roundness is presented in Psyk et al. (2004b). It is shown that in a free forming process, a higher charging energy and accordingly increased magnetic pressure amplitude without significant change of the rise time will cause a higher deformation and velocity of the workpiece. Psyk et al. (2004b) found that this is correlated to a deterioration of roundness and to an increasing wrinkling effect, respectively. Moreover it is shown that in order to achieve a defined radial deformation either a pressure pulse with a longer rise time and a lower maximum or with a shorter rise time and a higher maximum can be applied. Thereby, a faster rise of the pressure leads to higher strain rates and a better roundness of the compressed tube. This result correlates well with the investigations presented in Balanethiram and Daehn (1992). Here, it is shown that, compared to quasistatic forming technologies, high speed forming via electromagnetic forming and electrohydraulic forming are less sensitive to localizing effects and therefore in many cases allows an extension of forming limits. This means that the current and pressure courses have to be dimensioned considering the achievable process efficiency and the achievable roundness and these two aspects can lead to contradictory demands. However in Psyk (2010) it is shown that, in the case of rather fast pressure pulses with pressure rise times of less than 15 μs, no significant further improvement of the roundness can be expected by applying pulses with even shorter rise times.

[2] In the case of a conventional direct acting tool coil with constant width of the winding and in the case of a symmetric fieldshaper with a cylindrical contour in the concentration area, this is typically the middle cross-section of the deformed area.

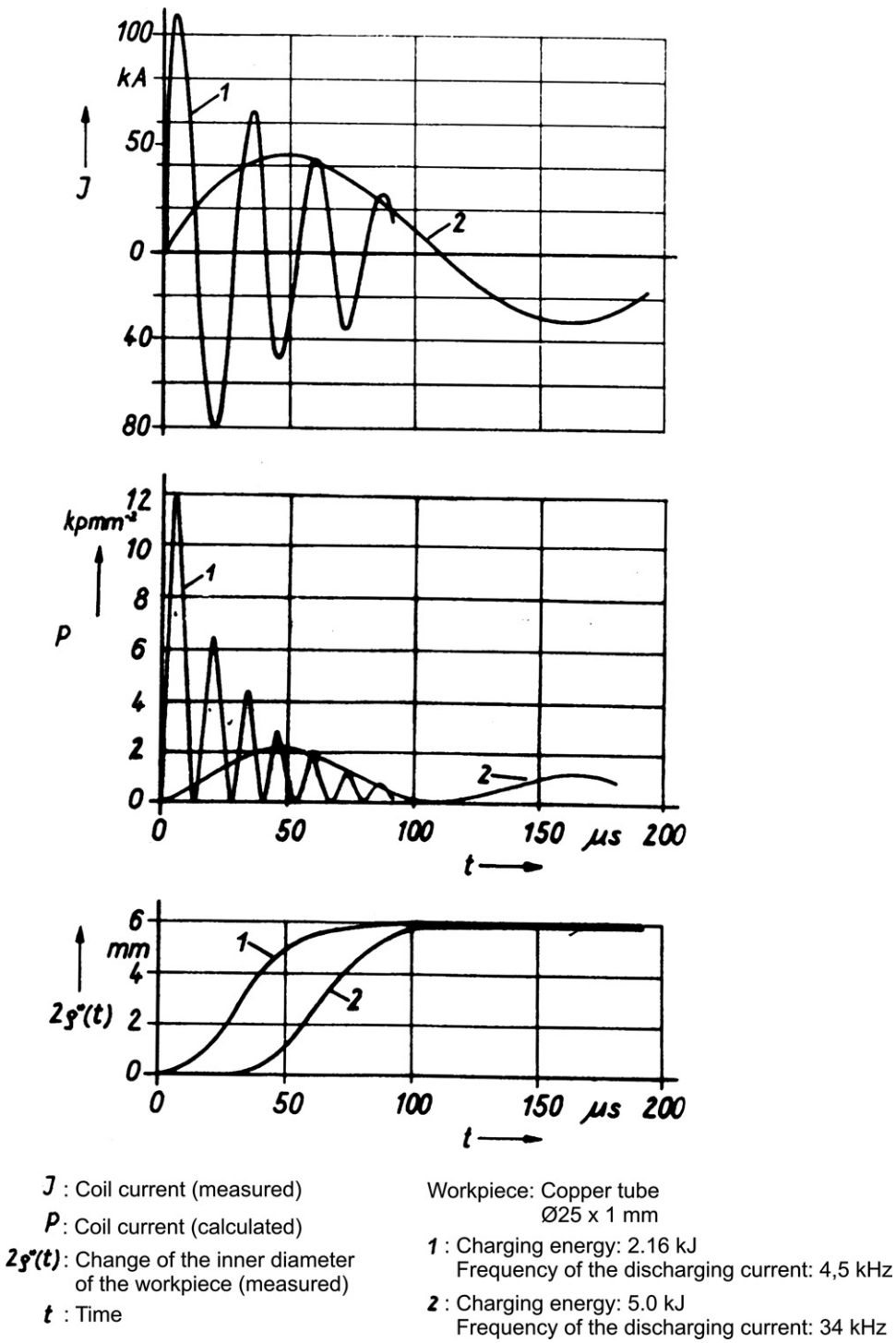

Fig. 10. Current and pressure course as well as workpiece deformation during a free electromagnetic compression process according to Daube (1973).

As suggested in Psyk et al. (2005) and investigated in more detail in Psyk and Tekkaya (2009) wrinkling in tube compression processes is triggered by material or geometrical inhomogeneities in the semi-finished part. The sensitivity of the electromagnetic compression process considering such inhomogeneities decreases with decreasing strength as well as with increasing stiffness of the tube.

Apart from the regarded influence of the current and pressure pulse on the deformation of the tube, there exists a retroactivity of the workpiece deformation on the pressure pulse. For a detailed analysis of this effect Beerwald (2005) used a stepwise coupled finite element simulation. Important results are summarized in Fig. 11.

It can clearly be seen that neglecting the workpiece deformation can lead to a significant overestimation of the magnetic pressure. Furthermore, it can be recognized that due to the increasing gap volume, the qualitative distribution of the magnetic pressure changes over the process time. At the beginning, the pressure maximum is located in the middle of the tool coil and consequently here the maximum deformation results. Due to this, the maximum gap width between the tool coil and workpiece occurs in the middle area of the coil and in turn the pressure decreases faster, here.

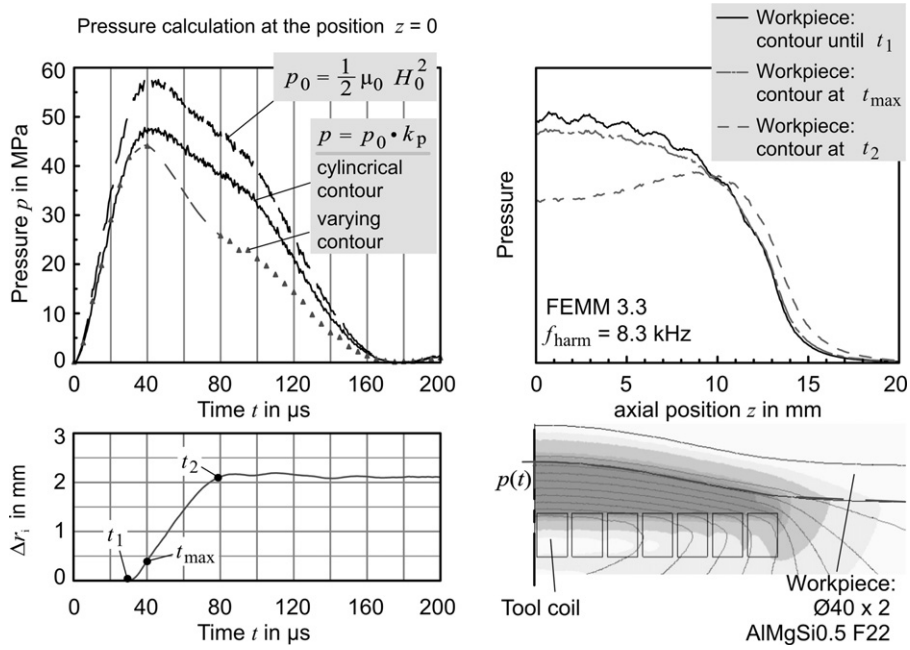

Fig. 11. Influence of the workpiece deformation on the pressure course (Beerwald, 2005).

Thus, the pressure maximum moves from the center to the outer regions of the coil during the deformation process.

3.2.2. Tube expansion process

The major difference between a tube compression and a tube expansion process is the temporary development of the workpiece's geometric stiffness considering radially acting loads. This stiffness decreases with increasing tube diameter and decreasing wall thickness. Therefore, during an expansion process the stiffness decreases due to the tube deformation, while in the case of compression the stiffness increases over the process time. In the case of lower workpiece stiffness, the influence of inertia forces is higher.

Considering the interdependencies between acting loads and workpiece deformation, the conclusions drawn on the basis of compression processes can partly be transferred to the tube expansion. Thus, the beginning of the workpiece deformation affects the current and the pressure curve in the same manner than in the case of tube compression, while the end of the workpiece deformation cannot always be identified that clearly (Beerwald, 2005).

3.2.3. Electromagnetic sheet metal forming

In the case of sheet metal forming the effect of inertia forces is more distinctive than in the case of tube forming. For this process variant frequently spirally wound tool coils are used. In these cases the center of the workpiece is not pressurized and the sheet remains in the initial position at the beginning of the process (see Fig. 12). The saw-tooth shape of the pressure versus radius curve is caused by the turns of the coil. Due to the acceleration of the pressurized parts of the workpiece, the center of the workpiece will be dragged in the drawing direction as the process progresses (Takatsu et al., 1988). Depending on the pressurized area, some parts of the workpieces will be distinctively bent and unbent. Thus, different strain hardening and material strength evolves during the forming process in the workpiece.

During the deformation stages a continuously decreasing pressure can be observed because of the decreasing magnetic field strength which is related to an increasing gap volume. As soon as the workpiece leaves the area of influence of the tool coil and the pressure decreases to a negligible level, the process is only driven by inertia forces. At this moment, the movement of the workpiece cannot be influenced anymore.

Fischer (1983) analyzed the influence of the discharging frequency regarding the electromagnetic sheet metal forming. In his analytical investigation he simplifies a spirally wound flat tool coil to a circular ring and neglects the workpiece deformation. The analysis shows that an increase of the discharging frequency causes an increase of the magnetic pressure. Beerwald et al. (2003) focus on the velocity of the sheet. They show that, similar to the tube compression process also in the case of sheet metal forming, the same workpiece deformation can be realized either by applying a short pressure pulse with a high maximum or a longer lasting pressure pulse with a lower frequency. The occurring velocities as well as the required capacitor charging energy are approximately the same. Risch (2009) investigates the influence of the discharging frequency in free electromagnetic sheet metal forming of materials with different mechanical and electrical properties, keeping the charging energy constant in all cases. It is shown that by applying varying current impulses the same characteristic shape but different maximum drawing depths were achieved. However, depending on the material properties like strength or electrical conductivity this effect can be observed more or less distinctive.

3.3. Energy transfer during electromagnetic forming

As already mentioned in Section 2 the energy for the electromagnetic forming process is initially stored as capacitive energy in the pulsed power generator. At the end of the process the forming energy has been used in order to change the shape of the workpiece. In-between these two stages, a complex energy transfer takes place. Daube et al. (1966) claims that the energy stored in the capacitor (see Eq. (1)) is only partly transferred to the coil. Losses occur, e.g. due to the heating of the supply lines, energy losses in the switches and reactive energy in the pulsed power generator (compare Fig. 13). Furthermore, fractions of the energy transferred to the coil are lost due to heating of this tool and leak fields, so that the exploitable magnetic field energy is reduced. The exploitable magnetic field energy in turn is only partly transferred to forming

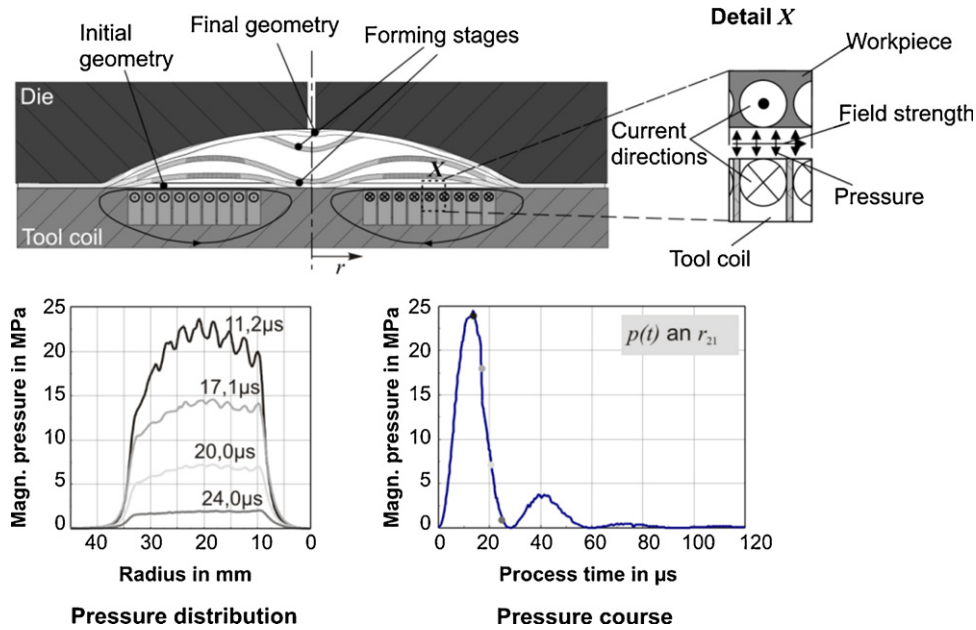

Fig. 12. Process principle of electromagnetic net-shape forming (Risch, 2009).

energy. Here, the losses can be attributed to heating of the workpiece due to eddy currents and to field energy that is not exploited. Daube et al. (1966) mention a total efficiency of the electromagnetic forming process in the range of 10–40%.

Bühler and Bauer (1968a) consider the mechanical energies in the system (i.e. the kinetic energy and the forming energy) in order to determined the material strength for the process-specific high strain rates. For this purpose the time-dependent trajectory of the kinetic energy, the forming energy, and the accumulated mechanical energy is determined.

This idea is partly resumed in Psyk et al. (2007). Here, the energy transfer is regarded, focusing on its effect on the forming result. The capacitor charging energy E_c is transferred into a magnetic pressure pulse p. This magnetic pressure pulse in turn is transferred into kinetic energy E_{kin}, which is reflected in the velocity distribution of the workpiece and into forming energy E_{def}.

At the moment, when the pressure has decreased to zero, the kinetic energy stored in the workpiece is available in order to finish the forming process. In a free forming operation the process ends as soon as the kinetic energy is completely transferred into deformation energy.

In the case of tube compression of light metals (aluminum or magnesium alloys), the kinetic energy is typically not sufficient to continue the deformation. Beerwald (2005) states that the deformation is usually completed during the first half wave of the coil current and the magnetic pressure, respectively, in these cases. In contrast during the compression of metals with higher densities (steel or copper) and in the case of sheet metal forming, the deformation period can be significantly longer than the pressure pulse. An example of such a case is presented in Bauer (1969).

When forming into a die or onto a mandrel, the workpiece is suddenly decelerated as soon as it hits the form defining tool. In

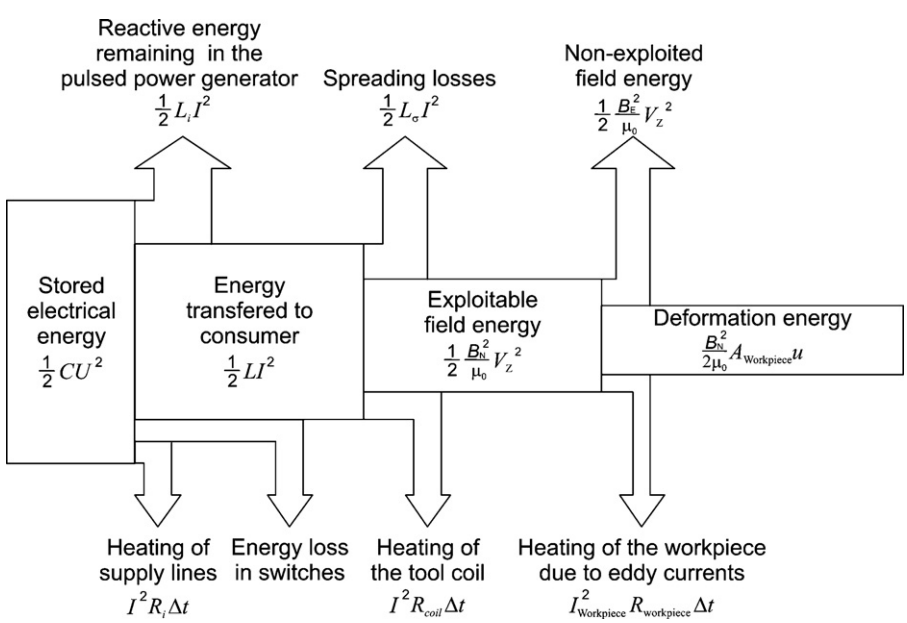

Fig. 13. Energy transfer during electromagnetic forming (Daube et al., 1966).

Table 2
Typical efficiencies for different electromagnetic forming applications.

Technological application									
Compression			Expansion				Sheet metal forming		
Free compression	Compression to an insulated mandrel	Compression to a conductive mandrel	Free expansion	Expansion in an insulated die	Expansion in a conductive die	Hole punching	Faces bending	Forming	Hole punching
10–25 Efficiency in %	4–8	2–4	10–25	6–10	4–8	2–4	4–8	3–4	2–4

this case the remaining kinetic energy in the workpiece has to be absorbed by the form defining tool in the area of contact. If this transfer and dissipation cannot be entirely guaranteed, especially in sheet metal forming the remaining energy in the workpiece can cause further undesired deformations, resulting in the so-called rebound of the workpiece, which is analyzed in Risch et al. (2004). On the other hand the remaining kinetic energy in those areas where the desired shape of the workpiece is not yet achieved, must be sufficient to complete the forming task. Otherwise an insufficient form filling results.

A quantitative analysis of the energy transfer during electromagnetic sheet metal forming into a die is presented in Risch (2009) on the basis of two exemplary forming tasks. In the first forming task an aluminum sheet is formed into a die with a spherical cavity. Here, electrical efficiency describing the quality of the transfer of capacitatively stored energy to inductive energy in the tool coil is 65%. The mechanical efficiency, describing the transfer of inductive energy to forming energy is 36%. The total efficiency of the process is 23%. Contrary, in the second example, which considered the forming of an aluminum sheet into a conical die, only 25% of the applied charging energy was transferred into coil energy. However the mechanical efficiency was 81%, so that the overall process efficiency was determined to 28%. The high mechanical efficiency is attributed to the high workpiece velocity during this forming operation and the resulting high kinetic energy. In comparison, Klocke and König (2006) noticed that the efficiency of the deep drawing process is typically in the range of 50–70%, whereby lower values are achieved for cups with a small wall thickness while in the case of cups with thicker walls higher efficiencies are possible.

The process efficiency calculated in Risch (2009) is significantly higher than values stated in earlier publications. For example in Bauer (1969) for an exemplary tube compression process using a multiturn coils wound from spring steel, an efficiency in the range of only 2% is stated. Typical efficiencies for different applications as calculated in Kuchinski (1973) are listed in Table 2.

Thus, it can be concluded that depending on the special forming example and the applied tools, the achievable efficiency can differ dramatically.

3.4. Electrical conductivity of the workpiece

As known from the literature, the electromagnetic forming process is suitable for materials with a high electrical conductivity. Therefore, aluminum as well as copper alloys are very applicable. von Finckenstein (1967) found that the maximum amplitude of the magnetic pressure is nearly proportional to the square root of the electrical conductivity. Furthermore, the smaller the electrical conductivity of the workpiece, the more energy will be transferred into joule losses. This effect can be detected by an increase of the workpiece temperature as shown in Al-Hassani et al. (1967). Therefore, a high electrical conductivity is essential in order to achieve a high transmission of power with only small losses. According to Wilson (1964) the electrical conductivity should not be smaller than 6.6 MS/m, so that useful results can be produced. An excerpt of materials with the corresponding electrical conductivity is given in Table 3.

In the case of a comparably low electrical conductivity of the workpiece, e.g. when forming steel, the magnetic field penetrates the workpiece very fast. This effect is shown in Fig. 14. It can clearly be seen that in case of the highly conductive workpiece material (Al99.5) the magnetic pressure is focused to the area of the coil winding and here especially to the gap between tool coil and workpiece and the surfaces of these to components. The density of the field lines and the strength of the magnetic field are significantly stronger than in case of the lower conductive material (DC06). Hence, the lower electrical conductivity of the workpiece causes a comparably small magnetic pressure, although all other parameters are kept constant.

Birdsall et al. (1961) describe another effect related to the penetration of the magnetic field: If the workpiece is formed against an electrically conductive die or joining partner the penetrated magnetic field can cause eddy currents in this component and consequently a counter pressure can occur which decelerates the workpiece deformation. As a result the process efficiency is decreased and formation of a joint and complete filling of a die cavity can be prevented. This effect is more pronounced if the electrical conductivity of the die or joining partner is higher than the conductivity of the workpiece. Apart from the electrical conductivity the penetration also depends on the thickness of the workpiece and on the parameters of the discharging process. Here, especially the frequency is relevant (compare Eq. (7). Therefore, Belyy et al. (1977) state that the minimum thickness of the workpiece depends on this penetration effect.

The penetration of the magnetic field through the workpiece can be retarded by applying a conductive layer on the workpiece or by using a driver, so that the forming behavior of these workpieces can be improved. Weimar (1963) suggests the use of a copper layer as a driver, which might be galvanized or cladded. Tillmann et al. (2008) introduce a thermal sprayed layer to enhance the electrical conductivity of the formed workpiece, whereby in Tillman et al. (2005) other coating processes are used to create a conductive layer.

With regard to the forming of steel like the typical deep drawing steel DC06, apart from the lower electrical conductivity also the permeability is a frequently discussed subject. However, according to Pfestorf and Wiznerowicz (1964) within the analysis of ferromagnetic materials, the material permeability can be set to 1, because for the representative inductances in the range of 10 T to 100 T saturation is achieved.

Table 3
Electrical conductivity of selected materials according to Ruge and Wohlfahrt (2007).

Material	Electrical conductivity	Material	Electrical conductivity
Silver	62.5 MS/m	AlMg3	18 MS/m
Copper	59.8 MS/m	Brass	15.9 MS/m
Gold	43.2 MS/m	DC06	7.94 MS/m
Al99,5	34 MS/m	Stainless steel	2 MS/m
Magnesium	22 MS/m	Titanium	1–2 MS/m
EN AW-5182	19 MS/m		

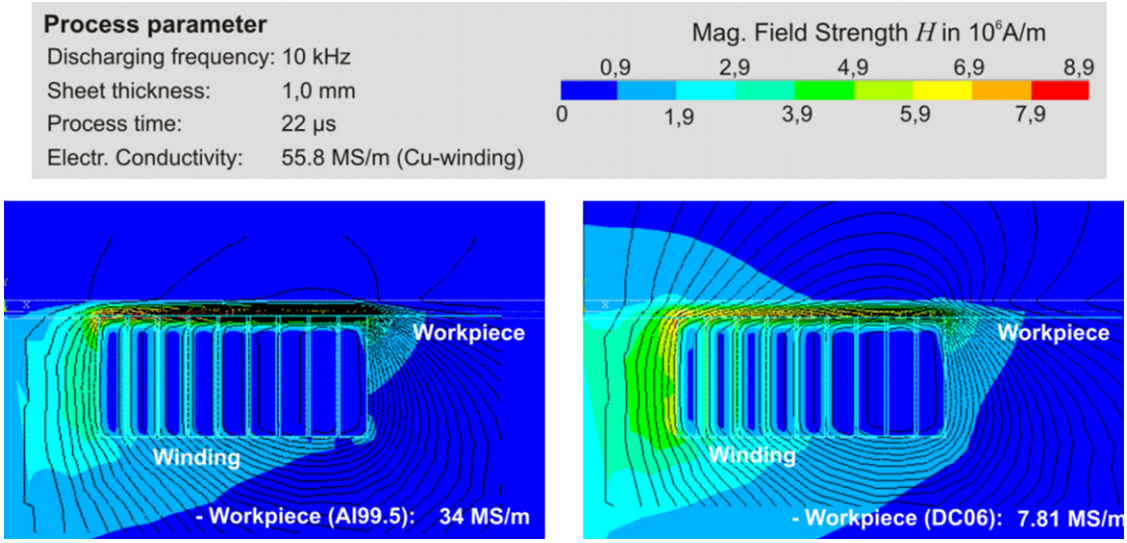

Fig. 14. Distribution of the magnetic field for a high electrically conductive workpiece (left) and a low electrically conductive workpiece (right) (Risch, 2009).

4. Material behavior at high strain rates

During electromagnetic forming, high strain rates and elevated temperatures are achieved. Therefore, a physical, coupled understanding of these effects is required to characterize the material behavior for numerical simulations and analytical modeling.

Over the years it has been shown several times that the forming behavior of some materials can significantly differ from the quasistatic forming behavior if high forming velocities are applied. Hu and Daehn (1996) point out that the earliest report about strain rate sensitivity of materials is Clark and Wood (1950). These authors state that the ductility of specimens loaded in dynamic tensile tests is higher than in the case of quasistatic experiments. Bühler and Bauer (1968a) state that the flow stress in electromagnetic forming is higher than the conventional quasistatic flow stress. The authors conclude that for copper as well as for steel (St35) an increase of the strength occurs for strain rates of 100 s^{-1} or more. Quantitative values for the flow stress are determined, but the temperature influence could not be separated from the strain rate influence, here. Dietz and Hammann (1975) also mention a change of the material flow behavior. According to these authors, in the dynamic forming process the flow stress is usually increased and the ductility is decreased, but they admit that due to the challenges considering the measurement technique at that time no reliable quantitative data existed. Meanwhile, this topic has been investigated by different authors leading to the conclusion that depending on the material an increase or a decrease of the ductility can be observed. An increase was reported, e.g.

- for interstitial free iron in Balanethiram and Daehn (1992),
- for copper in Balanethiram and Daehn (1994),
- for high strength steels in Meyer et al. (1981),
- for aluminum alloys 6061-T4 and 5754 in Golovashchenko (2007),
- for stainless steels in Wood (1967),
- for Tantalum in Gianotta et al. (1985),
- for titanium alloys in Takeda and Kobayshi (1990),
- for the aluminum alloy EN AW 7075 in El-Magd and Abouridane (2004), and
- for some magnesium alloys including cast alloys as AZ80 in El-Magd and Abouridane (2004) and wrought alloys as AZ 31 and ZEK 100 in Psyk et al. (2006a).

For the titanium alloy Ti–6Al–4V with increasing strain rate at first an increase and then a decrease is reported in El-Magd and Abouridane (2004).

This strain rate effect on the flow stress (σ) can be incorporated into the constitutive model for the material by including a strain rate ($\dot{\varepsilon}$) term and strain rate sensitivity (m) exponent into the power hardening law of the material:

$$\sigma = C\varepsilon^n \dot{\varepsilon}^m \tag{29}$$

where C is the strength coefficient and n is the strain hardening exponent. The C, m and n values are material parameters and therefore affected by parameters such as alloying elements. For example, Lindholm et al. (1971) compare strain rate sensitivity parameters of pure aluminum as well as several aluminum alloys with the results of different scientists. A summary is given in Fig. 15. The diagram shows that the strain rate dependency decreases with the degree of alloying. Note that these tests were conducted at strain rates on the order of 1 s^{-1}, which are significantly less than those observed in electromagnetic forming.

In addition to strain rates, temperature affects the forming behavior of metals with increases in temperature decreasing the flow stress and increasing the elongation or strain at failure through activation of additional slip systems in the material for dislocation motion. This is of interest due to the adiabatic nature of the high

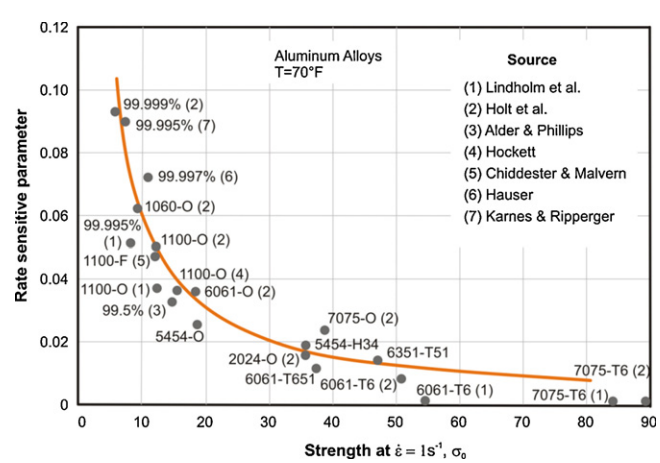

Fig. 15. Strain rate sensitivity of different aluminum alloys according to Lindholm et al. (1971).

speed forming process as the forming heat cannot be transferred in a short time scale. Consequently, the material will be heated and soften resulting in a decrease of the flow stress. Furthermore, at high strain rates (in contrast to low strain rates in superplastic forming), the deformation will be localized at weak locations in the material. Shear bands will be generated, leading to the specimen finally failing as discussed in Abouridouane (2005). The transfer from the isothermal to the adiabatic behavior of the process with high strain rates was described already in the 1940s Zener and Hollomon (1944). Vohnout and Daehn (2002) have clarified the thermal influence caused by the occurring Joule losses (i.e., resistive heating) in the workpiece (estimated to be 320 C). Thereby an increased fracture strain was determined for the specimens, which are heated by the induced eddy currents in the workpiece.

Constitutive material laws have been developed based on experimentally determined results, which can be used as input data in finite element simulations (see Emde et al., 2006; El-Magd et al., 2003) and analytical models. One model used to relate σ, ε, $\dot{\varepsilon}$, and temperatures is the Johnson–Cook (J–C) model:

$$\sigma = (A + B\varepsilon^n)(1 + C\ln\dot{\varepsilon})\left(1 - \left(\frac{T - T_0}{T_m - T_0}\right)^m\right) \tag{30}$$

where A, B, and C are material constants; T is the temperature; T_0 is a reference temperature (e.g. room temperature), and T_m is the melting temperature of the material. A shortcoming of the J–C model is the inability to represent variations of flow stress with strain rate. Lesuer et al. (2001) evaluated the strain rates due to discrete obstacle controlled plasticity and drag controlled plasticity, which are both related to theoretical dislocation motion through the lattice structure during deformation. More accurate predictions of flow stress based on the strain rate induced (experimentally from 10^{-4} to $10^4\ s^{-1}$) were obtained.

An additional concern with empirical models such as the J–C to characterize the deformation behavior is that the material parameters are only constant for a relatively small range of ε, $\dot{\varepsilon}$, and T values. Thus, a theoretical approach where a specific range of process parameters is considered would be advantageous. El-Magd and Abouridouane (2006) created a constitutive relationship for "damping controlled deformation at high strain rates" which would be applicable for electromagnetic forming operations:

$$\dot{\varepsilon} = \dot{\varepsilon} * \left\{\exp\left[-\frac{\Delta G_0}{kT}\left(\beta_0 T + \ln\left(\frac{\sigma *}{\sigma_0 *}\right)\right)\right] + \frac{\xi}{\sigma - \sigma_h}\right\}^{-1} \tag{31}$$

where * indicates the thermally activated strain and stress components, ΔG is the activation free enthalpy, and k, ξ, and β_0 are material parameters. With additional terms, their model was effective at modeling deformation over a large range including transition between three specified regions with respect to σ, $\dot{\varepsilon}$, and T.

Additional material modeling efforts by Zerilli and Armstrong (1987) included microstructural terms in the constitutive relationship. For a fcc material with a two-phase structure:

$$\sigma = \sigma_g + c_2\varepsilon^{0.5}\exp(-c_3 T + c_4 T\ln\dot{\varepsilon}) + kd^{-0.5} \tag{32}$$

and for a bcc material:

$$\sigma = \sigma_g + c_1\exp(-c_3 T + c_4 T\ln\dot{\varepsilon}) + c_5\varepsilon^n + kd^{-0.5} \tag{33}$$

where k is the microstructural stress intensity, d is the average grain size diameter, and σ_g (which is dependent on the initial dislocation density and solute elements) and $c_{1\text{–}5}$ are material constants. Majta et al. (2003) demonstrated the usefulness of this material model for the dynamic loading of niobium–microalloyed steel. Furthermore, Husson et al. (2003) incorporated microstructural effects into a continuum damage model. The flow stress was determined by summing an athermal term and a temperature and strain rate dependent term. Results provided accurate results for OFHC copper under both quasi-static and dynamic loading.

In addition to Eqs. (30)–(33), other relationships have been developed by researchers to model the material behavior during electromagnetic forming conditions (Song et al., 2001; Rusinek et al., 2005; Domblesky et al., 2005). Experimental validation of such constitutive models is difficult to achieve due to the high strain rate and temperature conditions required. However, adequate representation of the material response has been achieved.

Finally, note that failure in sheet metal forming is often predicted in industry based on the strain-based forming limit diagram (i.e. a plot of in-plane major and minor failure strain values for various deformation paths). In Golovashchenko (2007), the EMF and quasi-static forming limit curves (FLCs) were nearly identical when forming into an open die. However, when forming into a conical or V-shaped die, the FLC shifted upward significantly (approximately 15% to 30% with respect to the major strain value). This effect is attributed to the hydrostatic stress and bending/unbending due to the impact with the die and the varied deformation in EMF (Imbert et al., 2005). Thomas and Triantafyllidis (2007) used a Marciniak–Kuczynski model to theoretically predict failure using this strain based approach in EMF, which included material property variations based on the electrical current induced in the process. The upward shifting of the FLCs with respect to n, m, temperature, and current density were provided. Analytical results from this model were compared to experimental measurements in Thomas et al. (2007).

5. Equipment for the electromagnetic sheet metal forming process

As known from conventional forming processes, also in the case of electromagnetic forming the applied equipment significantly influences the forming process and the achievable forming result. Essential components of this equipment are the forming machine (pulsed power generator) and the tool coil including a fieldshaper if applicable, as well as potential form defining tools, an assembly fixture and component transportation devices (Bertholdi and Daube, 1966). However, von Finckenstein (1967) emphasizes that in contrast to most conventional forming operations in the case of electromagnetic forming not only the geometric and mechanical properties but also the electrical parameters are crucial and need to be adapted to the planned forming task.

5.1. Pulsed power generators for electromagnetic forming

Since in electromagnetic forming high electrical energies are required in a very short time, energy storage is necessary. Kapitza (1924) declared that considering a condenser battery, though it is the most obvious solution for storing energy in order to build up a magnetic field, it is extremely difficult to store sufficient energy to induce a very strong magnetic field. Therefore, he decided to use chemical storage. However, Furth and Waniek (1956) show that a capacitative storage is the most economic solution considering the energy level typically required in electromagnetic forming. Therefore, already in machines from the 1960s and in modern pulsed power generators as well a capacitor bank is the typically used for this purpose. Bertholdi and Daube (1966) mention that the first commercially available forming machine, the Magneform Model 1 was presented by the General Dynamics Corporation, San Diego, CA, USA in 1961. The typical machine physically consists of:

- the capacitor bank,
- high current switches,

- the charging unit including a high voltage source, a charging switch, and a short-circuiting device,
- the energy transfer system carrying the energy from the capacitor to the tool coil (the busbar), and
- control devices.

According to Belyy et al. (1977) the capacitor bank must have a low self-inductance and has to stand a high number of pulse discharges. Furthermore, it should be minimum weight, dimensions, and depreciation deductions for one process operation. Characteristic parameters of the capacitor bank are the capacitance C as well as the maximum allowable charging voltage U_{max}. These two values determine the maximum allowable capacitor charging energy $E_{c,max}$. Aspects to be considered when choosing these characteristics are also described in Belyy et al. (1977). Bauer (1980) states that the allowable voltage of the machine should be as high as possible for economic reasons. At the same time a high voltage allows minimizing the machine dimensions as stated by Löschmann et al. (2006). However, due to limitations considering the insulation, a voltage in the range of 20–25 kV is a maximum value. For forming small components according to Al-Hassani et al. (1967) machines with a maximum charging energy in the range of 6–20 kJ are common. The biggest machine reported in literature had a maximum charging energy of 240 kJ and was used for forming and embossing of large parts for the Saturn-V-moon-rocket (Schwinghammer, 1966).

The charging of the capacitor bank can be realized via a suitable high-voltage-constant-current-power supply or via an invariant voltage source supply. However, the constant current supply is more efficient while the constant voltage supply is simpler and therefore cheaper (Belyy et al., 1977). The discharge via the tool coil is triggered by the discharging unit and the high-current-switch, respectively. One of the first publications dealing with high current switches is Kapitza (1924). Daube et al. (1966) indicates that in pulsed power machines for electromagnetic forming the switches must be able to discharge extremely high currents (in the range of 10^4 A) in a very short time (less that 10^{-7} s) synchronously. Possible technological solutions that can be applied are spark-gap switches (Weimar, 1963), ignitrons (Davies and Austin, 1970), thyratrons (Harvey and Brower, 1962) or vacuum and different air three-electrode dischargers and various two-electrode mechanical switches. The design of some exemplary solutions is depicted in Belyy et al. (1977). Löschmann et al. (2006) indicate that spark-gap-switches require intensive maintenance while ignitrons in fact are maintenance free, but hold a safety risk due to the quicksilver-cathode. Therefore, especially over the last years the development of reliable semi-conductor switches able to switch the process-specific high power has been sought (see Welleman and Fleischmann, 2006). Löschmann et al. (2006) apply such switches are, e.g. in a 100 kJ machine.

In order to provide a powerful machine, a low inner inductance L_i is required (Lange, 1993). The (natural) inductance of a short circuited pulsed power generator represents a lower limit considering the inductance of the complete resonant circuit, because adding a load (i.e. a tool coil, fieldshaper, and a workpiece) will cause a rise of the inductance and the resistance of the resonant circuit in any case. Thus, in order to achieve a maximum possible flexibility considering the adaptation of the current course via a corresponding design of the tool coil, the inductance and resistance of the machine should be as low as possible. According to von Finckenstein (1967) this can be achieved via paralleling of capacitors, switches and supply lines. Moreover, the length of the wires should be chosen as short as possible and wires of especially low specific resistance and inductance (coaxial cables) are favorable. In Golovashchenko (2007) a numerical example is given. Golovashchenko states that by using three coaxial cables with a length of 1.5 m each and connecting them in parallel, the efficiency of the connection can be improved by a factor of 6 compared to using a 3-m-long conventional one-cable connection of the applied Magnepress system with the coil. Considering the choice of the cables the forces between the inner and the outer conductor resulting from the high currents have to be considered. The maximum allowable current in a serial application, for which plastic deformation can be avoided, depends on the strength and the diameter of the outer conductor as well as on the strength of the cable coating as shown in Römheld et al. (2008).

5.2. Tool coils

The coil is the actual tool of the electromagnetic process and analogous to conventional forming processes it needs to be adapted to each specific forming task. The major task of the tool coil is conducting the current and consequently establishing a suitable temporary course and local distribution of the magnetic field and pressure. According to Belyy et al. (1977) it must also provide:

- A high conversion coefficient of the capacitor bank energy to the work of the workpiece deformation.
- High mechanical resistance.
- Optimal frequency of the discharging current.
- Resistance to electrical over-voltages.
- A reliable connection to the machine.
- A simple design performance.

Therefore, the design of the geometry is as important as the consideration of the mechanical characteristics, i.e. especially the strength, and the electrical properties, i.e. inductance and resistance, for the dimensioning of a tool coil.

In the case of tube compression and expansion typically cylindrical coils are used, so that the geometry can be parameterized by the length and diameter of the winding and by the pitch of the coil (i.e. the number of turns per unit of length), which is related to the cross-section of the single turn. Furth et al. (1957) specify 4 different types of cylindrical coils: single-layer single-turn coils, single layer multi-turn coils (helix), multi-layer multi-turn coils (bobbin) and multi-layer single-turn coils (spiral). These are illustrated in Fig. 16.

While the helix coil is usually used for tube compression or expansion processes, the spiral coil type, which is often called pancake-coil, is typically applied for forming rotationally symmetric sheet metal components. However, as shown, e.g. in Daehn et al. (2000) the scope of possible winding geometries for tool coils for the electromagnetic sheet metal forming is much wider. It includes different coils for forming oblong geometries as a tridental coil geometry (Vohnout, 1998), ellipsoidal (Conraux et al., 2006), superellipsoidal geometries (Psyk et al., 2004a), meander-shaped (Furth and Waniek, 1962), square (Uhlmann et al., 1999) and rectangular (Golovashchenko et al., 2006a) geometries and many more.

Although in connection with electromagnetic sheet metal forming, often the term flat coil is used, the process is not limited to the forming of flat sheets but it can also be used in order to process three-dimensionally preformed components which have been produced, e.g. by deep drawing as described in Vohnout (1998). In these cases the surface shape of the coil needs to be adjusted to the workpiece geometry in order to guarantee a small gap width between the tool coil and workpiece. An example of such a three-dimensionally curved tool coil is shown in Vohnout (1998). A more detailed description of a coil setup for a similar forming task is given in Psyk et al. (2007).

Considering the strength and – related to this – the durability of a tool coil it needs to be considered that according to the third Newton axiom "*actio = reactio*", the forces required in order to achieve

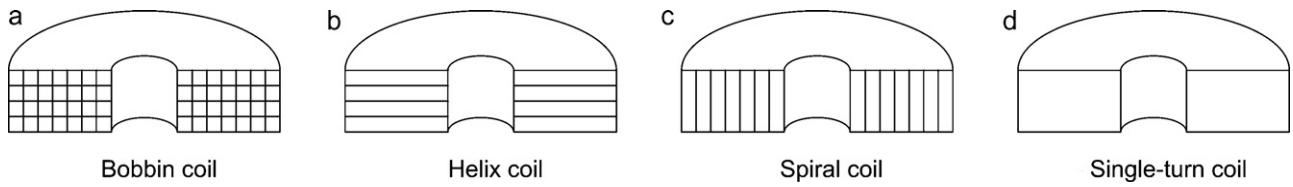

Fig. 16. Basic toroidal coil types (Furth et al., 1957): a) the bobbin; b) the helix; c) the spiral; d) the single-turn coil.

the desired deformation of the workpiece act also as so-called reaction forces on the tool coil in the opposite direction. The tool coil has to absorb these reaction forces as well as forces between the separate turns of the winding without any deformation (Bauer (1973). Seen from the mathematical point of view it is possible to design so-called force-free coils, but as shown in Dicke (1968) a practical realization of these concepts is not possible. Pioneer work in the field of the coil development was done by Furth and Waniek (1956), who defined several approaches to estimate the reaction forces.

Especially in the case of expansion coils and flat coils depending on the distance between the tool coil and workpiece, different load cases can occur as shown in Fig. 17 for a typical pancake coil and in Tekkaya et al. (2007) for an expansion coil.

In contrast to tube compression processes, for these two process variants the desired forces can only be established if an electrically conductive workpiece is positioned close to the coil winding so that the magnetic field and accordingly the force is concentrated in the gap between the workpiece and tool coil. This is the desired load case and the tool coil has to be designed in such manner that this force can be endured. Without a workpiece in direct proximity to the tool coil the magnetic field is concentrated in the volume compassed by the turns and the major forces acting on the coil are vectored radially in the outward direction. These forces are higher the lower the volume compassed by the turns (i.e. the smaller the inner diameter of the coil is). Therefore, Belyy et al. (1977) states that for the electromagnetic expansion of tubes with a diameter that is smaller than 40 mm coils do not have sufficient mechanical strength so that the coil lifetime is only short. This load case is undesired. In order to enable a preferably small gap width between the tool coil and workpiece especially in the case of expansion coils, the armoring against such forces is marginal so that this load direction will lead to a reduced coil lifetime. By doing experiments without the workpiece, the tool coil is exposed to extreme loading conditions and defines an extreme case during the practical use. Since the distance between the tool coil and workpiece changes during the process the load case can vary depending on the course of the workpiece deformation. Thus, the load cases need to be well-known and considered during the coil design.

Besides the mechanical loading, there are the electrical as well as thermal loadings acting on the tool coil. Here, thermal loadings occur at high cycle times and by high discharge currents. High temperature increases can cause thermal fracture on components of the tool coil (e.g. winding, connectors, etc.) (Furth and Waniek, 1956; Furth et al., 1957).

In general there are two different approaches for designing a tool coil with regard to the acting loads. Most of the relevant literature dealing with coil development aims at designing durable coils, but according to Baines et al. (1965) especially for the manufacturing of prototypes also disposable tool coils (which are often referred to as single-shot coils) represent an interesting alternative. As it can be concluded from the feasibility study performed by Woodward et al. (2011), this topic is still relevant today.

Lange (1993) states that for a durable coil, a tool life of 10^6 pulses is desirable, but there exist only very few papers in the literature, which contain some information about the durability. In Daube and Borowski (1969) about 10,000 discharges are reported as a reference value concerning a wound compression coil made of stainless steel, whereby no mechanical or electrical fracture was detected. (No information about the loading conditions was given here.) In order to realize a coil lifetime in this magnitude, high strength and stiffness of the coil is required. Therefore, often massive coils with one single or only very few turns have been applied. For example, Schmidt (1976) designed a coil with a width of the turn of 100 mm for the electromagnetic compression of a tube of 100 mm diameter. Fischer (1983) suggests that the gap width between the single turns should not be smaller than 2 mm, and Golovashchenko (2001) suggests that the width of the turns should be at least 5 mm to guarantee the required stiffness.

On the other hand, the number of turns of the winding is crucial, because it significantly influences the resistance and the inductance of the coil and the coil workpiece unit, respectively. The product of the number of turns and the current flowing through the turns is a decisive parameter with regard to the achievable deformation, Bauer (1973). For coils with only a few turns, this parameter is certainly relatively low. Alternatively, Henselek et al. (2004) state that in the case of single turn coils and coils with very few turns the process efficiency is usually very low due to the extremely low inductance. Although according to Henselek et al. (2004) the efficiency of a multiturn coil is typically higher compared to single turn coils, von Finckenstein (1967) determines an efficiency of only 2% for his multiturn coil. He claims the Joule losses in the coil and the fieldshaper to be the major part of the energy losses. However, it needs to be considered here, that von Finckenstein (1967) uses a coil made of spring steel, which is of rather low conductivity. Thus, a significant improvement of the process efficiency is achievable when using coils and fieldshapers of a material of higher electrical conductivity as copper. To combine the strength and stiffness of a steel coil with the efficiency of a copper coil, von Finckenstein (1967) suggests using spring steel cladded with copper. Daube and Borowski (1969) state that copper beryllium alloy is an excellent material to realize the tool coil, because it offers a good compromise of strength and conductivity. This alternative is also tested in Schmidt (1976). Other materials that are recommended in Belyy et al. (1977) are zirconium and cadmium coppers, tungsten, and molybdenum. In order to guarantee an electrical insulation between the single turns of the winding, the coils are encapsulated with plastic materials. Here, Belyy et al. (1977) suggest using lavsan, ftoroplast and polymid films, mica, glasstextolite, epoxies and composites, as, e.g. glass fiber reinforced epoxy. Information about the characteristics of these materials as well as of the suggested materials for the solenoid are included in Belyy et al. (1977). Schmidt (1976) tested different plastic materials including glass fiber reinforced ones, but he rates all tested materials to be insufficient for a use in an industrial series production. Therefore, he suggests again the application of self supporting coils made of high strength material and realizing the electrical conductivity by a corresponding coating on the surface of the coil that faces the workpiece.

The general principle of separating the functions and fulfilling them by different components in the coil is still applied in today's coil construction in a slightly different form. In Beerwald (2003) it is suggested to use a highly conductive copper wire which can be thin and of low strength, because any deformation of this wire is

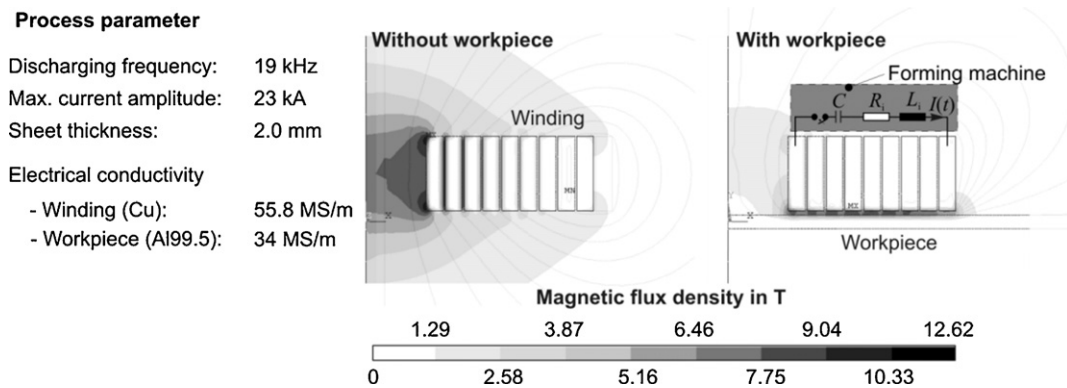

Fig. 17. Loading types acting on the tool coil according to Risch et al. (2008b).

prevented by a resin soaked fiber-matrix which acts as a kind of armoring of the tool coil. Alternatively, Kevlar fibers can be used as reinforcement, offering the essential advantages of an extreme high tensile strength (ca. 2900 MPa) and vibration-isolating properties. However, one disadvantage of the Kevlar fibers is the low thermal conductivity. In Beerwald (2003) it is further stated that such armoring is not necessary at that surface of the coil where the highest field strength occurs. (This is typically the surface facing the workpiece or the fieldshaper, respectively.) This design concept allows reducing the coil dimensions significantly while the efficiency is increased. For a series production it is possible to implement a cooling system. In the case of small pressures this can be, e.g. by means of air or water streamed capillary tubes while in the case of higher charging energies, heat transferring copper parts can be used as described in Beerwald (2003).

Apart from spooling an isolated wire, alternative manufacturing strategies especially for flat coil windings are cutting processes including milling (Bauer, 1967), laser- and jet cutting (Uhlmann et al., 1999), and eroding (Dicke, 1968). According to Golovashchenko et al. (2006a), windings which are produced by jet cutting feature higher stiffness and lower residual stresses in comparison to spooled ones. In Golovashchenko (2007) a detailed discussion of failure modes of flat coils is presented and conclusions for an improved coil design are drawn. Here, three different failure modes, shown in Fig. 18, are differentiated. The most important point with regard to failure is that a deformation of the coil is initiated in the central turn. According to Golovashchenko (2007) it occurs due to an expansion of the clearance between the first and second turns. Depending on the armoring, which is realized via an insulation block and a steel bandage, the deformation of the inner turns can lead to:

- an expansion of the bandage and fracture of the insulation block in case of a relatively weak bandage (compare Fig. 18a) or to;
- a telescoping effect. In this case the coil looses its flatness and the central turn deforms outside the original coil plane (compare Fig. 18b). Further use of such deformed coils lead to short circuit and mechanical failure.

As another important aspect with regard to coil failure, it is mentioned that the insulation thickness must not be smaller than the clearance between the turns, because otherwise the forces between the parallel turns cause a deformation of the coil as shown in Fig. 18c.

Moreover, it is advised to use micarta as insulation material, because experience has shown that it performs much better than insulation blocks made from delrin.

Concludingly, Golovashchenko points out that the strength of the coil is not defined by the strength of the material of the spiral, but it is mainly dictated by the reinforcement of the coil against the observed failure modes. He suggests improving coil lifetime using a high strength bandage made of steel and additionally implementing additional reinforcing elements Golovashchenko et al. (2006a). Again cooling channels for a liquid or gaseous fluid can be provided. A lifetime study considering an accordingly designed coil, presented in Golovashchenko et al. (2006b), has shown that even after 50,000 discharges no damage occurs.

In addition to the advantages mentioned above, coil windings produced by means of cutting feature an enlarged design freedom. These technologies represent, e.g. an easy method for producing winding geometries with locally varying width of the turns. According to Beerwald and Henselek (2003) this design strategy can be applied in order to locally adjust the magnetic pressure, which is proportional to the square of the magnetic field strength that in turn is proportional to the pitch of the coil. Locally increasing the width of the turns reduces the pressure and vice versa. This principle is introduced in Wolf (1974) for compression coils and transferred to flat coils in Beerwald and Henselek (2003). It is used for focusing the pressure to form an aluminum sheet into V-shaped die geometries in Psyk et al. (2004a) and to realize a specially contoured tube by electromagnetic compression in Psyk et al. (2006c).

Altogether, current investigations and publications dealing with coil design mainly focus on flat coils. Bauer (1973) already stated that the development of compression coils could be finished. Nevertheless there is still ongoing work, whereby especially the development of separable compression coils, required, e.g. for joining of closed frame structures is addressed. With regard to this specific problem Auerswald (1968) suggests assembling the turns of the coil winding from several parts which intertwine via a dovetail joint. In Deeg (1967) it is suggested to use the magnetic field outside a cylindrical coil for compressing the workpiece which is positioned outside the tool coil (compare Fig. 19).

In order to bring the magnetic field to the workpiece, a so-called transducer is used. In principle this is a special fieldshaper, which encloses the tool coil and the workpiece each with a part of its surface. In order to close the current path the segments of the transducer are connected electrically with each other. In order to avoid welding effects, current densities have to be controlled in the connecting area. Therefore, the shape and the contact elements in this zone are crucial. In order to avoid or reduce the forces in the contact zone Beerwald and Henselek (2005) suggest that U- or V-shaped contact sheets can be applied in such a manner that the magnetic pressure bends the elements up and thus increases the contact pressure. A practical implementation of this concept is presented in Henselek et al. (2004).

An alternative approach for a realization of a separable tool coil is suggested in Golovashchenkon et al. (2005). A practical implementation of the coil is presented in Golovashchenko (2006) and shown in Fig. 20. The coil consists of two independent multi turn windings connected in series—each mounted in its own shell. Both

Fig. 18. Failure of a flat coil according to Golovashchenko (2007): a) failure by fracture of the insulation block; b) failure by a telescoping effect; c) failure by turn deformation due to insufficient insulation thickness.

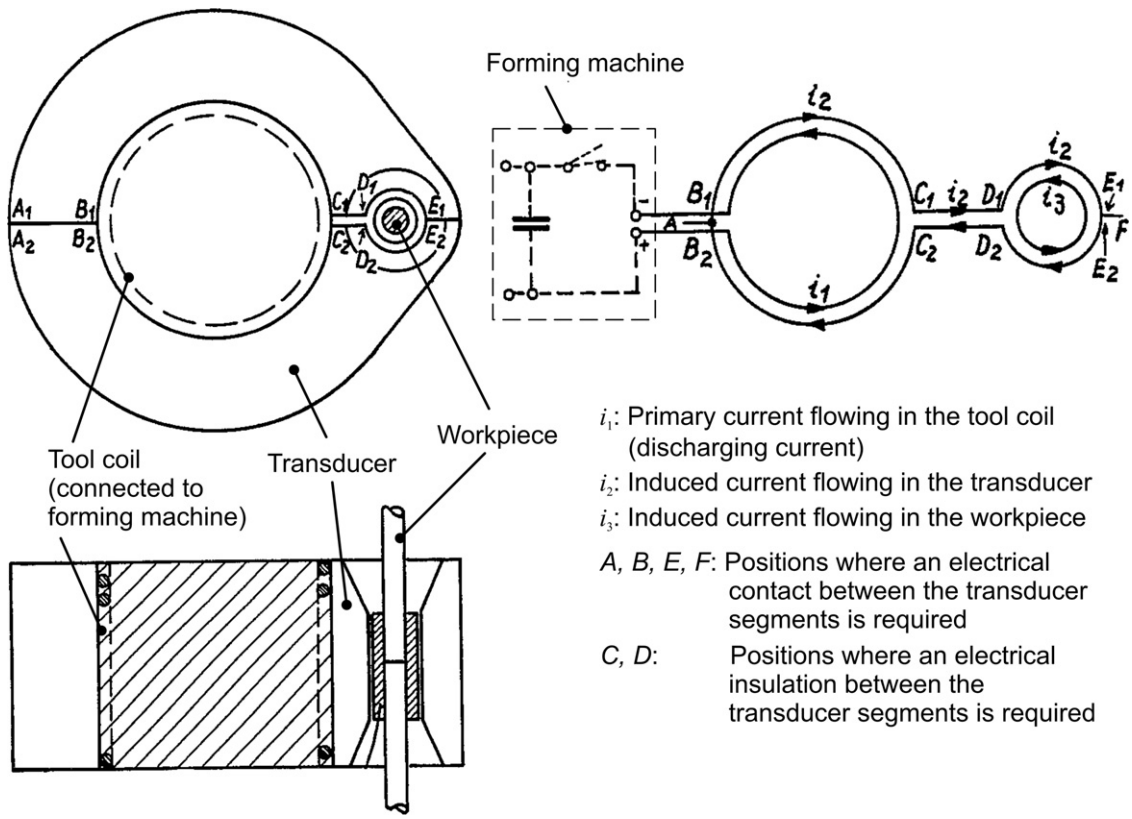

Fig. 19. Principle sketch of an openable tool coil according to Deeg (1967).

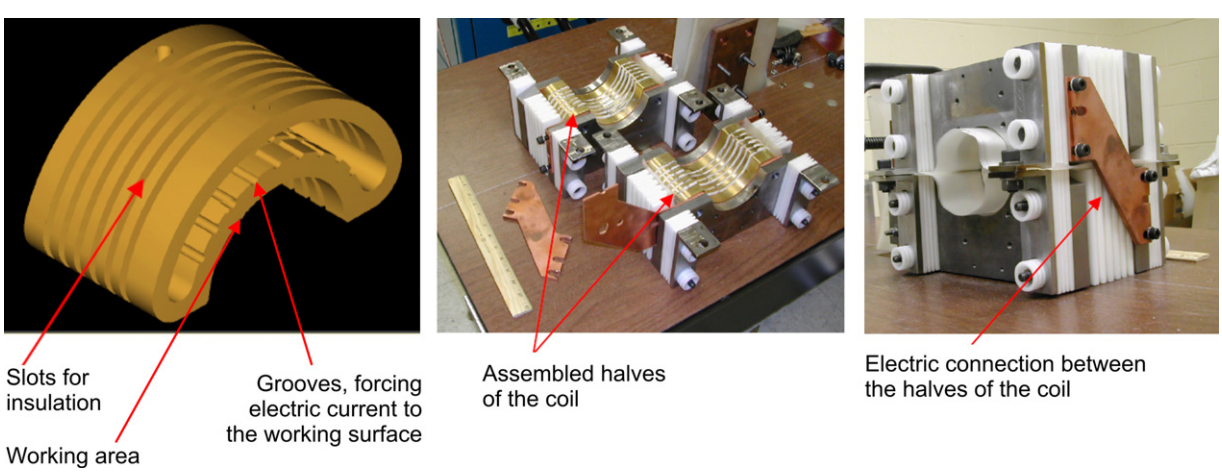

Fig. 20. Openable tool coil according to Golovashchenko (2006).

windings feature a concave work zone with the shape of a tubular component. They are positioned in such a manner that the two work zones enclose the workpiece and thus form a closed loop. The major advantage of this coil variant is that electrical contacting of the winding segments is not required.

Similarly, Uhlmann et al. (2007) suggested using at least two independent coil segments, which are arranged at the circumference of the workpiece. However, in this approach the single segments are similar to coils with spiral winding geometry and a three-dimensionally shaped surface, which are used in electromagnetic forming of three-dimensionally curved sheet metal components. Here, again no electrical contact between the coil segments is required, but compared to a conventional compression coil the pressure distribution along the circumference features significant inhomogeneities. However, according to Uhlmann et al. (2007) this concept was realized and successfully applied for joining closed frame structures.

5.3. Fieldshaper

The principle requirements to be made on a fieldshaper are similar to those which need to be considered when designing a tool coil. Here, again the major task is the application of a suitable magnetic pressure. At the same time a long lifetime is desired. So, on the one hand, an efficient energy transfer to the workpiece is required and, on the other hand, the fieldshaper has to be able to bear high mechanical loads. As shown in Neubauer et al. (1988) a compromise has to be made considering these two criteria. In Fig. 21 an overview about different fieldshaper designs and their specific advantages and disadvantages is given.

In many sketches the fieldshaper-surface facing the tool coil is frequently even, but as shown, e.g. in Tikhonovich et al. (1974) it can also feature recesses in which the windings of the coil are directly integrated. This design variant is applicable for sheet metal forming (compare Fig. 6) as well as for tube compression processes. An approach to calculate inductors with such fieldshapers depending on a given maximum strain, a given speed of impact with the die, a given magnetic field intensity in the operating gap, or a given work of deformation of the workpiece is suggested in Belyy et al. (1977). According to Tikhonovich et al. (1974) the major disadvantage of such a fieldshaper is that axial forces act on the windings in the recesses, which are not balanced in the area of the radial slot. Consequently the winding fails in this area early. In order to counteract this effect Tikhonovich et al. (1974) suggest implementing current conducting inserts, which are insulated from the fieldshaper, in order to bridge the radial slot as shown in Fig. 22. Minimum dimensions that should be kept in mind when designing such a fieldshaper are given in Belyy et al. (1977). Apart from aspects related to the mechanical strength also the heating of inductor in a series production and according requirements considering the cooling of the tool are regarded here.

In contrast to direct acting tool coils in the case of a fieldshaper, additional forces in the circumferential direction occur, because in the axial gap a high magnetic field is induced and consequently a high magnetic pressure results. Especially in the case of asymmetric fieldshapers, i.e. such fieldshapers with a concentration area not located in the center plane, high mechanical loads result so that the fieldshaper should be made of a high strength material and the dimensioning should not be chosen too small (Wolf and Meinel, 1972). With regard to the efficiency of the energy transfer, a material of high electrical conductivity should be chosen, so that here again, a compromise between the requirements considering the strength and considering the conductivity has to be found. Frequently used materials are copper and copper-alloys, aluminum and aluminum alloys, brass and bronze.

With regard to the geometry of the fieldshaper it should be considered that the overall length of the fieldshaper should be adjusted to the coil length. If the fieldshaper is shorter than the tool coil an inhomogeneous loading of the coil occurs which will finally lead to a reduced coil lifetime. If the fieldshaper is longer than the tool coil the energy transfer is of lower efficiency. Dietz et al. (1967b) noticed that the concentration area should not be too short, because otherwise the magnetic field will penetrate it and the required magnetic pressure cannot be built up. The length should not fall below a value of three times the skin depth.

Beerwald (2005) investigates the influence of the fieldshaper geometry on the force distribution by means of a two-dimensional FE-analysis. It is shown that compared to a direct acting tool coil, applying a fieldshaper with cylindrical geometry in the concentration area leads to a more homogeneous distribution of the magnetic field and consequently of the pressure, in which the single turns of the coil cannot be identified any longer. The reason for this is the homogeneous distance between workpiece and fieldshaper. However, this is not valid for those areas where the fieldshaper features axial slots. As a result of this geometric inhomogeneity a local reduction of the magnetic field and the forces occurs, which is more significant, the wider the slot is.

Moreover, Beerwald (2005) points out that the geometry in the concentrating area characterized by the depth and the length of the step significantly influences the acting forces. In addition a defined field and force distribution can be adjusted by a contouring of the fieldshaper, which results in a target-oriented modification of the gap between workpiece and fieldshaper. Here, already very small modifications in the range of some tenths of a millimeter affect the force distribution considerably. According to Beerwald (2005) such a contouring can be exploited in order to manufacture different workpiece contours and in order to influence the trajectory of the forming process.

5.4. Form defining tools

In electromagnetic sheet metal forming it is frequently necessary to apply a form defining tool – a so-called die – in order to establish the desired workpiece geometry. During the deformation the workpiece ideally aligns to this tool and copies its shape. The same concept can also be applied when forming tubular semi-finished parts. In the case of electromagnetic expansion the die surrounds the workpiece while in the case of electromagnetic compression the form-defining tool – typically called mandrel – is positioned inside the specimen.

Due to the high forming velocity, Romanovskiy (1971) claims that it is necessary to provide holes in the die in order to provide that the air exits the cavity. He also gives special advice about the positioning, the size and the shape of these holes.

According to Daube et al. (1966) and Neubauer et al. (1989), in high speed forming processes form defining tools can be made of different materials as, e.g. reinforced concrete, wood, hard plaster or steel. Weimar (1963) mentions that dies and mandrels respectively made of plastic, Bakelite or wood can be used in the case of electromagnetic forming. According to Romanovskiy (1971) the productivity, the type of operation, the geometry, and the shape of the workpiece as well as its material properties and the depth of penetration of the magnetic field in the workpiece are important aspects that need to be considered when choosing the die material. Considering the last point the electrical conductivity of the die material can be decisive with regard to the achievable forming result. Especially if the electrical conductivity of the workpiece is low and the penetration depth of the magnetic field is accordingly high, the workpiece deformation can be damped due to a counter pressure created by the magnetic field between the die and the workpiece. Additionally, the surface quality can be deteriorated due

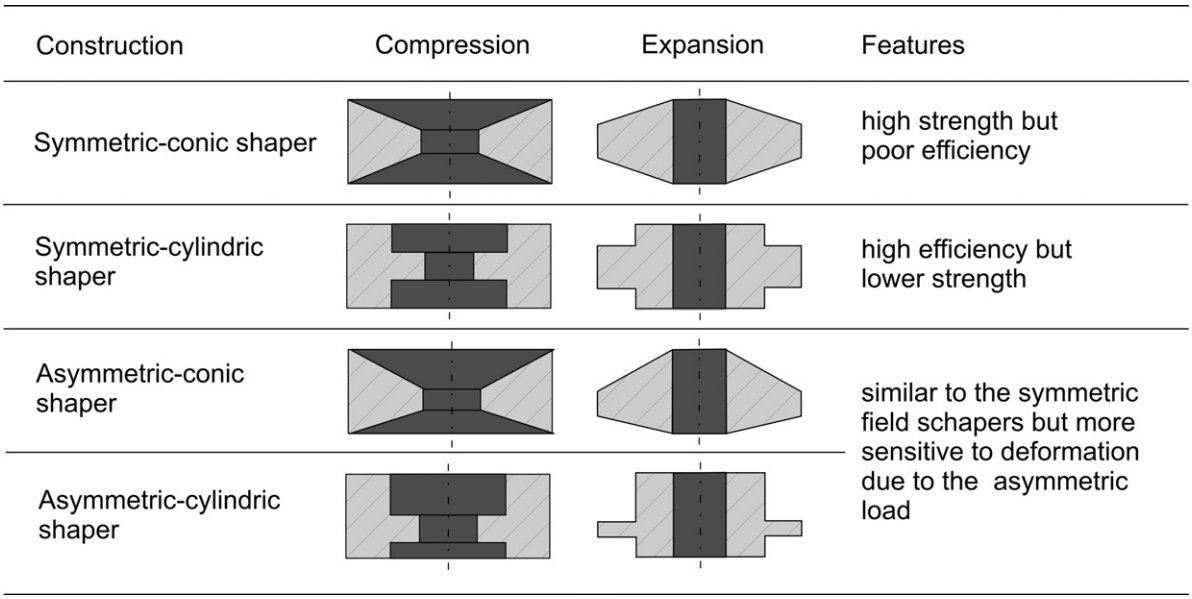

Fig. 21. Various fieldshaper designs with corresponding advantages and disadvantages according to Neubauer et al. (1988).

to arcing. Therefore, Romanovskiy (1971) recommends using form defining tools made of insulating epoxy based materials with reinforcing fillings for workpieces made of copper or aluminum of low thickness (<2 mm) and for large curvature radii. For forming of solid materials and for forming small curvature radii different steels are suggested. Wood and textolite are suggested in case of small lot size (<10).

However, as already mentioned in Section 3.3 at the moment of contact, energy is transferred from the workpiece to the form-defining tool. The properties of the tool and especially the spring stiffness and the damping coefficient significantly influence the energy dissipation and consequently the achievable forming result as shown in a parametric study in Risch et al. (2004). Noland et al. (1967) also refers to the energy absorption when establishing conclusions regarding the geometrical as well as material design of the die within the high speed electrohydraulic forming process. He claims that the die has to be less massive, if the kinetic energy of the workpiece is already transferred into forming energy when the workpiece contacts the die the first time. In this case the die is used only for the final shape, while the forming process mainly is just a free forming operation.

vom Ende (1991) reports that the sheet metal manufacturing processes with elastic tools achieved a production stage in Germany and the USA in the middle of the twentieth century. In Guérin (1940) the deep and stretch forming of sheet parts with a rubber pillow was patented. This so-called Guérin-method was developed against the background of finding new and economic operations to produce flat deep drawing and bending parts especially in the aerospace industry. In Sachs (1951) practical experience was published. In the beginning rubber materials were applied as a pressure medium, but later on in the 1960s Polyurethane was used. This material class replaced and extended the procedures with rubber materials due to their advantages like higher hardness, higher wear resistance as well as lower sensitivity to oils and chemicals. In practice flexible tools are used for example in the manufacturing of sinks, heat exchangers, cladding parts, window profiles, lamp screens and reflectors (vom Ende, 1991). Thiruvarudchelvan (2002) indicates that for the forming of aluminum, flexible tools made of Polyurethane and rubber can be applied instead of conventional tools made of steel. In Woodward et al. (2011) a rubber pad is successfully used for the calibration of aviation components by means of electromagnetic forming.

According to Schneider and Horst (1966) disk-shaped material made of wood has become more important in the field of manufacturing, despite the fact that the strength limits can be exceeded during the impact. Recently, Kolleck et al. (2008) successfully replaced a steel punch with a deep drawing punch made of wood with no detrimental effects to the quality of the final product.

The applicability of different die materials (wood, elastopal, and steel) for electromagnetic sheet metal forming processes is investigated in Risch et al. (2008b). To quantify the energy absorption potential of the different materials under impulsive loading, a model experiment is established. Based on these investigations, electromagnetic forming experiments are carried out and the results are evaluated, e.g. considering the surface quality of the workpiece, achievable form filling, accuracy, rebound, economic factors, handling, and durability of the die. Risch et al. (2008b) point out that a steel die is extremely good with regard to the achievable accuracy and the handling while the wooden die led to workpieces with an excellent surface quality, but the handling was complicate, here.

In contrast to electromagnetic sheet metal forming in the case of tube compression, the major concern considering the design on the form defining tool is the removal of this mandrel after the forming process. A mandrel is typically applied if the achievable roundness in a free forming operation is not sufficient, e.g. due to the properties of the semi-finished parts, on the one hand, and the required deformation, on the other hand. In such cases an increase of the charging energy and the magnetic pressure, respectively, leads to an improved forming result as exemplarily shown in Psyk (2010).

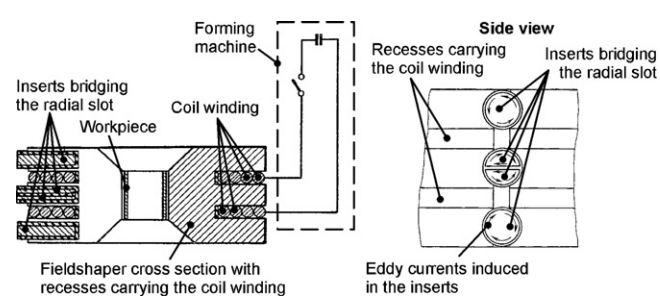

Fig. 22. Fieldshaper with recesses to carry the coil winding and conductive inserts bridging the radial slot according to Tikhonovich et al. (1974).

A reasonable upper limit for the magnetic pressure is given by the forces required to remove the mandrel from the workpiece after the compression process. As frequently stated in the literature, the joining of a tube and mandrel by means of electromagnetic compression is one of the most important applications. In the case of shape forming onto a mandrel the same mechanisms as in the case of joining are acting and depending on the properties of the workpiece and tool as well as on the process parameters, a connection of tube and mandrel can results which cannot be separated without damaging either of the joint partners. Belyy et al. (1977) claims that this effect can be even more severe due to a heating effect which can occur during the process. The shrinking during the cooling of the workpiece promotes the formation of a joint. Therefore, it is suggested to make the mandrels sectioned or provide a small cone to insure easy removal of the parts from the mandrel. Psyk (2010) mentions additional measures which help to reduce the required forces for the removal of the mandrel and to avoid spoiling the workpiece or the tool. With regard to the process design:

- the magnetic pressure can be reduced and/or;
- lubrication can be applied.

Considering the tool design:

- the choice of the material (steel, elastomer, granular materials, etc.),
- an adjustment of the geometry,
- the application of segmented tooling, or
- elastically pre-strained mandrels can contribute to a reduction of the removal forces.

Psyk (2010) concludes that the most efficient of these strategies with regard to the reduction of the removal forces is the application of elastically pre-strained mandrels.

Another interesting aspect regarding the application of mandrels in an electromagnetic tube compression processes is the forming of undercuts. Referring to this, Weimar (1963) mentions that divided dies and mandrels respectively made of plastic, Bakelite or wood can be used.

In addition to the axis-symmetric reduction of the tube diameter, the application of a mandrel with a corresponding geometry also allows a local change of the cross-section geometry. As shown in Psyk et al. (2005), e.g. flattened, waisted and square cross-section geometries can be realized, providing that the circumscribed circle of the mandrel geometry is not larger than the inner diameter of the tube and that the two orthogonal measurements of the cross-section are not too different in length (see Fig. 23).

6. Applications and application-oriented research work

By Neubauer et al. (1988) the EMF technology can be applied in various different manufacturing processes. Especially in the field of sheet metal processing, applications frequently consider electromagnetic forming in the classical meaning, but it is also possible to perform joining or cutting operations or even a combination of the mentioned applications. A detailed review focusing on the potential of primary shaping by means of powder compaction is given in Mamalis et al. (2004), so that this area will be disregarded in the following.

6.1. Forming

Applications and application-oriented work considering electromagnetic forming operations focus on both sheet and tubular metals. However, in case of tube compression mere forming operationshave not found broad application. Belyy et al. (1977) give wrinkling effects and the difficulties of removing the compressed tube from the mandrel after the process as reasons for this development. However, some suggested applications are described in the following.

The free electromagnetic forming can only be applied if the requirements on the accuracy are relatively low. One possible application considering tube compression is the production of preforms which are further processed by subsequent forming operations (see Section 6.4) which is investigated in Psyk (2010). In this simple process variant, the achievable forming result significantly depends on the properties of the semi-finished part, which is applied. Wrinkling is caused by compressive stresses and instability. In Psyk and Tekkaya (2009) it is shown that wrinkling effects are also directly related to inhomogeneities considering the microstructure, e.g. due to longitudinal extrusion seams. Moreover, inhomogeneities considering the workpiece geometry, i.e. the roundness and wall thickness distribution along the circumference of the tube cause wrinkling as shown in Psyk et al. (2005).

Another application for which the tolerances achievable in a free forming operation are sufficient is contouring very large tubes. Weimar (1963) states that such accordion-shaped tubes formed by means of electromagnetic expansion can compensate longitudinal strains, so that curvatures can be avoided.

Electromagnetic tube forming with a form defining tool has a high potential for calibrating tube ends to a diameter with narrow tolerances. In Beerwald et al. (2001) the influence of the charging energy on the achievable roundness of a compressed tube was investigated for different mandrel diameters. Due to the support by the mandrel the deformation of the tube is limited so that an increased magnetic pressure will not lead to an increased deformation but the workpiece will align to the form defining tool. Beerwald et al. (2001) proved that an increase of the charging energy results in an improved roundness of the inner tube radius and furthermore that the required charging energy increases with decreasing mandrel diameter and accordingly increasing workpiece deformation. Investigations in Psyk (2010) showed that if a mandrel is used in comparison to a free forming operation (i.e. without a mandrel) a slight increase of the charging energy leads to a significant improvement of the roundness, while a further raise of the charging energy will lead to a less distinctive reduction of the roundness tolerance thus indicating a saturation of the effect.

By Uhlmann and Forstmann (1998) it is possible to change the cross-section geometry by means of electromagnetic forming. In Psyk (2010) it was shown that also workpieces with non-rotationally symmetric or shifted cross-section geometry in the compressed area can be realized. A parameter study focusing on flattened cross-section geometries shows that depending on the measurements of the cross-section geometry and on the capacitor charging energy more or less distinctive defects regarding the shape of the workpiece occur. Thereby, different effects are identified. Analogous to the forming of rotationally symmetric parts, here increasing the charging energy causes significant improvement of the geometry at first, while a further increase leads to a less distinctive improvement.

Hashimoto et al. (1999) investigate the deformation behavior of aluminum tubes, which are electromagnetically compressed onto form defining tools featuring v-shaped axial grooves of different angles. The top of the v is located in the center of the tube cross-section. However, the motivation behind these investigations is analyzing the reaction of tubular structural parts or a pipelined if exposed to impact load as may occur during collision or seismic shock pulse. Consequently, no real parameter study with regard to an optimized forming result is performed. Nevertheless, it is shown that with an increasing width of the axial groove, bending of the workpiece propagates from the shoulder of the v-shaped groove

Forming machine: capacitance C=992μF; inner inductance L_i=50 nH; inner resistance: R_i=3,3 mΩ
Workpiece: material: EN AW-5754; initial geometry: Ø40 x 2 mm

Cross section	Round geometry	Flatened geometry	Waisted geometry	Square geometry
	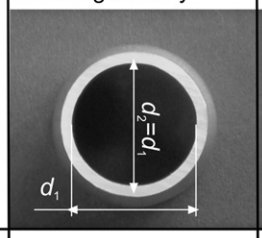	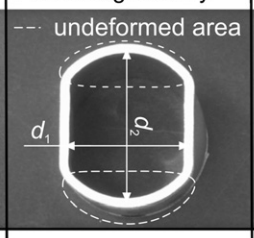	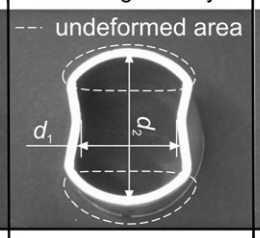	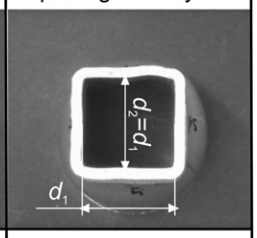
Tool coil	diameter D = 40 mm; length l =60 mm; number or turns n = 10	diameter D = 40 mm; length l =60 mm; number or turns n = 10	diameter D = 40 mm; length l =60 mm; number or turns n = 10	diameter D = 80 mm; length l =90 mm; number or turns n = 8
Field-shaper	no	no	no	concentration area: diameter D_{ca}= 40 mm; length l_{ca}=50 mm
Charging energy	3.2 kJ	3.2 kJ	3.8 kJ	10.2 kJ

Fig. 23. Exemplary cross-section geometries that can be formed by electromagnetic compression according to Psyk et al. (2005).

towards the center. Consequently, the workpiece aligns to the mandrel in the shoulder area, while the center is hardly deformed.

In Murakoshi et al. (1998) inside bead forming of aluminum tubes by electromagnetic compression is regarded via experimental as well as numerical investigations. Thereby, it is shown that increasing the charging voltage and thus increasing the charging energy as well as increasing the shoulder radius of the bead leads to an increased bead height due to an increased bending moment and consequently to an increased thickness strain of the part up to a limiting value. Exceeding this value causes a sudden change of the thickness strain which leads to an increase of the thickness at the top of the bead, while the thickness at the shoulder decreases and finally necking occurs, here. Furthermore, an increasing discharging voltage as well as an increase of the shoulder radius results in an increasing strain up to a certain limit, too. Above this value, saturation is reached and the longitudinal strain is not affected any longer. However, the longitudinal strain considered in this paper refers to the total length of the tube and does not focus on the beading zone.

Regarding electromagnetic sheet metal forming, Göbl (1969) performed parameter studies in view of the accomplishable flange angle at the forming of blanks. Within these studies the center of the workpiece was held down and the pressure acted only on the boundary area. So, conical workpieces were produced considering different materials and thicknesses. The tests were performed applying a defined charging energy interval whereas the flange angle and the outer diameter were varied. The author presented an interpretation method to characterize the “geometrical efficiency”. He obtained values between 0.95 and 1 as a result for his analysis of the optimal geometrical efficiency in consideration of the technical and aesthetic demands.

Fischer (1983) determined the influence of the mean deformation velocity for a given forming geometry, material and thickness in order to achieve a complete and wrinkle-free forming of the workpiece angle. He determined that the mean deformation velocity increases with increasing forming angle.

In recent years, investigations regarding the net shaping electromagnetic forming process are carried out focusing on different influence parameters like die geometry, stiffness, forming behavior, etc. Kleiner et al. (2005) focuses on the influence of the workpiece velocity on the form filling of the desired geometry. The velocity distribution in the workpiece strongly depends on the distribution of the magnetic pressure and thus on the geometry of the tool coil. Kleiner et al. (2005) shows that especially in the case of forming tasks with a relatively low drawing depth (e.g. in the range of 10 mm) and a low stiffness the forming result reacts sensitively to variations in the pressure and velocity distribution. Based on this result, a detailed analysis, considering the local stiffness distribution as well as the geometrical stiffness course over the process time is presented in Risch et al. (2007). It is shown that high forming velocity (and accordingly high kinetic energy) is required in order to form geometry-elements of high stiffness while in areas of lower stiffness this energy cannot be dissipated and consequently, rebound effects occur. This result is in good agreement with findings presented in Imbert et al. (2010). Here, the authors present the results of an experimental and numerical study focusing on the effect of the force distribution and the rebound on workpieces of conical and v-channel geometry. They state that in comparison to conical parts the v-channel-shaped workpieces are significantly more affected by force distribution as well as by rebound. Typically this oblong structure features a lower geometric stiffness in comparison to a rotationally symmetric one, providing that the cross-section is the same in both cases.

Apart from effects that are directly related to the velocity distribution as rebound and insufficient form filling also material failure has to be considered when analyzing the potential of electromagnetic net shaping. This aspect is focused on in Imbert et al. (2004) considering the example of forming different aluminum alloys (AA5754 and AA6111) into dies with conical cavities. Both alloys could successfully be formed with strains above the conventional forming limit diagram. Different failure modes have been identified for the regarded materials: The AA5754 parts failed by necking and fracture with significant thinning at the fracture tip. This is interpreted as a combination of plastic collapse and ductile fracture. Contrary, in the case of the AA6111 parts a crosshatch pattern of shear bands in the lower half of the part, and tears in the area close to the tip were observed and interpreted as an indicator of shear fracture. In Imbert et al. (2006) this investigation is widened by including free formed parts. In contrast to the net shaping electromagnetic forming, a comparison to the conventional forming limit diagram showed no significantly increased formability for these parts. Based on results of an FE-analysis the authors explain the increased formability during the forming into conical dies by a complex stress state that occurs during the interaction of sheet and die.

Here, high hydrostatic stresses create a stress state favorable to damage suppression and increasing ductility.

Imbert et al. (2004) mentions that the vacuum hole in the die affects the quality of the formed parts significantly. Investigations on electromagnetic forming into a conical die show buckling in the area of the vacuum hole. Referring to an exemplary rectangular part with a flat bottom, Neugebauer et al. (2006) compare forming results achievable for different qualities of the vacuum. They show that in the case of insufficient vacuum air cushions are created which result in imperfections in the workpiece after EMF.

The main focus of current investigations regarding electromagnetic sheet metal forming was put on aluminum and aluminum alloys, respectively. But considering the increasing importance of implementing lightweight construction concepts also the forming of magnesium alloys becomes more and more important. In Belyy et al. (1977) it is stated that electromagnetic forming of magnesium and magnesium alloys is only possible at elevated temperatures. Uhlmann and Jurgasch (2004) show the possibility to do a warm electromagnetic forming of magnesium. Thereby, the heating of the magnesium sheet was integrated in the experimental setup of the electromagnetic sheet forming operation. However, in Psyk et al. (2006a) electromagnetic compression of tubes is performed at room temperature. In Ulacia et al. (2009) the cold forming of magnesium sheets with electromagnetic forming operation is presented. It is shown that even at room temperature AZ 31 (a standard magnesium wrought alloy) exhibits significant strain rate sensitivity. In uniaxial tensile tests as well as in the case of biaxial strain the application of high strain rates as achieved during electromagnetic forming leads to an improved formability.

Furthermore, investigations on materials with less electrical conductivity are more and more important. Here, Seth et al. (2005) investigate the deformation behavior of five steels. Despite large differences in the quasi-static ductilities of the steels, their ductilities were similar when formed using EMF. In addition, first investigations regarding the forming of AZ31B-0 magnesium and CP grade 1 titanium were presented in Revuelta et al. (2007) for quasi-static deep drawing and EMF experiments. Although the tools and dies were the same for the tests, the location of severe deformation was different which lead to improved formability for the EMF process. During the experiments for both of these studies, an aluminum driver sheet was used.

Some examples produced by electromagnetic forming are summarized in Fig. 24 and presented in the following:

An industrial example of shaping is the light reflector shown in Fig. 24a. According to Zittel (1975) the rotationally symmetric preform was produced by spinning and subsequently the complex pattern of the diamond-shaped flats was produced by electromagnetic calibration (i.e. a final EMF process to produce the final part geometry based on the corresponding die). By this way a better shape was accomplished but especially considerably better reflecting attributes compared to conventional manufacturing processes were achieved.

In recent years, Kamal and Daehn (2007) did feasibility studies focusing on the potential of the electromagnetic forming process with regard to embossing using the developed “Uniform Pressure Actuator”, which generates a homogeneous pressure allocation in the forming zone (Kamal, 2005). They show that the pressure occurring during impact is sufficiently high for embossing a flat sheet on a die with a holographic image. For forming operations Kamal and Daehn (2007) suggest using multiple-discharge-forming. According to Kamal and Daehn (2007) due to the wide distance between the tool coil and workpiece and the according poor inductive coupling, multiple discharges will not significantly increase the forming depth, but they can help to improve the workpiece geometry and reduce the demands considering the evacuation of the die during high speed forming. In Kamal et al. (2007) they use this principle in order to manufacture mobile phone cases from the material Al 2219-0 (see Fig. 24b). Here, in a first step the part is electromagnetically preformed and then the geometric details are electromagnetically calibrated in two more discharges, in which a copper driver was applied. Finally the edges were flanged, using a ring-shaped coil. The parts, manufactured in such a manner feature a good mould filling and accuracy of the geometry details without any sign of material failure, a result which could not be realized in a single forming operation. Similarly to this procedure, Löschmann (2007) also utilizes a multiple step strategy for the manufacturing of a door handle.

Lebedev et al. (1970) investigated the application of electromagnetic sheet metal forming for beading axially symmetric parts made of different aluminum alloys and different shapes. Beading or circular plates along the outer edge is considered as well as beading of rings along their inner edge. It is shown that compared to conventional beading operations using a rubber-tool the application of electromagnetic forming leads to less springback and allows increased beading heights. Furthermore, the manufacturing by means of electromagnetic forming requires less forming steps, so that tooling costs and production times can be reduced.

Schäfer and Pasquale (2009) have formed by electromagnetic compression the crashbox shown in Fig. 24c from an aluminum tube. During the process also the holes were cut whereby the mandrel served as the cutting die.

In Bradley et al. (2005) forming of fuel cell bipolar plates by applying the “Uniform Pressure Actuator” is patented. Kamal et al. (2006) present a prototype formed from 0.13 mm thick stainless steel. The component specific modest forming over large areas makes the “Uniform Pressure Actuator” especially suitable, here. However, the direct electromagnetic forming of this material is not possible due to its low electrical conductivity. Considering commercialization aspects Shang et al. (2010) decided to use the special process variant introduced in Livshitz et al. (2004) (see section 1) which they refer to as “compliant layer electromagnetic forming”. Using a prototype machine manufacturing of sub-sized fuel cell bipolar plates with a production rate of 5 parts per second could be realized proving the commercial viability of the technology. Coil life as well as die wear have been regarded and Shang et al. (2010) claim that the results prove that this bipolar plate manufacturing process can be regarded as commercially viable.

Another application in which a similar forming variant is applied is presented in Beerwald et al. (2010). Here, the force is transferred to the workpiece via a fluid working medium (water) instead of an elastomeric layer. However, a rubber membrane is used in order to seal the water basin from the electromagnetic equipment. The technology, which is referred to as the impulse hydroforming method, is applied in order to form a blister for pharmaceutical packaging from a multilayer foil consisting of some plastic layers and a 45 μm aluminum layer in between. Although the electrical conductivity of aluminum is typically high enough for a direct electromagnetic forming process the achievable forming result was not sufficient, which is explained by the extremely low thickness of the aluminum layer. Contrary, using the impulse hydroforming method the blister could be formed successfully, providing that the forming limits of the aluminum foil were not exceeded and that the die cavities are completely dry. A parameter study performed using tin plated steel as it is used for food packaging shows that the forming result depends on the temporary course of the pressure pulse. Neither too fast nor too slow pressure pulses will lead to an efficient energy transfer and an accordingly optimized forming result.

6.2. Joining

Joining by electromagnetic forming can be applied for connecting tubes as well as sheet metal. A tubular workpiece can be

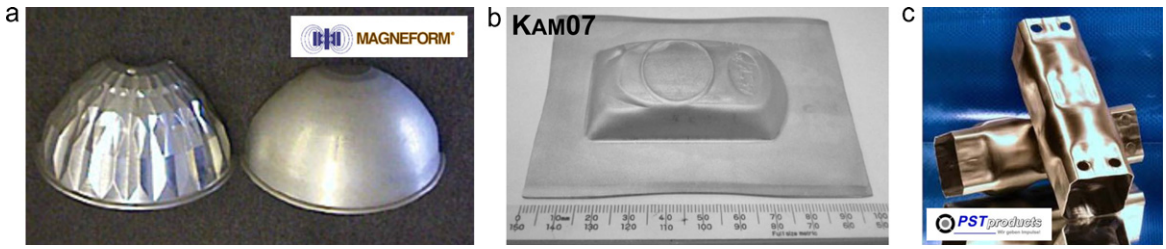

Fig. 24. Applications of electromagnetic forming.

electromagnetically compressed onto an internal joining partner (e.g. a mandrel) or electromagnetically expanded into an external joining partner (e.g. a collar). The resulting connections can be subdivided according to the dominating joining mechanism into

- Interference-fit joints (crimping), which are based on an elastic-plastic bracing of the joining partners (see Section 6.2.2).
- Form-fit joints, which are based on shaping an undercut in order to transfer the load (see Section 6.2.3), and
- impulse welded joints, which are based on a clamping of the joining partners on a microstructural level (see Section 6.2.4).
- Moreover, in a special process variant, the thermally assisted joining by electromagnetic forming has been used for special material-combinations (see Section 6.2.5).

For profile-shaped workpieces in general all three mechanisms and any possible combination of them can be used and the most suitable mechanism has to be chosen considering the special joining task e.g. regarding the materials to be connected. In the case of connections including at least one sheet metal partner (i.e. sheet-sheet-connections and profile-sheet-connections), only form-fit joints, impulse welded joints or a combination of these two mechanisms is possible. Depending on the joining mechanism different material combinations are possible. While impulse welded joints are possible for different combinations of metallic joining partners the other joining mechnisms even allow combinations of metallic and non-metallic components. However, Belyy et al. (1977) states that for joining by electromagnetic compression the inner joining partner should be made of a lower conductive material in order to avoid a counter pressure in-between the two joining partners, which will decrease the process efficiency. The other way round in case of joining by electromagnetic expansion the inner joining partner should be of higher electrical conductivity for the same reason.

Different industrial applications were reported, especially in the 1960s and 1970s. Among the first reported applications was swaging of copper tubes to the ends of coaxial cables (Birdsall et al., 1961). In Hurlimann (1965) among others the joining of high pressure hoses by electromagnetically compressing an aluminum jacket and the hose to a jagged fitting is reported. Testing of these joints proved tightness up to the failure pressure of the tube (approx. 24 MPa). In Belyy et al. (1977) it is stated that for sealed connection of tubes and metal tips, which can stand a test pressure up to 10^7 N/mm^2, can be realized by electromagnetic forming. Furthermore, joining of an aluminum tube with cooling fins to a fuel cell is mentioned. In Rowland (1967) applications in the automotive industry as e.g. the sealing of rubber protective boots to ball joint housing, assembly of air brake hose and in the electrical industry as e.g. joining of metal fittings to ceramic insulators or joining of high voltage coaxial cables are listed. Belyy et al. (1977) refers among other things to the pressing of cable tips and mentions that two wires can be joint by a connecting tube. They state that the electrical contact resistance of such a joint is 1.5–2 times less than that of a joint produced by using a conventional hydraulic press and that the filling coefficient of the pressed part is close to one. This statement correlates well with an example shown in Shribman and Tomer (2006). Sanderson (1967) also mentions the automotive and electrical industry as fields of application and additionally reports that aluminum sheaths have been swaged onto rods for nuclear reactors. However most of these publications only list applications without giving further information. In contrast Wolf (1974), Wolf and Meinel (1989), and Zittel (1975) describe special application examples from automotive, electrical and appliance industry as well as from the nuclear and defense industries. Zittel (1975) also provides comprehensive graphical material.

6.2.1. Joint strength

When testing joints manufactured by electromagnetic forming not only the maximum achievable force, but also the failure mode and force-elongation curves can be of interest. Regarding failure modes, according to Weddeling et al. (2011)

- Failure in the form of a detachment between the joining partners and
- failure in the form of cracking of a joining partner can be distinguished.

With regard the force-elongation curves Weddeling et al. (2011) report that failure due to cracking of a joining partner occurs more suddenly. With respect to DIN 7182 Bühler and von Finckenstein (1968b) identified two especially significant values. These are

- The force for which the first relative movement between the joining partner occurs and
- the maximum force.

Bühler and von Finckenstein (1968b) state that with regard to practical applications the force for which the first relative movement between the joining partners occurs is more relevant. However, due to fretting effects during loading the difference between the two forces can be significant. As pointed out by Kleiner et al. (2006) this seizing effect can be significant with regard to safety, because failure initialization can be identified early and measurements can be taken, before ultimate failure occurs.

6.2.2. Interference-fit joints

For the manufacturing of interference-fit joints by electromagnetic compression or expansion, the workpieces are coaxially positioned. Marré et al. (2004) underlines that the gap between the two joining partners is decisive with regard to the achievable strength of the joint and without this gap no significant strength can be realized. However, this is valid only for joining of two metallic components. As reported in Hwang et al. (1992) in the case of joining aluminum tubes to polyurethane cores by means of electromagnetic compression, a gap in the initial condition affects the achievable pull-out strength negatively. Eguia et al. (2004) state that an accurate coaxial positioning of the components is required to guarantee process-safe production, which according to Homberg

et al. (2004) is a decisive production-related demand that has to be considered during joint design.

After positioning, a radial pressure is applied to the tubular workpiece – i.e. the inner joining partner in the case of electromagnetic expansion (see Fig. 25a) and the outer joining partner in the case of electromagnetic compression (see Fig. 25b). Consequently, it impacts and aligns to the joining partner (phase 1).

As reported in Marré et al. (2004), the impact velocity significantly influences the strength of the joint. This impact velocity in turn is determined by the pressure pulse (however in most publications the capacitor charging energy is the parameter referred to), on the one hand, and by the gap between the joining partners in the initial condition, on the other hand. As shown on the basis of recordings of the velocity measured in free forming experiments, the workpiece is accelerated up to a certain maximum velocity and afterwards it decelerates. In order to exploit the energy as much as possible, the gap between the joining partners in the initial conditions should be chosen considering the displacement for which the maximum velocity is achieved. In order to achieve sufficiently high impact velocities for small gaps (and accordingly short acceleration distances) significantly higher charging energies and/or pressure pulses are required.

After impact both components are deformed together up to a maximum radial deformation. Thereby the tube is deformed elastically in the beginning (see Fig. 25, phase 2) and plastically at the end of the deformation process. The joining partner (i.e. the collar and the mandrel, respectively) preferably should be formed merely elastically (see Fig. 25, phase 3). After the magnetic force diminishes the elastic deformation of both joining partners recedes. A force fit connections results if the complete relaxation of the elastic deformation of the mandrel and the collar respectively is prohibited by the plastically deformed tube. In this case interference and an according pressure in the contact zone remains (see Fig. 25, phase 4).

The strength of this joint is determined by

- the remaining interference stress in the contact zone together with
- the friction coefficient, and
- the area of the contact zone.

The deformation and the conditions in the contact area are significantly influenced by the material of the mandrel and the collar, respectively. According to Eguia et al. (2004) compared to metallic mandrels significantly higher interference strains are achieved, if an elastomeric mandrel (e.g. G10) is applied, providing the same process parameters. The authors conclude that the interference strains increase with decreasing mandrel stiffness. However, for all regarded mandrel materials the interference strain increases with increasing charging energy. A more detailed study considering joining of aluminum tubes to massive polyurethane cores by means of electromagnetic compression, which is especially of interest with regard to applications in the field of underwater sonar, ocean structures, or chemical plants, is presented in Hwang et al. (1992). The authors found that the pull-out strength of such connections is directly related to the deformation. Increasing charging energy leads to increasing deformation and increasing pull-out strength. Applying the same charging energy to a longer joining area or a tube of higher thickness leads to decreasing deformation and decreasing strength. Applying multiple discharges leads to increasing deformation and increasing pull-out strength. Hwang et al. (1992) point out that considering joints including elastomeric components, the radial shrinkage of the elastomer during pulling has to be taken into account when estimating the achievable pull-out force. In Hwang et al. (1993) the authors extended the investigations to joining of copper tubes on polyurethane tubes which are supported by aluminum cores. They found that the roundness must not be disregarded for this joining task. With increasing charging energy the roundness of the joint is improved at first, because the aluminum core, which features narrow tolerances, acts as a kind of form defining tool. However, if a critical deformation is exceeded the roundness quality decreases and this causes a reduction of the pull-out force.

Kleiner et al. (2006) investigate the influence of yield strength and stiffness (i.e. Young's modulus) for joining of aluminum tubes to massive metallic mandrels by electromagnetic compression. They show that higher yield strength as well as higher stiffness of the mandrel lead to higher strength of the joint. Therefore, the authors suggest using mandrel materials of higher strength than the tube material.

Bühler and von Finckenstein (1968a) estimate the interference stress of such a connection on the basis of a model experiment and a spring diagram. The influence of the mandrel stiffness on the joint strength is investigated in detail using copper tubes and steel mandrels. To realize different stiffnesses, hollow mandrels are applied. The stiffness is characterized by the ratio Q of inner diameter D_i and outer diameter D_a. This means that a ratio $Q = 0$ represents a solid mandrel of high stiffness while a value of $Q \approx 1$ represents an extremely thin-walled mandrel of very low stiffness. The authors identified three characteristic areas with regard to the resulting push-out force. In the case of high stiffness the deformation of the mandrel is only small and consequently the achievable interference stress and joint strength is low. Increasing the Q above a certain case-specific value leads to a significant increase in the maximum achievable push-out force. However, if Q exceeds a critical value the push-out force decreases drastically, because the deformation of the mandrel is now elastic plastic and no longer merely elastic. In Kleiner et al. (2006) it is proved that this correlation is also valid for the interference fit joining of aluminum tubes on steel mandrels by means of electromagnetic compression. In Barreiro et al. (2006) in addition to the pull-out strength of force-fit joints also the joint quality with regard to cyclic loading (swelling load) is regarded.

With regard to the process design, apart from the impact velocity and the strength and stiffness of the mandrel especially the surface design in the contact area is decisive. The influence of shot peening and of different machining parameters on the surface properties and the resulting joint strength is investigated in Hammers et al. (2009). It is shown that an increase of the surface roughness as well as a surface hardening is suitable in order to increase the pull-out force of the joint. The consequential continuation of this approach is a micro-contouring of the surface. For example in Marré et al. (2007) mandrels with cut-knurled surfaces are investigated. By Psyk et al. (2009), the resulting surface structure corresponds to a roughness of $R_a = 250\,\mu m$. As shown in Marré et al. (2007), compared to joints applying no special surface structuring the transferable load of the joints applying cut-knurled mandrels is significantly higher, although the strain in the tubular joining partner is lower (max. 1%). In Eguia et al. (2004) joining onto mandrels with different surface structuring (knurls and screw threads) is regarded. They found that finer structures result in higher joint strength and that also for these mandrels the transferable load can be increased, if the impact velocity is increased. The authors attribute these correlations to a better engagement of the joining partners' surfaces and suggest applying mandrels with fine pitches and features that result in full engagement. In Bühler and von Finckenstein (1969) joining to mandrels featuring profiles of narrow channels of different pitches is investigated. It is stated that increasing the depth of this profile results in incomplete filling while increasing the pitch leads to better filling and consequently to higher joint strength. Considering the application of torque tubes in aircrafts, Eguia et al. (2004) do not exclusively focus on joint strength under axial loading, but they consider torsion strength of crimped tube-to-mandrel

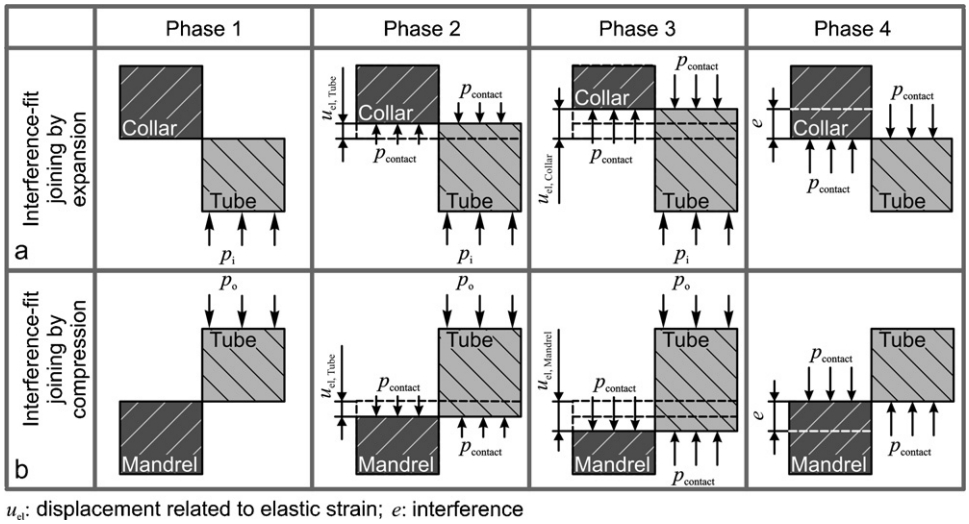

Fig. 25. Principle of interference-fit joining by electromagnetic compression and expansion according to Al-Ahmad (1980).

joints, too. It is reported that by applying fine-knurled mandrels the torsion strength of the tube could be reached.

Bauer (1980) shows that the strength of the interference-fit joint can be improved by applying an elastomeric layer that increases the friction coefficient or glue in-between. However, although Bauer (1980) states that interference-fit joints without such supplements are not suitable for transferring high loads it is shown in Marré et al. (2004) that the achievable push-out strength can reach the strength of the weaker joining partner (usually the tube) if appropriate process parameters are chosen. This joining mechanism is especially interesting

- if sensitive materials as e.g. fiber-reinforced composites are considered, because here any damaging of the fibers caused by sharp-edged geometry elements has to be avoided (Marré et al., 2004),
- if no extensive deformation can be tolerated. According to Marré et al. (2007) this is e.g. the case when composite extrusions with continuous reinforcing elements are applied, because defects of such composites in the form of detached interfaces between the matrix and the reinforcing element or in the form of necking of the element were observed already at small strains, or
- if multiple components as e.g. cords or wires shall be connected and assembled, respectively. Such applications are frequently mentioned in the literature. For example Pfestorf and Wiznerowicz (1964) report that assembling speaker and transformer components can be realized by an electromagnetically formed enclosure. More recently, in Shribman and Tomer (2006) assembed a 55 mm^2 aluminum cable.

6.2.3. Form-fit joints

If the surface structures discussed before are increased to a macro-structural level a transition between dominating inference-fit and dominating form-fit is reached. Bühler and von Finckenstein (1968b) define form-fit joining as joining to a partner which features one to five grooves while multiple small channels are still considered as force-fit joining. This form-fit joining mechanism is based on the formation of an undercut due to the forming of one joining partner into geometric features as e.g. grooves of the other joining partner. In early studies Bühler and von Finckenstein (1968b) investigate form-fit joining into circumferential grooves of different dimensions. Thereby, the charging energy is adjusted in order to guarantee that the tube is formed into the groove in such manner that the bottom of the grove is just touched. In the publication the influences on the force for which the first relative movement between the joining partners occurs and on the maximum force are discussed in detail. But with regard to practical applications in the following only influences on the force for which the first relative movement between the joining partners occurs will be regarded. Bühler and von Finckenstein (1968b) observe that for annealed tubes higher detachment forces are reached. Furthermore, they report that higher push-out forces are related to stronger deformation of the workpiece in the area of the groove. This can be achieved by increasing the charging energy or choosing a frequency of the discharging current that leads to higher process efficiency. A comparison shows that in the case of rectangular and trapezoidal grooves for the same charging energy approximately the same workpiece deformation results if the length at the outer radius of the mandrel is the same. However, applying the same charging energy, a configuration of two grooves is beneficial with regard to the transferable load. Considering the influence of the groove width Bühler and von Finckenstein (1968b) found that there is an optimum groove width, which depends on wall thickness and hardness of the tube and on the available charging energy. In Bühler and von Finckenstein (1969) application-oriented guidelines for the dimensioning of suitable grooves are presented. The authors differentiate between coating materials of relatively low strength (e.g. in the range of up to 100 N/mm^2) and a rill profile or a thread with a pitch of 0.125–0.5 is recommended. For higher strength materials grooves are recommended and experimentally determined diagrams for estimating the strength of such joints depending on the deformation are provided.

In Bühler and von Finckenstein (1971) an analytical-empirical model for estimating suitable tool and machine parameters for joining a special form-fit is suggested. For this purpose, the maximum achievable forming pressure of a magneform-machine for electromagnetic compression of tubes with different conductivities and different measurements is calculated on the basis of equations setup by Dietz et al. (1967a,b, 1968). The minimum required pressure to initiate forming into a groove is determined. On this basis a piecewise linear approximation of the acting pressure is assumed in order to calculate the impetus and its application time is determined. A comprehensive empirical study is presented in order to determine the resulting deformation and the according strength of the joint.

While Bühler and von Finckenstein (1968b) analyze the form-fit joining with rectangular grooves circular grooves are regarded in Golovashchenko (2001). Similarly to Bühler and von Finckenstein

(1968b) the charging energy is adjusted to the groove geometry in order to make sure that the deformed tube just touches the bottom of the groove. It is proved that the filling of wider grooves requires less magnetic pressure but at the same time the strength of the joint decreases. With regard to the required charging energy and the according coil lifetime Golovashchenko (2001) recommends using a minimum groove width that corresponds to the quadruple wall thickness of the workpiece. Contrary, increasing the groove depth requires higher magnetic pressure in order to guarantee form filling, but results in higher strength of the joint. On the basis of these basic investigations, a strategy for determining the optimum combination of groove dimensions necessitating the minimum magnetic pressure in order to provide a defined axial strength of the joint and considering space limitations is presented. Thereby, Golovashchenko (2001) suggests applying a groove shape that corresponds to the workpiece shape after forming into a rectangular groove, because in this case the contact area between the joining partners is maximized.

Another study considering the groove design in form-fit joining by electromagnetic compression is presented in Park et al. (2005). In contrast to Bühler and von Finckenstein (1968b) and Golovashchenko (2001), here one and the same charging energy is applied in order to form the tube into the different grooves. The regarded mandrels are hollow ones featuring rectangular grooves. It is shown that also in this case an increase of the groove depth leads to an increase of the joint strength, but if a critical depth is reached shearing occurs at the groove edges and consequently the strength of the joint decreases again. With regard to this shearing effect also the groove radius is significant. Here, an optimum value considering the achievable joint strength was detected. Considering the groove width, Park et al. (2005) found that applying the same charging energy to wider grooves leads to a larger contact area at the groove base and due to the residual hoop stresses in this area an interference-fit was generated here, which increases the joint strength. This effect is more significant, the wider the grooves are. However, if a critical width is exceeded wrinkling occurs, which reduces the contact area and consequently the strength of the joint. Park et al. (2005) have also shown in their research that additional grooves in the joining zone will significantly increase the strength of a form-fit connection.

In recent work Weddeling et al. (2011) studied the influence of different groove shapes (rectangular, circular, and triangular) and of the charging energy on the pull-out force considering different groove measurements. In this study the following four strengthening mechanisms were identified:

- Higher deformation/higher stiffness in the tube due to the mandrel groove geometry,
- smaller resulting angle of the tube wall at the edge of the groove,
- partial shearing of the tube at the groove edge (locking mechanism), and
- interference stresses at the tube-mandrel-interface.

Increasing the depth of the groove as well as decreasing the width of the groove leads to higher tube deformation and consequently to higher stiffness, a smaller angle of the tube wall of the groove and a higher chance for partial shearing of the tube at the groove edge. Increasing the charging energy decreases the resulting angle α and creates an interference fit between the tube and the mandrel. Considering the groove shape it is proved that the highest joint strength can be achieved for rectangular grooves, while triangular grooves were shown to reach the lowest strength.

Considering form-fit joining of sheet metal workpieces, electromagnetic hemming of aluminum sheets is investigated in Jimbert et al. (2007). Aluminum, which is prone to cracking during hemming, was joined to a steel component, here. Evaluating the resulting geometry after the hemming process, it is shown that the achievable quality in electromagnetic hemming is comparable with the result of a conventional hemming process, providing that the flange length is not too high. A two-step electromagnetic flanging and hemming process is investigated in Jimbert et al. (2008). For basic investigations considering the influence of the relative positioning of workpiece and tool coil and of the charging energy, circular specimens were regarded. Considering the flanging operation it is found that an increased overlap of tool coil and workpiece leads to less damaging of the workpiece, but it requires a higher charging energy to reach the desired final diameter. Considering the hemming step it is stated that bending of the inner joining partner is the process limit, here. This effect occurs if the pressure is applied too close to the bend in the flange. A process window considering the maximum allowable overlap depending on the part diameter is quantified and applied for the process dimensioning of a complex part including areas of different radii as well as straight zones. It is shown that for this part the same hemmed union geometry is achieved for all areas using one single coil and one single discharge. A detailed study of electromagnetic hemming applying experimental as well as numerical methods is presented in Jimbert et al. (2011).

6.2.4. Impulse welded joints

Applying electromagnetic forming for generating joints of tubes as well as of sheet metal parts basing on metallic bonding was patented in Lysenko et al. (1970). However, the interface morphology, the detailed bonding mechanism, and the forming of intermetallic phases in the weld zone still are frequently discussed issues in current publications.

In order to generate an electromagnetic weld, the workpieces are positioned in a defined distance. Applying a magnetic pressure pulse accelerates one (or both) joining partner(s) resulting in the high velocity impact during which the joint is generated. Already in Brown et al. (1978) it is described that the high-velocity impact causes plastic deformation and that due to the high strain rates the material behaves like a high viscosity fluid although it remains solid. This theory is transferred from investigations considering explosive welding and cladding. During the process the so called jetting effect – a self-cleaning of the surfaces by ejecting a small surface layer – occurs. In Miller (1998) the composition of jets are investigated experimentally. One important result is that with decreasing wall thickness as well as with increasing impact angle the relative abundance of projectile in the jet rises, but no systematic dependency of the jet composition considering the impact velocity could be proved. A descriptive illustration of the weld formation including the jetting effect and the typical resulting appearance of the weld is given in Shribman and Tomer (2006). An excerpt of this is presented in Fig. 26. In Shribman and Tomer (2006) it is suggested that the joining is due to propelling the atoms towards each other with such enormous force that they overcome their natural repulsion forces and result in a stable equilibrium because they share and exchange electrons. A high quality metallic bonding can be achieved if the impact velocity and the impact angle are well adjusted to the special welding task (Shribman and Tomer, 2006).

Regarding the joint mechanism itself, there are two proposed explanations for impulse joint welding: solid state welding and rapid melting/solidification. At the interface of the two components, a wavy pattern may develop as shown in Fig. 30. In Brown et al. (1978) it is emphasized that electromagnetic welding is accomplished without reaching the melting temperature. However, it is also reported that in the first third of the joint small melt pockets can be found but the chemical composition in these regions does not differ from that of the cladding tube and the end plug. Accordingly, Shribman and Tomer (2006) state, that the forma-

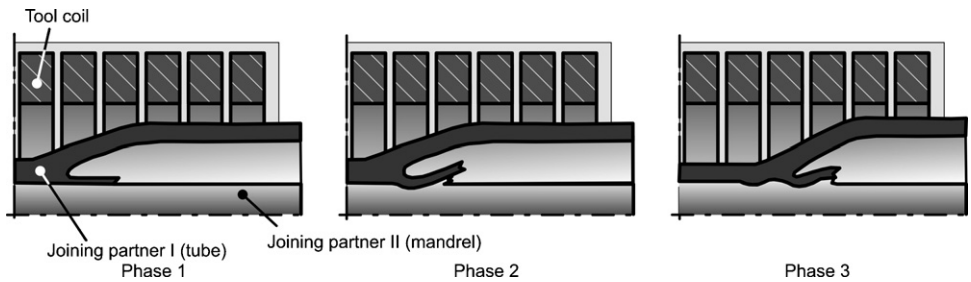

Fig. 26. Development of an electromagnetic welding process according to Shribman and Tomer (2006).

tion of intermetallics is avoided during electromagnetic welding, because the joint formation is based on pressure and not on heat. According to this theory the high rates and plastic deformation may simply produce a solid state weld. This opinion is supported by findings presented in Hisashi et al. (2009). Here, a numerical study of the electromagnetic welding is presented. One important conclusion is that in the regarded case of electromagnetic welding of aluminum to steel the increase of the temperature at the joint interface is not sufficient to melt either of the joining partners. Numerical investigations performed by Uhlmann and Ziefle (2010) lead to the same conclusion. Experimental investigations and according microstructural analysis and XRD presented in Kore et al. (2009b) certify that also in the case of welding aluminum to magnesium no eutectic microstructure and no intermetallic phases were found. Therefore, it is concluded that the temperatures are not high enough to cause melting, in the regarded case.

However, for some cases, impulse welded joints contain a micro-structural combination of the two joining partners, which may indicate melting and solidification. Okagawa and Aizawa (2004) assumed that directly at the interface between the two welding partners a high temperature occurs but without heating up the workpieces largely. They claim that the welding effect can be attributed to both: the magnetic pressure and the joule heat. Recently, in Göbel et al. (2010) intensive metallographic investigations were performed on aluminum tubes which were electromagnetically welded to copper cylinders. According to Göbel et al. (2010) the absence of any diffusion layers in these welds leads to the conclusion that local melting is mainly involved in the phase formation and the bonding process. Depending on the charging energy only the component featuring the lower melting temperature or – at higher charging energies – both materials can be partly melted.

All publications agree in the statement that the resulting welds are of high strength because if exposed to tensile tests, failure typically occurs in the parent material and not in the welding zone. However, according to Okagawa and Aizawa (2004) this is true only if the initial gap width between the welding partners is well chosen. It must be high enough, so that the deformed component can be sufficiently accelerated and the required kinetic energy can be established before collision. On the other hand, it should not be too high in order to avoid decreasing of the kinetic energy. Okagawa and Aizawa (2004) assume that the current flowing after the collision can influence the weld positively because this can still receive energy in the form of joule heating from this current. Therefore, the gap must be chosen carefully considering the discharge energy and the sheet thickness. Considering these correlations during investigations on aluminum-aluminum welds Kore et al. (2007) found that increasing the charging energy increases the field and consequently the shearing strength of the joint, provided that the gap in the initial condition is kept constant. Similarly, reducing the width of the coil's cross section leads to the same effect, provided that the charging energy and the gap in the initial condition is kept constant. In Kore et al. (2008) it is proved that the same dependencies are also valid for aluminum-steel welds. Kore et al. (2008) also agrees with Okagawa and Aizawa (2004) considering the fact, that regarding the initial gap width between the welding partners an optimum value exists. However, in order to accelerate the stainless steel plates, aluminum driver sheets are applied in Kore et al. (2008). Similarly, in Kore et al. (2009a) aluminum driver sheets are applied for electromagnetically welding thin copper sheets. Here, the electrical conductivity of the workpiece in principle is high enough for direct forming, but the disadvantageous ratio of skin depth and sheet thickness requires the application of additional drivers. For the same reason aluminum drivers are applied in Kore et al. (2009b), where the feasibility of electromagnetic welding of magnesium to aluminum is proved (Fig. 27).

Considering the morphology, it is stated in Brown et al. (1978) that the welded interface features a wavy or rippled pattern, which is characteristic for impact bonding. Uhlmann et al. (2007) agree that the formation of a wavy interface is a prerequisite to guarantee a high strength weld. In Aizawa et al. (2007) several aluminum sheets (A1050, A2017, A3004, A5182, A5052, A6016 and A7075) as well as steel materials are regarded and it is stated that in all cases a wavy pattern without any significant heat-affected zone occurs. In Watanabe et al. (2006) electromagnetic welding of aluminum to iron, aluminum to nickel and aluminum to copper is investigated and also in this publication a wavy interface was detected in all material combinations. Moreover, an intermediate layer was detected in the weld seam. A parameter study shows that with increasing charging energy and accordingly increasing impact velocity amplitude and the wavelength of the wavy interface increases up to a critical energy and after exceeding this energy both values decrease again. Numerical investigations presented in Elsen et al. (2010) also prove that wavelength and amplitude increase with increasing impact velocity but at least in the investigated velocity range no reversal of this dependency can be observed. However, since Watanabe et al. (2006) refers to charging energies and not directly to velocities a quantitative comparison is not possible, here. Shribman (2006) also agrees that the morphology of the welded interface significantly depends on the properties of the metals and the process parameters. As shown exemplary in this publication, it can either show the frequently reported wavy pattern or be waveless. This statement is reconfirmed in Göbel et al. (2010), who claims the specimen geometry to be the most significant aspect with regard to the morphology formation and verifies that a wavy interface is not a categorical prerequisite for the weld formation. Recently, Ben-Artzy et al. (2010) have proved that in tubular magnetic pulse welds interface waves are formed in a Kelvin–Helmholtz instability mechanism. They claim reflected shock waves to be the source for interferences at the weld interface. In the publication it is calculated and experimentally verified that the wavelength of the interface wave is proportional to the free path of shock wave propagation in the inner part of the welded components.

Deep investigations of steel aluminum welds are presented in Lee et al. (2007). Here, it is stated that the wavy interface in the

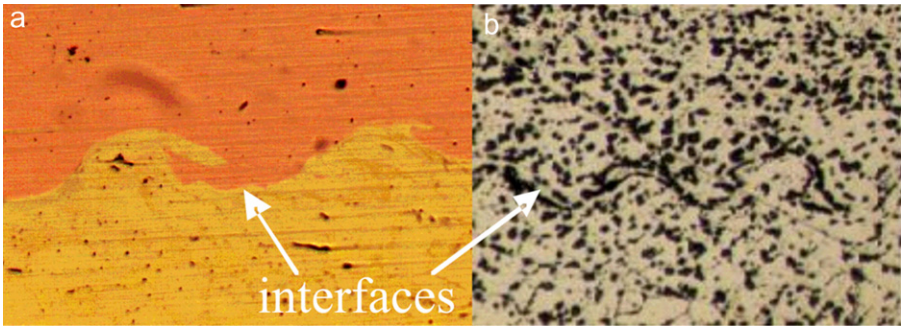

Fig. 27. Wavy pattern at the interface for a) Cu-Brass and b) Al 6061-Al 6061 impulse welded joints (Shribman, 2009).

weld seam corresponds to the shape of the intermediate layer in-between the two welding partners. The interface between the steel and the intermediate layer is identified to be wavy, while the interface between the aluminum and the intermediate layer is relatively flat. TEM micrographs and electron diffraction pattern indicate that the intermediate layer consists of fine aluminum crystal grains and even finer equiaxed crystal grains assumed as Fe–Al intermetallic compound. Similarly, in Aizawa et al. (2005) for welds of aluminum and steel, in Psyk et al. (2008) for welds of aluminum and a titanium alloy (TiAl6V4), and in Kore et al. (2006) for welds of aluminum and aluminum an inhomogeneous transition layer was found in parts of the weld but without giving further identification of the composition. Kore et al. (2006) and Psyk et al. (2008) attribute this effect to the transition area between the weld with metal continuity and the un-welded zone as well as to lower charging energies. Göbel et al. (2010) did a comprehensive experimental study on electromagnetic welding of aluminum tubes to copper cores. Basing on this, they state that in the formation of intermetallic phases could not be avoided. However the significance of these phases can be significantly influenced. It is pointed out that in the case of wavy interfaces the intermetallic phases are concentrated in so-called "melt pockets" while in the case of waveless intersections intermetallic phases form a film of varying thickness. This statement is in good agreement with Zhang et al. (2011), where it is stated that in electromagnetic welding extensive intermetallic phase formation in the corner of wave vortex can be detected. Furthermore, it is stated in Göbel et al. (2010) that for low pulse energies a relatively thin intermetallic phase film is formed and that with increasing pulse energy the thickness increases and cracks, voids, and pores are revealed. This detailed study confirms findings presented in Psyk et al. (2008) which indicate that microfractures can occur, if the energy in impact welding is chosen too high. In Faes et al. (2010) magnetic pulse welding of copper tubes to brass mandrels featuring a step is investigated and it is shown that brittle intermetallic layers and melting can occur if the process parameters are not chosen optimally. Both effects can lead to cracking in the welding zone and thus deteriorate the weld quality.

Another important aspect frequently regarded in the literature is the shape of the weld cross section and especially the continuity of the weld. Considering welding of tubular components it is shown in Faes et al. (2010) that three different zones can be identified in the weld. Here, actual welding occurs in the middle where the typical wavy interface can be identified. The wavelength increases towards the end of the welds and at the edges an un-welded run-in and run-out zone can be detected.

Considering the cross section of lap joints of sheet metal Watanabe et al. (2006) demonstrate that in the center of the seam no welding could be achieved, while at the sides two bulging sections occur and in these regions bonding of the two welding partners takes place. The width of these bonding areas increases with increasing charging energy. Accordingly, Kore et al. (2006) reports the same principal shape for direct welding of aluminum to aluminum sheets. This is confirmed in Lee et al. (2007). As possible reasons in Kore et al. (2006) entrapped oxides, rebound due to normally acting Lorentz forces, and the complex deformation state at the interface are mentioned. However, when applying driver sheets this effect cannot be identified any longer. As shown in Kore et al. (2008) in these cases continuous weld without no-weld areas in the center occurs. This different behavior is explained on the basis of numerical investigations in Kore et al. (2010). The simulations prove that in the case of direct welding aluminum to aluminum normally acting Lorentz forces and a rebound effect are the reason for the un-welded areas in the center of the weld. If driver sheets are applied, the acting force has a shear component in the middle and therefore, continuous welds can be realized.

A more technologically oriented view of the electromagnetic sheet welding process is presented in Zhang et al. (2010a). Focusing on the prerequisite that the impact angle and the impact velocity have to be well adapted in order to guarantee good welding quality, three different configurations:

- A direct lap joint,
- a pre-flange lap joint, and
- a lap joint with embedded wires

are regarded and according tool coil geometries are suggested. During the experiments the impact velocity is measured by Photon Doppler Velocimetry as introduced in Section 3.1.2. On the basis of these measurements a weldability map, indicating matching values for impact angle and impact velocity which allow generating a metallic bonding between 0.254 mm thick copper sheets is deduced. The joint quality is characterized by lap shearing and peel tests, proving that failure occurs in the parent material. Accordingly, microstructural investigations as well as nano-indentation tests show that significant grain refinement and hardness increase can be found in the weld seam. A numerical modeling of the pre-flange lap joint on the basis of the electromagnetic module, implemented in LS DYNA and introduced in Section 3.1.2 is presented in Zhang et al. (2009) and it is shown that the calculated and the measured velocities are in good agreement.

6.2.5. Thermally supported joining by electromagnetic forming

An exotic material combination is investigated in Rafailoff and Schmidt (1975). Here, metallic tubes are connected to porcelain components by electromagnetic compression. This joining task is extremely difficult, because of the poor geometric accuracy, the low impact strength, and the extremely low formability of the porcelain. Considering these special issues "conventional" joining by electromagnetic compression holds a high risk of fracturing the porcelain. Therefore, a combined electromagnetic and thermal joining process was developed. In the process the metallic tube is heated and electromagnetically compressed at elevated tempera-

ture to a porcelain part guaranteeing that fracture of the porcelain is avoided. However, this deformation is not sufficient to generate a joint of sufficient strength. The final strength of the connection is reached after cooling and according thermal shrinking of the tube. The process variant was successfully applied in order to connect metallic tubes to cylindrical porcelain parts (interference-fit joints) and to such, featuring one or several grooves (form-fit joints). By applying a special sealing element even tighter connections could be realized.

Electromagnetic forming at elevated temperatures was suggested for the first time in Alf (1963) in order to reduce the forces required for electromagnetic forming and thus the mechanical load acting on the tool coil. Alf (1963) further suggests using an inductive heating of the workpiece ideally applying the same equipment for heating and forming as well. While Rafailoff and Schmidt (1975) do not explicitly mention how the heating of the tubes was realized, Uhlmann and Hahn (2003) applied the combined inductive heating and electromagnetic compression in order to join magnesium tubes. The reason for choosing electromagnetic forming at elevated temperatures is that the formability of magnesium is significantly extended at such temperatures and that joining at room temperature is not possible at all. However, since the electro-technical, thermal, and mechanical requirements on a tool coil suitable for inductive heating differ from those on a tool coil for electromagnetic forming, a special tool concept was developed. It includes two coils which are focused to the same workpiece area by a common fieldshaper. Here, again interference-fit joints as well as form-fit joints were realized. Tensile tests on the joints proved that in the case of form-fit joints higher load can be transferred. The detaching force increases with increasing temperature of the workpiece and with increasing groove width.

Brower (1969) reports that thermally-supported joining by electromagnetic forming can also be beneficially applied if mere heat shrinking is not possible due to unfavorable length to diameter ratio and small dimensional change or when an exceptionally hard material has to be formed into grooves in a soft or weak material. Belyy et al. (1977) mentions that also in case electromagnetic compression at room temperature during to the process a heating of the workpiece can result. This heating together with the subsequent cooling of the workpiece can lead to additional stresses with improve the quality of an assembly operation.

6.3. Cutting

The punching, or rather cutting, of a blank shaped semi-finished product is another application of electromagnetic sheet metal forming although, according to Kautz (2008) only a few publications consider this task. The workpiece material is, in consequence of high load energies, quickly accelerated and cut at die edges. Breitling (1998) notices that a better quality of the trimmed edge results if higher process velocities are applied. However, Breitling regards high-speed blanking using a mechanical and an electromagnetic impact press but not the direct electromagnetic cutting in the sense of replacing one cutting tool by a tool coil. The maximum velocity regarded in Breitling (1998) is 4 m/s. In addition to comprehensive numerical investigations, it is shown experimentally that velocities attainable with a mechanical high-speed press lead to high productivity but do not significantly influence the shearing result. Contrary, the application of even higher cutting rates by using the electromagnetic impact press results in less plastic deformation (rollover), a shorter and smoother fracture zone, and a reduced burr. Breitling (1998) points out that behavior can be attributed to the process temperature and therefore it is especially relevant in the case of steel workpieces. Due to the higher thermal conductivity of copper and aluminum the advantages are less pronounced for these materials, but they are still measurable.

The direct electromagnetic cutting of sheets is briefly mentioned in Uhlmann and Forstmann (1998) and in Uhlmann et al. (1999). The feasibility is shown on the basis of a simple ring-shaped geometry in Uhlmann and Forstmann (1998) and for a more complex geometry in Uhlmann et al. (1999). Uhlmann and Scholz (2003) investigate the direct electromagnetic cutting of sheets in more detail and compare it to conventional quasistatic shearing. They claim the electromagnetic cutting to be advantageous, because

- common disadvantages of conventional cutting of aluminum like buildup welding or loose burrs (i.e. slivers) are avoided due to the contact free force application in electromagnetic cutting,
- the tool coil offers high flexibility, and
- production costs are reduced because of the savings in cutting punch and according guidance.

In the publication it is shown that in contrast to conventional shearing, where the force is applied by the punch in direct proximity of the cutting edge, in the case of electromagnetic cutting the force is applied in a region of the pinch-off defined by the coil geometry and near the cutting edge, respectively. Therefore in the case of conventional shearing the cutting process is characterized by shearing and subsequent shear fracture, while in the case of electromagnetic cutting it is characterized by bending and subsequent cracking. Accordingly the resulting geometries of the cutting edge differ significantly from each other as shown in Fig. 28. It is obvious that in the case of electromagnetic cutting no shear zone and a significant rollover occurs.

Considering the required force Uhlmann and Scholz (2003) found that although the process time in the case of conventional shearing is approximately a factor of 1000 longer than in the case of electromagnetic cutting, the required forces for electromagnetic cutting are only slightly higher. In the regarded example the factor is less than 1.5. A parameter study considering the burr height showed that it can be reduced by increasing the charging energy and decreasing the cutting edge radius (Uhlmann and Scholz, 2003).

In Golovashchenko (1996) the cutting of tubes by electromagnetic compression is investigated. Here, two mandrels with sharp edges and polished surfaces were placed inside the workpiecewith an axial distance of 14.4 mm in-between them. Tubes featuring a diameter of 45 mm and a wall thickness of 1.5 mm were successfully cut by applying a pressure pulse with a frequency of 41,300/s and an amplitude of 360 MPa. In addition to experimental investigations the shearing process is analyzed in finite element simulations. This study shows that with the increase on the radial displacement of the tube two regions of fracture are developing. On the one hand, fracturing caused by meridional bending and tension originates on the external surface. On the other hand, a second fracture originates from the internal surface close to the edge of the mandrel. These fractures approximate each other and consequently the sections of the tube are separated from each other.

Newer developments of electromagnetic cutting are presented by Kautz (2008). In contrast to the previously mentioned work, here the cutting of hollow profiles by means of electromagnetic expansion is regarded. In order to provide a standardized nomenclature and definitions, he extends the systematic production technologies according to DIN and VDI by the process variants of electromagnetic cutting. In Kautz (2008) this nomenclature is available in German, only, but in Maier-Komor et al. (2010) it is partly translated to English. In order to analyze the basic principles during the electromagnetic cutting a FE-model is established in Kautz (2008). Theoretical and numerical investigations show that the stress state in the cutting area during the process is dominated by shearing stresses. Depending on the tool, process, and workpiece parameters axial tensile and compression stresses can be superimposed. Considering the electromagnetic cutting of hollow profiles

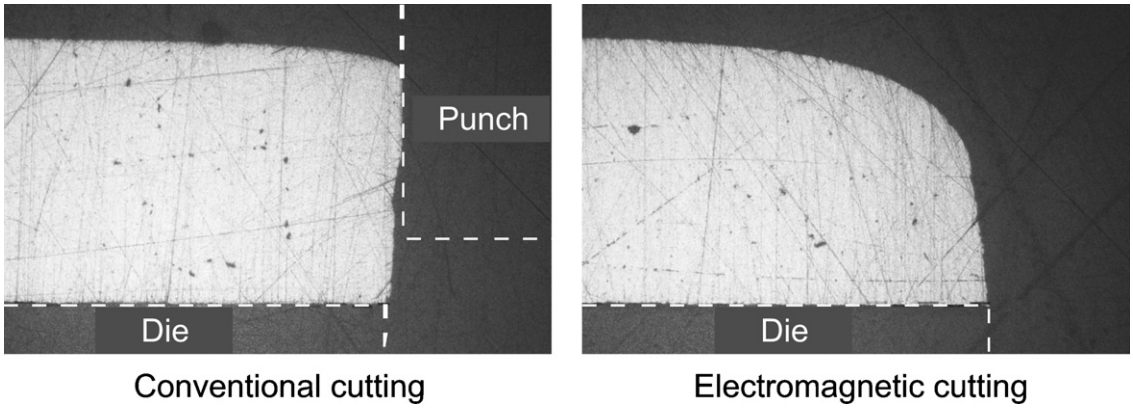

Fig. 28. Comparison of the cutting edge for conventionally sheared and electromagnetically cut parts (sheet thickness: 1 mm; sheet material: AlMgSi0.5) according to Uhlmann and Scholz (2003).

by electromagnetic expansion, Kautz (2008) differentiates a process variant with a cutting cylinder and a supporting cylinder from a variant with a cutting cylinder but without a supporting cylinder (compare Fig. 29). On the basis of extensive numerical and experimental investigations it is stated that with regard to the required pressure and the achievable part properties as well, the process variant with a cutting cylinder and a supporting cylinder should be favored. A method for a semi-empirical estimation of the required pressure for this process variant is presented. Moreover, it is shown that the required pressure increases if the supported length falls below a critical value.

In Maier-Komor et al. (2010) also the cutting of tubular components is investigated. Here, three different approaches – the cutting by electromagnetic expansion and the cutting by electromagnetic compression with and without a fieldshaper – are compared especially considering the required discharging energy. It is found that in the case of electromagnetic compression more energy is required, which is attributed to compressive radial stresses during the reduction of the tube diameter. Moreover, it is proved that the process efficiency is reduced if a fieldshaper is applied. Considering the shape of the cutting edge, the same principle geometry as already shown in Uhlmann and Scholz (2003) is identified here, too. As expected, it is stated that disregarding the mirror symmetry the cutting surface looks the same for compression and expansion.

An industrial application of an electromagnetically cut component – a crashbox shown in Fig. 24c – is presented in Schäfer and Pasquale (2009). Here, it is emphasized that electromagnetic compression is applied for forming and cutting in one and the same pulse. In Kräusel et al. (2010) it is mentioned that even the cutting of high strength steel (22MnB5; sheet thickness 0.9 mm) is possible.

6.4. Process combinations

Innovative approaches combine electromagnetic and conventional forming operations in order to exploit the process specific advantages complementarily. The feasibility of the following process combinations and integrations has already been proven successfully:

- Combined deep drawing and electromagnetic calibration in Vohnout (1998).
- Combined profile curving, electromagnetic compression and tube hydroforming in Psyk et al. (2004b).
- Combined extrusion and electromagnetic compression in Jäger et al. (2009).
- Combined bending and electromagnetic calibration in Golovashchenko et al. (2004).
- Combined flexible roll forming and electromagnetic forming in Eguia et al. (2010).

6.4.1. Combined deep drawing and electromagnetic calibration

The suitability of combining conventional deep drawing and subsequent electromagnetic calibration in order to enhance forming limits was investigated in different research projects. Considering examples from the automotive industry, more precisely a “door inner” and a “hood” Vohnout (1998) shows that by using this process combination higher strains and more complex geometries can be realized compared to the mere deep drawing process. Here, special geometrical details are calibrated by electromagnetic sheet metal forming after a deep drawing step. The principle setup is illustrated in Fig. 30.

Burden et al. (2000) have performed his studies on the example of a “door handle”. He found out that the best result regarding

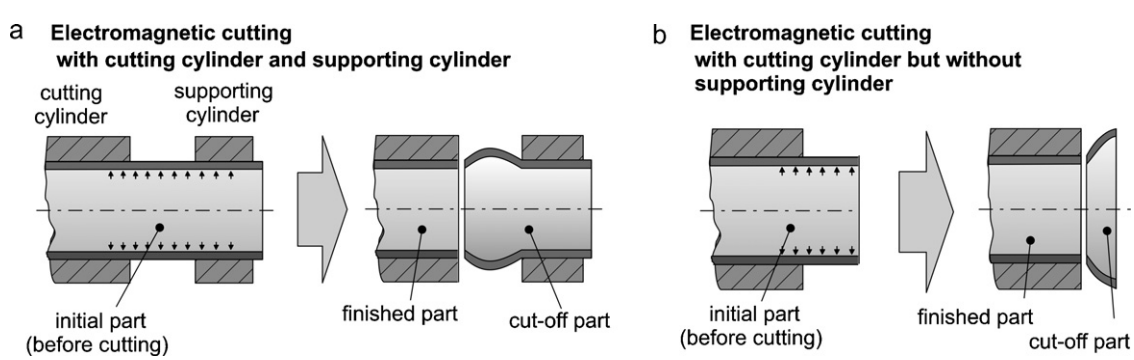

Fig. 29. Cutting of hollow profiles by electromagnetic expansion a) with a cutting cylinder and a supporting cylinder; b) with a cutting cylinder but without a supporting cylinder (Kautz (2008)).

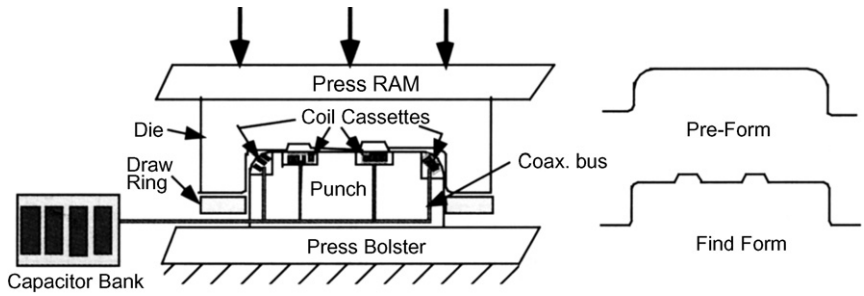

Fig. 30. Principle setup of the combined deep drawing and electromagnetic sheet metal forming (Vohnout et al., 1999).

the form filling can be achieved if the pressure distribution in the forming zone is homogeneous. A relatively homogeneous pressure distribution was realized by applying a so-called "double pancake flat tool coil". Integration in a real tool was planned, but no information about the realization is given.

An integration of the electromagnetic sheet metal forming into a conventional deep drawing process is presented in Psyk et al. (2007) as well as Risch et al. (2008a). In these investigations a three dimensional curved tool coil was integrated into the deep drawing tool. In Psyk et al. (2007) the tool coil was integrated in the deep drawing punch, while in Risch et al. (2008a) the tool coil was implemented in the deep drawing die. The forming task can be achieved regarding both examples in a good order. However, depending on the specific forming task it might be necessary to make special demands on the deep drawing equipment in order to achieve a good forming result. If the form-defining element in a special region changes from one process step to the next – e.g. if the workpiece aligns to the punch after deep drawing and to the die after electromagnetic forming depending on the drawing gap – geometric deviations can occur.

In Vohnout et al. (2004) another variant of this process combination is suggested. Here, again actuator coils are embedded in stamping tools, but in contrast to the previously mentioned research work these coils are not necessarily operated in a single high pulse, but they can also be used to provide several lower pulses during the deep drawing stroke. As shown in Vohnout et al. (2004) this procedure reduces the maximum strain levels by engaging more of the part material in the forming process. Thus, lubrication can be saved and fewer forming steps and/or tools are required. Moreover, this strategy allows forming stronger and less formable material and at the same time springback can be reduced (see also Section 6.4.4).

6.4.2. Combined profile curving, electromagnetic compression and tube hydroforming

Another process combination offers the possibility to enhance the forming limits of the conventional hydroforming process. The electromagnetic tube compression process can be applied in order to realize an optimized contoured perform for subsequent hydroforming.

Starting with a semi-finished part of a medium sized diameter the cross-section is locally reduced by electromagnetic compression. This pre-contoured semi-finished part is then used in a hydroforming process in order to enlarge the cross-section locally and calibrate the preformed regions. Thus, the spectrum of cross-section geometries achievable within one and the same part can be increased. This principle is illustrated in Fig. 31.

This process is suggested in Psyk et al. (2004b) and considering the application in the process chain, basic investigations regarding the workpiece deformation and the forming result caused by electromagnetic compression are documented here (see also Section 3.2.1). The principal feasibility of the combined electromagnetic compression and hydroforming process is proved in Psyk et al. (2005) on the example of laboratory tests. Thereby, the free as well as the form-defined electromagnetic compression are considered. It is shown with regard to the feasibility of the combined process, geometric aspects and the remaining formability must be balanced. The application of a mandrel is recommended if the preform geometry will be widely adjusted to the finished part in the compression area. In this case more strain hardening is acceptable during preforming. Contrary, less accuracy of the preform geometry is acceptable if the remaining formability allows sufficient further deformation e.g. in order to reverse wrinkling effects. The industrial applicability was verified on the basis of an automotive component – more precisely a roofrail – in Psyk et al. (2006c). Here, the investigations were extended by including a bending operation before electromagnetic compression. A comprehensive study of the complete process chain considering also an alternative curving operation – the curved profile extrusion, which was invented by Kleiner et al. (2001), feasibility proved for two-dimensionally curved parts in Arendes (1999), improved accuracy and process reliability in Klaus (2002), and transferred to three-dimensionally curved components in Becker (2009) – is given in Psyk (2010).

6.4.3. Combined extrusion and electromagnetic compression

A further enhancement of the forming limits can be achieved, by a suitable heat treatment between the single forming steps, but such additional production steps will lead to an increased production time and energy consumption and, thus, to rising production costs. As an alternative, the electromagnetic compression can be directly coupled to an extrusion process.

This means that the extruded strand is guided through and compressed by the tool coil, and subsequently a controlled cooling of the workpiece material is realized in order to adjust the microstructure. This reduces the process forces and thus the mechanical load acting on the tool coils while increasing the workpiece formability at the same time. This process combination is patented in Jäger et al. (2009). A setup used for first feasibility tests considering this combination is developed in Tekkaya et al. (2009). Results of basic investigations considering the geometric accuracy, the process limits and defects are documented in Jäger et al. (2011). A possible application suggested in Tekkaya et al. (2009) is the gradation of the energy absorption of tubular crash boxes as part of a car bumper system.

In this process combination the electromagnetic compression is carried out as a hot working operation, so that the resulting influences on the relevant material properties have to be considered. For example the flowstress is significantly decreased so that a lower magnetic pressure is required to achieve a specific strain. At the same time the maximum formability can be increased significantly. On the other hand the electrical conductivity decreases with increasing temperature and the thermal load of the equipment and especially the tool coil has to be compensated with suitable cooling mechanisms as e.g. water or air cooling or by implementing heat

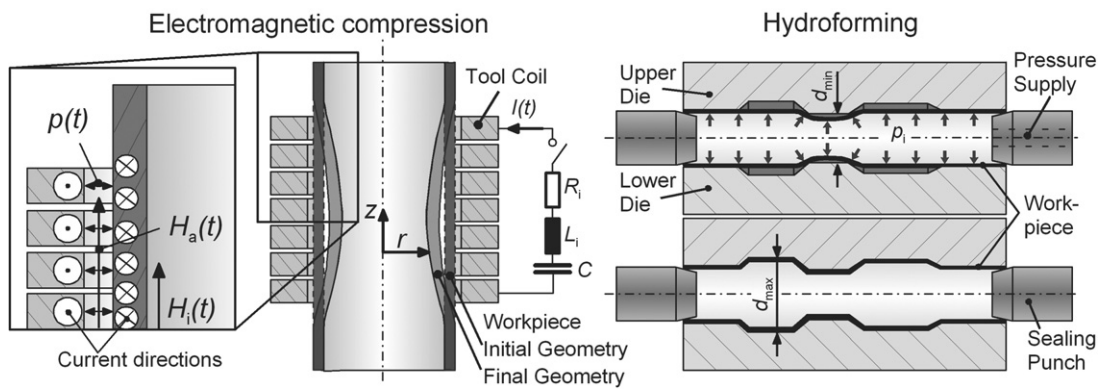

Fig. 31. Principle of the combined electromagnetic compression and hydroforming (Psyk et al., 2005).

conveying metal parts in the armoring as suggested in Beerwald (2003).

6.4.4. Combined bending and electromagnetic calibration

Applying electromagnetic forming in order to reduce or eliminate springback was initially suggested in Golovashchenko et al. (2004). The basic idea is using electromagnetic forces in order to introduce an elastic wave that propagates through the blank multiple times and thereby eliminates elastic residual stresses without noteworthy deformation of the part. Golovashchenko (2005) gives evidence about the successful realization of this approach for aluminum (AA6111-T4) and for high strength steels (BH210, DP500, DP600) as well. In the feasibility study the sheets are bent into a U-shape over a steel mandrel and then flattened by a steel plate. After relieving the applied load springback occurs. In order to relieve the stresses, the sheet is clamped to a flat coil by a steel plate and one or multiple discharges are performed. It is proven that with increasing charging energy the more and more stresses can be eliminated and thus springback is significantly reduced. In Golovashchenko (2006) the possibility to calibrate U-channels using a special flat coil to apply electromagnetic forces to the bottom of the profile is proven for the aluminum alloys AA6111-T4 and AA5754 and for the steels BH210, DP500, and DP600. Iriondo et al. (2011) study springback calibration of L-shaped parts made of AA5754 and DP600. The principle setup of and selected results are shown in Fig. 32. Furthermore, the reshaping of a stamped rocket nozzle panel made of a soft copper alloy is described in this publication. For this industrially oriented application the best results were achieved by applying multiple discharges.

6.4.5. Combined flexible roll forming and electromagnetic forming

Similar to the combined extrusion and electromagnetic compression process also in this process combination electromagnetic forming is applied together with a continuous manufacturing process. Flexible roll forming is an innovative technology for manufacturing complex open and closed profiles, which was investigated in detail in Istrate (2002). In contrast to conventional roll forming this special process variant allows a variation of the cross-section along the axis of the component.

Eguia et al. (2010) shows that the integration of an electromagnetic forming operation is suitable forming shallow longitudinal ribs or stiffeners. The feasibility of the process combination is shown on an exemplary part made of high strength steel (ZStE 340). A U-shaped profile with varying width was roll formed and electromagnetic forming was used to realize a longitudinal strengthening rib in the vertical wall in the central section. In order to achieve the desired deformation a driver was applied and a charging energy of 45 kJ was required. The general setup as well as the produced part is shown in Fig. 33.

7. Conclusion and future research directions for electromagnetic forming

As this literature review shows electromagnetic forming aroused lively interest in the first years after being invented in the late 1950s. Several publications originate from that timeframe. Important fundamental research work considering the process analysis and the analytical calculation of significant parameters, which is still relevant today, was already published at that time. However, numerous papers are limited to describing the process principle and listing potential process advantages showing high expectations, which were made on the new technology. Different applications ranging from the forming of very special and highly demanding parts in a small number of items to series production with large lot sizes and high production rates are reported.

Despite or maybe even due to this euphoria and the emphasis on the process advantages without comparable mentioning of the process limits, which might have led to disappointment, a stagnation of interest can be deduced from the significant decrease in the number of publications in the 1970s and 1980s. Up to now, a real breakthrough of the technology in industrial production has not been achieved with only modest incorporation into applications. This might be ascribed to the following open questions and unsolved problems, which demonstrate the need for further research work.

- There are no tools available which enable the production engineer to estimate the feasibility of a special manufacturing task by means of electromagnetic forming, joining, or cutting. Such an assessment and building on that the detailed process design and secured process dimensioning requires experience and expertise which is typically not part of today's engineering education.
- Related to the previous point, there is a lack of commercially available and user-friendly finite-element-software that is suitable for the modeling of electromagnetic forming processes. The existing tools are frequently limited to two-dimensional or very simple three-dimensional models. They are typically not capable of calculating complex industrially relevant applications and the few exceptions, which might be suitable for such tasks, require extremely long calculation time, so that an economic process design and optimization is not possible.
- A quantitative simulation of the electromagnetic forming requires accurate material data that considers the process specific load case (i.e. especially the high strain rates) occurring. Currently, material data, determined in conventional quasistatic tests is used in many cases, but this allows only a qualitative simulation of the process.
- Only a few research works considering the tool design with regard to the forming task, on the one hand, and the coil lifetime, on the other hand, have been published. Recently, some progress

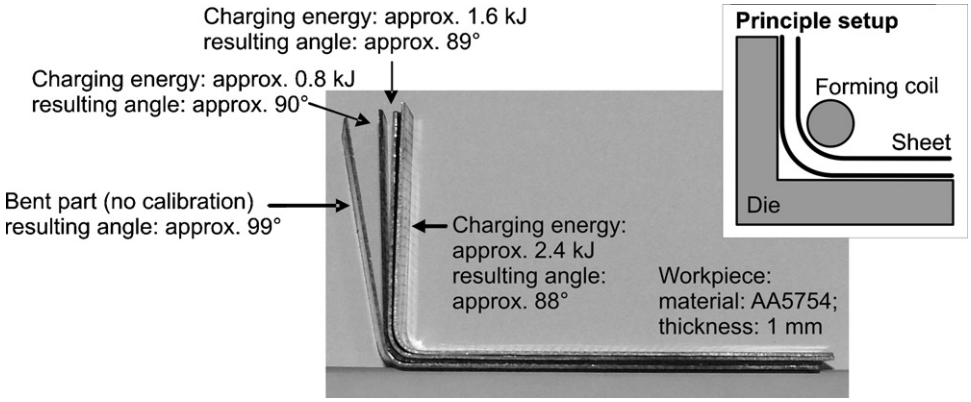

Fig. 32. Principle setup and selected results of springback calibration of L-shaped parts by electromagnetic forming according to Iriondo et al. (2006).

has been made considering the coil durability and some promising results have been reported, but they still refer to special case studies. Here, specific guidelines for the load-oriented coil design are required.

- Finally, modern production is based on costs, so that adequate calculations for specifying the costs of an electromagnetic forming process are necessary. This presumes among other things knowledge about the previously mentioned tool lifetime and the process efficiency. Here, statements can be found only rarely and the few specifications contradict each other, because there are a lot of parameters strongly influencing this value. The research work considering the energy transfer during the process is one contribution to close this gap in the knowledge, but here comprehensive parameter studies are necessary to build up a reliable data base.

Since the late 1990s a resurgence of electromagnetic forming in the scientific and industrial interest can be observed. This effect is related to the increasing importance of implementing lightweight construction concepts. Reasons for this can be found e.g. in the rising sense of responsibility for the environment and environmental protection in society and in rising gas prices. Lightweight construction concepts consider the material choice and special design strategies as well. To reduce product weight e.g. in a vehicle, the most suitable material for each separate component has to be identified and applied. This results in a sophisticated mix of different materials, which need to be connected to each other. Further weight reduction can be realized if structural components are optimally adapted to their specific load conditions and if more functions are fulfilled by one and the same component so that complete parts can be eliminated (i.e. integral construction concept). However, this design usually results in a higher geometric complexity of the remaining parts and at the same time modern lightweight materials typically offer a reduced formability compared to conventional steels. When realizing such complex components standard production concepts reach their limits, so that innovative forming and joining processes along with new processing strategies are required. Especially, since electrically highly conductive materials as aluminum alloys are frequently involved in lightweight construction concepts, electromagnetic forming is a promising technology and consequently a kind of renaissance can be recognized.

However, in order to avoid a new disappointment, which might lead to finite downfall of the technology, two different motivations for utilizing electromagnetic forming have to be differentiated. These are

- technologically oriented aims in the sense of applying electromagnetic forming as a *supplement* of conventional processing technologies in order to realize workpiece properties that cannot (or can hardly) be achieved by other methods and
- economically oriented aims in the sense of applying electromagnetic forming as a *replacement* of conventional processing technologies in order to realize similar workpiece properties as in the case of other manufacturing methods but at lower costs.

In the near future electromagnetic forming can be applied more beneficially in those cases, which are technologically motivated. These applications together with continuing research work can contribute to solve the currently remaining problems and answer

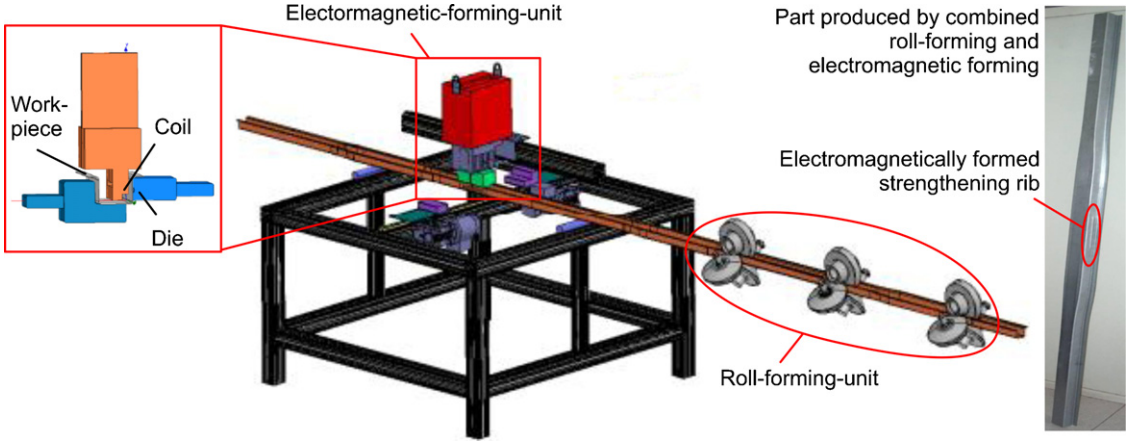

Fig. 33. Principle setup of the combined roll-forming and electromagnetic forming and exemplary part produced by this process combination according to Eguia et al. (2010).

the open questions. In order to promote the technology successful implementations in manufacturing tasks, for which electromagnetic forming is especially suitable should be published. In the long term the newly gathered experience might contribute to a beneficial implementation of electromagnetic forming also in those cases which are economically motivated.

References

Abouridouane, M., 2005. Bruchverhalten von Leichtmetallen unter Impact-Beanspruchung. Dr.-Ing. Dissertation, RWTH Aachen.

Aizawa, T., Kashani, M., Okagawa, K., 2005. Application of magnetic pulse welding for aluminium alloys and SPCC steel sheet joints. Welding in the World 49, 212–222.

Aizawa, T., Kashani, M., Okagawa, K., 2007. Application of magnetic pulse welding for aluminium alloys and SPCC steel sheet joints. Welding Journal 86, 119s–124s.

Al-Ahmad, N., 1980. Das Fügen rotationssymmetrischer Formelemente durch Umformen mit Impulsmagnetfeldern. Dr.-Ing. Dissertation, Ingenieurhochschule Zwickau.

Alf, F., 1963. Verfahren zur Verminderung der bei der Metallumformung durch Magnetfelder erforderlichen Kräfte. Auslegeschrift, 1157320.

Al-Hassani, S.T.S., 1975. Magnetic pressure distributions in sheet metal forming. In: Proceedings of the Conference on Electrical Methods of Machining, Forming and Coating , London, pp. 1–10.

Al-Hassani, S.T.S., Duncan, J.L., Johnson, W., 1974. On the parameters of the magnetic forming process. Journal Mechanical Engineering Science 16 (1), 1–9.

Al-Hassani, S.T.S., Duncan, J.L., Johnson, W., 1967. Analysis of electromagnetic forming process. In: Proceedings of the International American Society of Tool and Manufacturing Engineers , Deaborn, pp. 853–882.

Arendes, D., 1999. Direkte Fertigung gerundeter Aluminiumprofile beim Strangpressen. Dr.-Ing.-Dissertation, Universität Dortmund.

Auerswald, W., 1968. Spule zum magnetischen verformen von langen bzw. sperrigen Werkstücken. Patent 12577728.

Babat, G., Losinsky, M., 1940. Concentrator of Eddy currents for zonal heating of steel parts. Journal of Applied Physics 11, 816–823.

Bach, Fr.-W., Rodman, M., Rossberg, A., Weber, J., Walden, L., 2003. Verhalten von Aluminiumwerkstoffen bei der elektromagnetischen Blechumformung. In: Proceeding of the 2. Kolloquium Elektromagnetische Umformung , Dortmund, pp. 11–18.

Badelt, M., Beerwald, C., Brosius, A., Kleiner, M., 2003. Process analysis of electromagnetic sheet metal forming by online-measurement and finite element simulation. In: Proceedings of the 6th International Conference on Material Forming—ESAFORM 2003 , Salerno, pp. 123–126.

Bahmani, M.A., Niayesh, K., Karimi, A., 2008. 3D simulation of magnetic field distribution in electromagnetic forming systems with field-shaper. Journal of Materials Processing Technology, doi:10.1016/j.matprotec.2008.05.024.

Baines, K., Duncan, J.L., Johnson, W., 1965. Electromagnetic metal forming. Proceedings of the Institution of Mechanical Engineers 180 (3), 348–362.

Balanethiram, V.S., Daehn, G.S., 1992. Enhanced formability of interstitial free iron at high strain rates. Scripta Metallurgica et Materialia 27, 1783–1788.

Balanethiram, V.S., Daehn, G.S., 1994. Hyperplasticity: increased forming limits at high workpiece velocity. Scripta Metallurgica et Materialia 30, 515–520.

Barker, L.M., Hollenbach, R.E., 1972. Laser interferometer for measuring high velocities of any reflecting surface. Journal of Applied Physics 43 (11), 4669–4675.

Barreiro, P., Schulze, V., Löhe, D., Marré, M., Beerwald, C., Homberg, W., Kleiner, M., 2006. Strength of tubular Joints made by electromagnetic compression at quasistatic and cyclic loading. In: Proceedings of the 2nd International Conference on High Speed Forming , Dortmund, pp. 107–117.

Bauer, D., 1965. Messung der Umformkraft und der Formänderung bei der Hochgeschwindigkeitsumformung rohrförmiger Werkstücke durch magnetische Kräfte. Bänder Bleche Rohre 6, 575–577.

Bauer, D., 1967. Ein neuartiges Messverfahren zur Bestimmung der Kräfte, Arbeiten, Formänderungen, Formänderungsgeschwindigkeiten und Formänderungsfestigkeiten beim Aufweiten zylindrischer Werkstücke durch schnellveränderliche magnetische Felder. Dr.-Ing.-Dissertation, Technische Hochschule Hannover.

Bauer, D., 1969. Zur Physik der Metallumformung mit schnellveränderlichen Magnetfeldern. ETZ-A 90 (11), 268–271.

Bauer, D., 1973. Werkzeuge für das elektromagnetische Umformen. Kurzberichte der Hochschulgruppe Fertigungstechnik der Technischen Hochschulen und Universitäten der Bundesrepublik Deutschland, 73 (25).

Bauer, D., 1980. Elektromagnetisches Umformen: Entwicklungsstand und, Tendenz. Maschinenmarkt 86, 190–193.

Becker, D., 2009. Strangpressen 3-D-gekrümmter Leichtmetallprofile. Dr.-Ing. Dissertation, Technische Universität Dortmund.

Beerwald, C., 2005. Grundlagen der Prozessauslegung und—gestaltung bei der elektromagnetischen Umformung. Dr.-Ing. Dissertation, Universität Dortmund, ISBN 3-8322-4421-2.

Beerwald, C., Beerwald, M., Dirksen, U., Henselek, A., 2010. Impulse hydroforming method for very thin sheets form metallic or hybrid materials. In: Proceedings of the 4th International Conference on High Speed Forming—ICHSF 2010 , Columbus, pp. 150–158, online available at https://eldorado.tu-dortmund.de/handle/2003/27189.

Beerwald, C., Brosius, A., Homberg, W., Kleiner, M., Wellendorf, A., 1999. New aspects of electromagnetic forming. In: Proceedings of the 6th International Conference on Technology of Plasticity—ICTP, vol. 3 , Nürnberg, pp. 2471–2476.

Beerwald, C., Brosius, A., Kleiner, M., Psyk, V., 2003. Einfluss des magnetischen Druckes bei der elektromagnetischen Blechumformung. In: 2. Kolloquium Elektromagnetische Umformung, Dortmund, pp. 77–85.

Beerwald, C., Kleiner, M., Klocke, M., Kulig, S., 2001. Aspekte der Prozessführung beim Kalibrieren mittels elektromagnetischer Umformung. Kolloquium Elektromagnetische Umformung, Dortmund, pp. 45–54.

Beerwald, H., 2003. Mehrwindungsspule zur Erzeugung starker Magnetfeldimpulse. German Patent DE 100 20 708 C 2.

Beerwald, M., Henselek, A., 2003. Spiralförmige Spule zur magnetischen Umformung von Blechen. German Patent De 102 07 655 A 1.

Beerwald, M., Henselek, A., 2005. Teilbare Einwindungsspule zur Erzeugung starker Magnetfeldimpulse. German Patent De 102004016414A1.

Bely, I.V., Gorkin, L.D., Dmitriev, V.S., Khvorost, V.J., Khimenko, L.T., Mezhuev, A.T., 1975. Inductor for Magnetic-pulse Stamping of Flat Blanks. US Patent 3,921,426.

Belyy, I.V., Fertik, S.M., Khimenko, L.T., 1977. Spravochnik Po Magnitno-impul' Snoy Obrabotke Metallov [Electromagnetic Metal Forming Handbook]. English translation by Altynova, M.M., online available at http://www.mse.eng.ohio-state.edu/~Daehn/metalforminghb/index.html (shown on 04.11.2010).

Ben-Artzy, A., Stern, A., Frage, N., Shribman, V., Sadot, O., 2010. Wave formation mechanism in magnetic pulse welding. International Journal of Impact Engineering 37, 397–404.

Bertholdi, W., Daube, J., 1966. Die elektrohydraulische und die elektromagnetische Umformung von Metallen. Urania—Gesellschaft zur Verbreitung wissenschaftlicher Kenntnisse.

Bessonov, N., Golovashchenko, S., 2004. Numerical simulation of pulsed electromagnetic stamping process. In: Proceedings of the 1st International Conference on High Speed Forming ICHSF 2004 , Dortmund, pp. 83–91, online available at https://eldorado.tu-dortmund.de/handle/2003/27048.

Birdsall, D., Ford, F., Furth, H.P., Riley, R., 1961. Magnetic Forming! American Machinist/Metalworking Manufacturing 105 (6), 117–121.

Boulger, F.W., Wagner, H.J., 1960. High Velocity Metal Working Processes Based on Sudden Release of Electrical Energy. DMIC Memorandum, Defense Metals Information Center, Columbus.

Bradley, J.R., Schroth, J.G., Daehn, G.S., 2005. Electromagnetic Formation of Fuel Cell Plates. Patent US 2005/02173334 A1.

Breitling, J., 1998l. The challenges and Benefits of High-Speed-Blanking. Dr.-Ing. Dissertation, Universität Stuttgart. ISBN 3-88355-266-6.

Brosius, A., 2005. Verfahren zur Ermittlung dehnratenabhängiger Fließkurven mittels elektromagnetischer Rohrumformung und iterativer Finite-Element-Analysen. Dr.-Ing.-Dissertation, Technische Universität Dortmund.

Brosius, A., Beerwald, C., Homberg, W., Kleiner, M., Klocke, M., Kulig, S., 2003. Extended finite element modeling of electromagnetic forming. In: Proceedings of the 10th International Conference on Sheet Metal , Jordanstown, pp. 559–566.

Brower, D.F., Hayward, G.B., 1966. Electromagnetic Devices. US patent 3,231,842.

Brower, D.F., 1966. Forming Device and Method. US Patent 3,279,228.

Brower, D.F., 1969. Metals Handbook, vol. 4. ASM, Metals Park.

Brown, W.F., Bandas, J., Olson, N.T., 1978. Pulsed magnetic welding of breeder reactor fuel pin and closures. In: Proceedings of the AWS 59th Annual Meeting , New Orleans, USA.

Bühler, H., Bauer, D., 1968a. Ein Beitrag zur Formänderungsfestigkeit von metallischen Werkstoffen bei der Hochgeschwindigkeitsumformung durch magnetische Felder. Bänder Bleche Rohre 9 (4), 230–234.

Bühler, H., Bauer, D., 1968b. Ein Beitrag zur Magnetumformung rohrförmiger Werkstücke. Werkstatt und Betrieb 110 (9), 513–516.

Bühler, H., von Finckenstein, E., 1968a. Fügen durch Magnetumformung. Werkstatt und Betrieb 101 (4), 209–215.

Bühler, H., von Finckenstein, E., 1968b. Fügen durch Magnetumformung – Lösekräfte von Sickenverbindungen aus Stahl. Werkstatt und Betrieb 101 (11), 671–676.

Bühler, H., von Finckenstein, E., 1969. Beitrag zur Herstellung von Ummantelungen und Sickenverbindungen rohrförmiger Teile durch Magnetumformung. Bänder Bleche Rohre 10 (7), 413–418.

Bühler, H., von Finckenstein, E., 1971. Bemessung von Sickenverbindungen für ein Fügen durch Magnetumformung, 104. Werkstatt und Betrieb, 45–51.

Burden, R., Snowden, L., Hasegawa, K., Newman, D., Bauer, D., 2000. Elektromagnetisches Umformen (EMF). Neuere Entwicklungen in der Blechumformung, pp. 331–343.

Clark, D.S., Wood, D.S., 1950. The tensile impact properties of some metals and alloys. Transactions of ASM 42, 45–74.

Conraux, Ph., Pignol, M., Robin, V., Berghau, J.M., 2006. 3D finite element modeling of electromagnetic forming processes. In: Proceedings of the 2nd International Conference on High speed Forming—ICHSF 2006 , Dortmund, pp. 73–82, online available at https://eldorado.tu-dortmund.de/handle/2003/27071.

Daehn, G.S., Zhang, Y., Golowin, S., Banik, K., Vivek, A., Johnson, J.R., Taber, G., Fenton, G.K., Henchi, I., L'Eplattenier, P., 2008. Coupling experiment and simulation in electro-magnetic forming using photon doppler velocimetry. In: Proceedings of the 3rd International Conference on High Speed Forming—ICHSF 2008 , Dortmund, pp. 35–44, online available at https://eldorado.tu-dortmund.de/handle/2003/27105.

Daehn, G.S., Vohnout, V.J., Herman, E.A., 2000. Hybrid matched tool-electromagnetic forming apparatus incorporating electromagnetic actuator. US-Patent, 6, 128, 935.

Daube, J., 1973. Die Abhängigkeit der Durchmesseränderung elektromagnetisch umgeformter metallischer Werkstücke von Anlagen und Werkstückparametern. Dr.-Ing. Dissertation, Akademie der Wissenschaften der DDR.

Daube, J., Borowski, A., 1969. Auswechselbare Arbeitsspule mit Einspannvorrichtung für eine elektromagnetische Umformanlage. In: Drittes Kolloquium über

Grundlagen der elektrischen Hochgeschwindigkeitsbearbeitung , Berlin, pp. 67–77.
Daube, J., Götsch, A., Hänisch, H., 1966. Ausnutzung gespeicherter elektrischer Energie zur Magnetumformung von Metallen und Grenzen dieses Verfahrens. Fertigungstechnik und Betrieb 16 (2), 107–113.
Davies, R., Austin, E.R., 1970. Electromagnetic forming. In: Developments in High Speed Metal Forming, pp. 253–270.
Deeg, T., 1967. Verfahren und Anordnung zur Verformung von Werkstücken aus Metall durch impulsartige Einwirkung eines Magnetfeldes. Patent 438187.
Demir, O.K., Psyk, V., Tekkaya, A.E., 2010. Simulation of tube wrinkling in electromagnetic compression. Production Engineering 4 (4), 421–426, doi:10.1007/s11740-010-0243-4.
Dengler, K., Glomski, G., 1991. Die Hochleistungsimpuls-Technik – eine zukunftsträchtige Hochgeschwindigkeits-Umformtechnologie. Blech Rohre Profile 38 (4), 285–286.
Dicke, W., 1968. Zur Berechnung von optimalen Werkzeugen für das elektromagnetische Umformen. Dr.-Ing. Dissertation, Technische Universität Hannover.
Dietz, H., Hammann, J.-F., 1975. Hochgeschwindigkeitsverfahren zur Umformung metallischer Werkstücke. Siemens Forschungs- und Entwicklungs-Berichte 4 (3), 141–147.
Dietz, H., Lippmann, H.J., Schenk, H., 1967b. Theorie des Magneform-Verfahrens: Abge-stufter Feldkonzentrator. Elektronische Zeitschrift ETZ-A 88 (19), 475–480.
Dietz, H., Lippmann, H.J., Schenk, H., 1968. Theorie des Magneform-Verfahrens: Die Bewegung des Werkstücks. Elektronische Zeitschrift ETZ-A 89 (12), 274–278.
Dietz, H., Lippmann, H.J., Schenk, H., 1967a. Theorie des Magneform-Verfahrens: Erreichbarer Druck. Elektronische Zeitschrift ETZ-A 88 (9), 217–222.
Dolan, D.H., 2006. Foundations of VISAR analysis. Sandia Report Sand 2006–1950. Available from U.S. Department of Commerce National Technical Information Service.
Domblesky, J., Jones, D., Gebaur, K., 2005. Elevated temperature and strain rate constitutive data for process simulation. Wire Journal International, 124–127.
Eguia, I., Mangas, A., Iturbe, R., Gutiérrez, M.A., 2010. Electromagnetic forming of longitudinal strengthening ribs in roll formed automotive profiles. In: Proceedings of the 4th International Conference on High Speed Forming—ICHSF 2010 , Columbus, pp. 198–207, online available at https://eldorado.tu-dortmund.de/handle/2003/27184.
Eguia, I., Zhang, P., Daehn, G.S., 2004. Crimped-joining of aluminium tubes onto mandrels with undulating surfaces. In: Proceedings of the 1st International Conference on High Speed Forming ICHSF 2004 , Dortmund, pp. 161–170, online available at https://eldorado.tu-dortmund.de/handle/2003/27041.
El-Magd, E., Abouridane, M., 2004. High speed forming of the light-weight wrought alloys. In: Proceedings of the 1st International Conference on High Speed Forming ICHSF 2004 , Dortmund, pp. 3–12, online available at https://eldorado.tu-dortmund.de/handle/2003/27055.
El-Magd, E., Abouridouane, M., 2006. Characterization, modelling and simulation of deformation and fracture behaviour of the light-weight wrought alloys under high strain rate loading. International Journal of Impact Engineering 32 (5), 741–758.
El-Magd, E., Treppmann, C., Korthäuer, M., 2003. Constitutive modelling of CK45N. AlZnMgCu 1.5 and Ti–6Al–4V in a wide range of strain rate and temperature. Journal de Physique IV (Proceedings) 110 (1), 141–146.
Elsen, A., Ludwig, M., Schaefer, R., Groche, P., 2010. Fundamentals of EMPT-welding. In: Proceedings of the 4th International Conference on High Speed Forming—ICHSF 2010 , Columbus, pp. 117–126, online available at https://eldorado.tu-dortmund.de/handle/2003/27192.
Emde, T., El-Magd, E., Schillig, R., 2006. Modellierung des Einflusses von Dehngeschwindigkeit und Temperatur auf das mechanische Verhalten von Feinblechen. In: Proceedings 24. Tagung Werkstoffprüfung 2006, Fortschritte der Kennwertermittlung für Forschung und Praxis , Bad Neuenahr.
Erdösi, J., Meinel, M., 1984. Elektrische Hochgeschwindigkeitsbearbeitung. Fertigungstechnik und Betrieb 34 (10), 600–601.
Ertelt, D., 1982. Berechnung von Last- und Entladungsgrößen bei der magnetischen Hochleistungs-Impuls-Umformung. Wiss. Z. Techn. Hochschule Magdeburg 26 (4), 57–61.
Faes, K., Baaten, T., De Waele, W., Debroux, N., 2010. Joining of Copper to Brass Using Magnetic Pulse Welding. In: Proceedings of the 4th International Conference on High Speed Forming—ICHSF 2010 , Columbus, pp. 84–96, online available at https://eldorado.tu-dortmund.de/handle/2003/27195.
Fenton, G.K., Daehn, G.S., 1998. Modeling of electromagnetically formed sheet metal. Journal of Materials Processing Technology 75, 6–16.
Fischer, V., 1983. Gestaltung und Einsatz von Flachspulen für die elektromagnetische Umformung. Dissertation, TH Magdeburg.
Furth, H.P., Waniek, R.W., 1956. Production and Use of High Transient Magnetic Fields I. The Review of Scientific Instruments 27 (4), 195–203.
Furth, H.P., Levine, M.A., Waniek, R.W., 1957. Production and use of high transient magnetic fields II. The Review of Scientific Instruments 28 (11), 949–958.
Furth, H., Waniek, R., 1962. New ideas on magnetic forming. American Machinist/Metalworking Manufacturing, vol. 106, pp. 92–95.
Gianotta, J.C., Regazzoni, G., Montheullet, F., 1985. Ductility and Flow Rule of Tantalum at 20 °C and 500 °C. Journal of Physique 46, pp. C5-49–C5-54.
Göbel, G., Kaspar, J., Herrmannsdörfer, T., Brenner, B., Beyer, E., 2010. Insights into intermetallic phases on pulse welded dissimilar metal joints. In: Proceedings of the 4th International Conference on High Speed Forming—ICHSF 2010 , Columbus, pp. 127–136, online available at https://eldorado.tu-dortmund.de/bitstream/2003/27191/1/17.pdf.
Göbl, N., 1969. Elektromagnetische Umformversuche mit Flachspulen. In: Drittes Kolloquium über Grundlagen der elektrischen Hochgeschwindigkeitsbearbeitung , Berlin, pp. 78–94.
Golovashchenko, S., 1996. Impulsive electromagnetic tubes shearing process. In: Proceedings of 5th International Conference on Technology of Plasticity , Columbus, OH, pp. 939–942.
Golovashchenko, S., 2001. Methodology of design of pulsed electromagnetic joining of tubes. In: Proceedings of the 2nd Global Symposium on Innovation in Material Processing and Manufacturing: Sheet Materials , TMS Annual Meeting, New Orleans.
Golovashchenko, S., 2005. Springback calibration using pulsed electromagnetic field. In: Proceedings of NUMISHEET'2005 , Detroit, 2005, pp. 284–285.
Golovashchenko, S., 2006. Electromagnetic forming and joining for automotive applications. In: Proceedings of the 2dnd International Conference on High Speed Forming—ICHSF 2006 , Dortmund, pp. 201–206, online available at https://eldorado.tu-dortmund.de/handle/2003/27060.
Golovashchenko, S., 2007. Material formability and coil design in electromagnetic forming. Journal of Materials Engineering and Performance 16 (3), 314–320.
Golovashchenko, S., Bessonov, N., Davies, R., 2006b. Design and testing of coils for pulsed electromagnetic forming. In: Proceedings of the 2nd International Conference on High Speed Forming , Dortmund, pp. 141–151, online available at https://eldorado.tu-dortmund.de/handle/2003/27065.
Golovashchenko, S., Dmitriev, V., Canfield, P., Krause, A., Maranville, C., 2006a. Apparatus for electromagnetic forming with durability and efficiency enhancement. US Patent 2006/0086165.
Golovashchenko, S., Dmitriev, V., Krause A., Canfield, P., Maranville C., 2004. US Patent 10/967978.
Golovashchenkon, S., Dmitriev, V., Sherman, A., 2005. An Apparatus for Electromagnetic Forming, Joining and Welding. US patent 6,875,946 B2.
Gourdin, W.H., 1989. Electromagnetic ring expansion: experiment, analysis and application to high-strain-rate testing. Journal of Applied Physics 65 (1989), 411–422.
Guérin, H.E., 1940. The aviation rubber stamp. The Machinist 84, pp. 206–208 and 246–248.
Hammers, T., Marré, M., Rautenberg, P., Barreiro, V., Schulze, D., Biermann, D., Brosius, A., Tekkaya, A.E., 2009. Influence of Mandrel's Surface and Material on the Mechanical Properties of Joints Produced by Electromagnetic Compression, vol. 80. Steel Research International, Nr. 5, pp. 366–375.
Harvey, G.W., Brower, D.F., 1958. Metal Forming Device and Method. US-Patent Nr. 2976907.
Harvey, G.W., Brower, D.F., 1962. Verfahren zur Verformung von in fester Form vorliegenden leitenden, insbesondere metallischen Werkstücken. Patentschrift DE 1122188.
Hashimoto, Y., Hata, H., Sakai, M., Negishi, H., 1999. Local deformation and buckling of a cylindrical Al tube under magnetic impulse pressure. Journal of Materials Processing Technology 86, 209–212.
Heaviside, O., 1951. Electromagnetic Theory. The Complete & Unabridged Edition.
Henselek, A., Beerwald, M., Beerwald, C., 2004. Design and adaptation of emf equipment—from direct acting multi-turn coils to separable tool coils for electromagnetic tube compression. In: Proceedings of the 1st International Conference on High Speed Forming—ICHSF 2004 , Dortmund, pp. 275–284, online available at https://eldorado.tu-dortmund.de/handle/2003/27029.
Hisashi, S., Isao, S., Sherif, R., Hidekazu, M., 2009. Numerical study of joining process in magnetic pressure seam welding. Transactions of JWRI 38 (1), 63–68.
Homberg, W., Marré, M., Kleiner, M., 2004. Umformtechnisches Fügen leichter Tragwerkstrukturen. Aluminium, International Journal for Industrie. Research and Application 80 (12), 1396–1399.
Hu, X., Daehn, G., 1996. Effect of velocity on flow Localization in tension. Acta Materialia 44 (3), 1021–1033.
Hurlimann, J., 1965. Magnetische Pulsformung von dünnen Blechen. DGRR-Fachbuchreihe Fortschritte in der Raumfahrtforschung. Deutsche Gesellschaft, München, pp. 111–125.
Husson, C., Ahzi, S., Daridon, L., Courtin, 2003. Continuum damage modeling for ductile metals under high strain rate deformation. Journal de Physique IV 110, 63–68.
Hwang, W.S., Kim, N.H., Sohn, H.S., Lee, J.S., 1993. Joining of copper tube to polyurethane tube by electromagnetic pulse forming. Journal of Materials Processing Technology 37, 83–93.
Hwang, W.S., Kim, N., Sohn, H.S., Lee, J., 1992. Electromagnetic joining of aluminium tubes on polyurethane cores. Journal of Materials Processing Technology 34, 341–348.
Imbert, J., Winkler, S.L., Worswick, M.L., Oliveira, D.A., Golovashchenko, S., 2005. The effect of tool-sheet interaction on damage evolution in electromagnetic forming of aluminum alloy sheet. Journal of Engineering Materials and Technology 127, 145–153.
Imbert, J., Winkler, S.L., Worswick, M., Golovashchenko, S., 2004. Formability and Damage in Electromagnetically Formed AA5754 and AA6111. In: Proceedings of the 1st International Conference on High speed Forming—ICHSF 2004 , Dortmund, pp. 201–210, online available at https://eldorado.tu-dortmund.de/handle/2003/27037.
Imbert, J., Worswick, M., Golovashchenko, S., 2006. Contributing factors to the increased formability observed in electromagnetically formed aluminum alloy sheet. In: Proceedings of the 2nd International Conference on High Speed Forming—ICHSF 2006 , Dortmund, pp. 3–12, online available at https://eldorado.tu-dortmund.de/handle/2003/27078.

Imbert, J., Worswick, M., L'Epplattenier, P., 2010. Effects of force distribution and rebound on electromagnetically formed sheet metal. In: Proceedings of the 4th International Conference on High Speed Forming—ICHSF 2010 , Columbus, pp. 169–180, online available at https://eldorado.tu-dortmund.de/handle/2003/27187.

Iriondo, E., Gonzalez, B., Gutierrez, M., Vohnout, V., Daehn, G., Hayes, B., 2006. Electromagnetic springback reshaping. In: Proceedings of the 2nd International Conference on High Speed Forming—ICHSF 2006 , Dortmund, pp. 153–160, online available at https://eldorado.tu-dortmund.de/handle/2003/27064.

Iriondo, E., Gutierrez, M., Gonzalez, B., Alcaraz, J.L., Daehn, G.S., 2011. Electromagnetic impulse calibration of high strength sheet metal structures. Journal of Materials Processing Technology 211 (5), 909–915.

Istrate, A., 2002. Verfahrensentwicklung zum Walzprofilieren von Strukturbauteilen mit der Längsachse veränderlichen Querschnitten, Dr-Ing. Dissertation, TU Darmstadt.

Jablonski, F., 1976. Analyse der elektromagnetischen Umformung rohrförmiger Werkstücke. Dr.-Ing. Dissertation, Akademie der Wissenschaften der DDR, Berlin.

Jäger, A., Risch, D., Tekkaya, A.E., 2009. Verfahren und Vorrichtung zum Strangpressen und nachfolgender elektromagnetischer Umformung. German Patent, DE 10 2009 039 759.0.

Jäger, A., Risch, D., Tekkaya, A.E., 2010. Thermo-mechanical processing of aluminium profiles by integrated electromagnetic compression subsequent to hot extrusion. Journal of Materials Processing Technologies 211 (5), 936–943.

Jimbert, P., Eguia, I., Gutierrez, M.A., Gonzalez, B., Daehn, G.S., Zhang, Y., Anderson, R., Sundberg, H., Olsson, S.O., Brännström, P., 2008. Flanging and hemming of auto body panels using the electro magnetic forming technology. In: Proceedings of the 3rd International Conference on High Speed Forming—ICHSF 2008 , Dortmund, pp. 163–172, online available at https://eldorado.tu-dortmund.de/handle/2003/27093.

Jimbert, P., Eguia, I., Perez, I., Gutierrez, M.A., Hurtado, I., 2011. Analysis and comparative study of factors affecting quality in the hemming of 6016T4AA performed by means of electromagnetic forming and process characterization. Journal of Materials Processing Technology 211 (5), 916–924.

Jimbert, P., Perez, I., Eguia, I., Daehn, G., 2007. Straight hemming on aluminum sheet panels using the electromagnetic forming technology: first approach. Key Engineering Materials 344, 365–372.

Jurgasch, D., Damavandi, K., 2006. Berührungsloses Umformen im Zeitraffer. In: 1. Berliner Runde Prozess, Struktur und Simulation rund um die Werkzeugmaschine, pp. 33–51.

Kamal, M., 2005. A Uniform Pressure Electromagnetic Actuator for Forming Flat Sheets. Ph.D. Thesis, Ohio State University.

Kamal, M., Cheng, V., Bradley, J., Hatkevich, S., Daehn, G.S., 2006. Design construction and applications of the uniform pressure electromagnetic actuator. In: Proceedings of the 2nd International Conference on High Speed Forming—ICHSF 2006 , Dortmund, pp. 217–225, online available at https://eldorado.tu-dortmund.de/handle/2003/27058.

Kamal, M., Daehn, G.S., 2007. A uniform pressure electromagnetic actuator for forming flat sheets. Journal of Manufacturing Science and Engineering 129, 369–379.

Kamal, M., Shang, J., Cheng, V., Hatkevich, S., Daehn, G.S., 2007. Agile manufacturing of micro-embossed case by a two-step electromagnetic forming process. Journal of Materials Processing Technology 190, 41–50.

Kapitza, P.L., 1924. A method for producing strong magnetic fields. Proceedings of the Royal Society Serine A 105, 691–710.

Karch, C., Roll, K., 2005. Transient simulation of electromagnetic forming of aluminium tubes. Advanced Materials Research 6–8, 639–646.

Kautz, T., 2008. Impulsmagnetisches Beschneiden von dünnwandigen Hohlprofilen. Dr.-Ing. Dissertation, Otto-von-Guericke-Universität Magdeburg. ISBN 978-3-8322-6915-9.

Kegg, R.L., Haverbeck, K., 1962. Effect of process variables in electric discharge forming. Annals of the CIRP 11 (3), 131–137.

Khimenko, L.T., Mezhuev, A.T., Legeza, A.V., Sljusarev, A.K., Gavrjuschenko, A.D., Chudakov, V.A., Baranov, M.I., 1979. Inductor for forming metals by the pressure of a pulsed magnetic field. US-patent 4,143, p. 532.

Kim, Y.B., Platner, E.D., 1959. Flux concentrator for high-intensity pulsed magnetic fields. The Review of Scientific Instruments 30 (7), 524–533.

Klaus, A., 2002. Verbesserung der Fertigungsgenauigkeit und der Prozesssicherheit des Rundens beim Strangpressen. Dr.-Ing.-Dissertation, Technische Universität Dortmund.

Kleiner, M., Arendes, D., Klaus, A., 2001. Verfahren und Vorrichtung zur Herstellung von gekrümmten Strangpressprofilen. European Patent 1 169 146 B1.

Kleiner, M., Brosius, A., 2006. Determination of flow curves at high strain rates using the electromagnetic forming process and an iterative finite element simulation scheme. Annals of the CIRP, 55/1/2006.

Kleiner, M., Marré, M., Beerwald, C., Homberg, W., Löhe, D., Barreiro, P., Schulze, V., 2006. Investigation of force-fit joints produced by electromagnetic tube compression. Annals of the German Academic Society for Production Engineering, WGP XIII (1), 227–230.

Kleiner, M., Risch, D., Beerwald, C., Brosius, A., 2005. Influence of the velocity distribution during the process of electromagnetic sheet metal forming into dies. Production Engineering XII (2), 95–98.

Klocke, F., König, W., 2006. Fertigungsverfahren 4—Umformen. Springer-Verlag.

Kolleck, R., Koroschetz, C., Schickhofer, G., Augustin, M., 2008. Alternativer Werkstoff Holz spart Werkzeugkosten für die Blechumformung. Maschinenmarkt 38, 30–34.

Kore, S. D., Date, P.P., Kulkarni, S.V., 2006. Effect of process parameters on electromagnetic impact welding of aluminum sheets. International Journal of Impact Engineering, doi:10.1016/j.ijimpeng.2006.08.006.

Kore, S.D., Date, P.P., Kulkarni, S.V., 2007. Effect of process parameters on electromagnetic impact welding of aluminum sheets. International Journal of Impact Engineering 34, 1327–1341.

Kore, S.D., Date, P.P., Kulkarni, S.V., 2008. Electromagnetic impact welding of aluminium to stainless steel sheets. Journal of Materials Processing Technology 208, 486–493.

Kore, S.D., Date, P.P., Kulkarni, S.V., Kumar, S., Rani, D., Kulkarni, M.R., Desai, S.V., Rajawat, R.K., Nagesh, K.V., Chakravarty, D.P., 2009a. Electromagnetic impact welding of copper-to-copper sheets. International Journal of Material Forming, 117–121.

Kore, S.D., Imbert, J., Worswick, M.J., Zhou, Y., 2009b. Electromagnetic impact welding of Mg to Al sheets. Science and Technology of Welding and Joining 14 (6), 549–553.

Kore, S.D., Dhanesh, P., Kulkarni, S.V., Dat, P.P., 2010. Numerical modelling of electromagnetic welding. International Journal of Applied Electromagnetics and Mechanics 32, 1–19, doi:10.3233/JAE-2010-1062.

Kräusel, V., Schäfer, R., Engelbrecht, L., 2010. Gepulste elektromagnetische Felder schneiden hochfeste Bleche. Maschinenmarkt 4, 26–29.

Kuchinski, C.S., 1973. VYS0K0V0L'TNYYE IMPUL'SNYYE KONDENSATORI [High-Voltage Pulse Capacitors]. Leningrad, Energiya.

L'Eplattenier, P., Cook, G., Ashcraft, C., 2008. Introduction of an electromagnetism module in LS-DYNA for coupled mechanical thermal electromagnetic simulation. In: Proceedings of the 3rd International Conference on High Speed Forming—ICHSF 2008 , Dortmund, pp. 85–96, online available at https://eldorado.tu-dortmund.de/handle/2003/27100.

L'Eplattenier, P., Cook, G., Ashcraft, C., Burger, M., Imbert, J., Worswick, M., 2009. Introduction of an electromagnetism module in LS-DYNA for coupled mechanical-thermal-electromagnetic simulations. Steel Research International 80 (5), 351–358.

Lal, G.K., Hiller, M.J., 1968. The Electrodynamics of Electromagnetic Forming, vol. 10. Int. J. Mech. Sci., Pergamon Press, pp. 491–500.

Lamb, Horace, 1883. On Electrical Motions in a Spherical Conductor. Philosophical Transactions of the Royal Society of London 174, 519–549.

Lange, K., 1993. Umformtechnik, Bd. 4: Sonderverfahren, Prozesssimulation, Werkzeugtechnik Produktion. 2. Auflage. Springer-Verlag.

Lebedev, G., Komarov, A., Isarovic, G., Lysenko, D., 1970. Umbördeln der Öffnungen und des Außenrandes von Blechteilen durch Magnetumformung. Umformtechnik 4 (6), 13–20.

Lee, K., Kumai, S., Arai, T., Aizawa, T., 2007. Interfacial microstructure and strength of steel/aluminium alloy lap joint fabricated by magnetic pressure seam welding. Materials Science and Engineering A 471, 95–101.

Lesuer, D.R., Kay, G.J., LeBlanc, M.M., 2001. In: Lesuer, D.R., Srivatsan, T.S. (Eds.), Modeling the Performance of Engineering Structural Materials II. TMS (The Materials, Metals & Materials Society), pp. 75–86.

Lindholm, U.S., Bessey, R.L., Smith, G.V., 1971. Effect of strain rate on yield strength, tensile strength, and elongation of three aluminum alloys. Journal of Materials 6 (1), 119–133.

Lippmann, H, Schreiner, H., 1964. Zur Physik der Metallumformung mit hohen Magnetfeld impulsen. Zeitschrift für Metallkunde 55 (100), 737–740.

Livshitz, Y., Shribman, V., Izhar, A., Gafri, O., 2004. Pulsed Power Forming. In: Proceedings of the 1st International Conference on High Speed Forming—ICHSF2004 , Dortmund, pp. 221–228, https://eldorado.tu-dortmund.de/handle/2003/27035.

Lorentz, H.A., 1895. Versuch einer Theorie der elektrischen und optischen Erscheinungen in bewegten Körpern. E. J. Brill, Leiden.

Löschmann, F., 2007. Anlagentechnische Grundlagen für die Elektromagnetumformung im Automobilbau. Dissertation, Technische Universität Chemnitz.

Löschmann, F., Putz, M., Koch, T., 2006. Perspektivische Genauigkeitsanforderungen im Automobilbau. In: Proceedings of the 2nd International Conference on Accuracy in Forming Technology—ICAFT06 , Chemnitz, pp. 9–24.

Lysenko, D.N., Ermolaev, V.V., Dudin, A.A., 1970. Method of Pressure Welding. Patentschrift US 3,520,049.

Maier-Komor, P., Hoffmann, H., Ostermair, M., 2010. Cutting of hollow profiles using pulsed magnetic fields. In: Proceedings of the 13th International ESAFORM Conference on Material Forming—ESAFORM 2010 , Brescia.

Mamalis, A.G., Manolakos, D.E., Kladas, A.G., Koumoutsos, A.K., 2004. Electromagnetic forming and powder processing: trends and developments. Applied Mechanical Review 57 (4), 299–324.

Marré, M., Barreiro, P., Schomäcker, M., Brosius, A., Schulze, V., Tekkaya, A.E., Löhe, D., 2007. Characteristics of composite extruded tubes for joining by electromagnetic compression. In: Proceedings of the International conference on new forming technologies—ICNFT , Bremen.

Marré, M., Beerwald, C., Psyk, V., Homberg, W., Kleiner, M., 2004. Einfluss der Geschwin-digkeit beim kraftschlüssigen Fügen rohrförmiger Werkstücke durch elektromagnetische Kompression. In: Proceedings of the 11. Paderborner Fügesymposium, Mechanisches Fügen und Kleben , Paderborn, pp. 162–172.

Mattke, W., Dehoff, A., 1969. Zur Dimensionierung von Entladekreisen zum elektromagnetischen Umformen. In: Drittes Kolloquium über Grundlagen der elektrischen Hochgeschwindigkeitsbearbeitung , Berlin, pp. 41–53.

Majta, J., Zurek, A.K., Trujillo, C.P., Bator, A., 2003. Study of high strain rate plastic deformation of low carbon microalloyed steels using experimental observation and computational modeling. Journal de Physique IV 110, 117–122.

Maxwell, J.C., 1873. A Treatise of Electricity and Magnetism. Macmillan and Co. Publishers to the University of Oxford.
Meyer, L.W., Kunze, H.D., Seifert, S., 1981. Dynamic behaviour of high strength steels. Shock Waves High Strain Rate Phenomena in Metals, 51–63.
Miller, G., 1998. Jetting in oblique axissymmetric impacts. ICARUS 134, 163–175.
Mühlbauer, A., von Finckenstein, E., 1967. Magnetumformung rohrförmiger Werkstücke. Bänder Bleche Rohre 8 (2), 86–92.
Murakoshi, Y., Takahashi, M., Sano, T., Hanada, K., Negishi, H., 1998. Inside bead forming of aluminium tube by electro-magnetic forming. Journal of Materials Processing Technology 80–81, 695–699.
Neubauer, A., Schmicker, H., Kneiphoff, U., Borisewitsch, W.K., Wowk, W.T., 1989. Hochgeschwindigkeitsumformeinrichtungen in der Praxis. Umformtechnik, 23.
Neubauer, A., Stroppe, H., Wolf, H., 1988. Hochgeschwindigkeitstechnologie der Metall-bearbeitung. VEB Verlag Technik, Berlin.
Neugebauer, R., Löschmann, F., Putz, M., Koch, T., Laux, G., 2006. A production oriented approach in electromagnetic forming of metal sheets. In: Proceedings of the 2nd International Conference on High Speed Forming—ICHSF 2006 , Dortmund, pp. 129–139, online available at https://eldorado.tu-dortmund.de/handle/2003/27066.
Noland, M.C., Gadberry, H.M., Loser, J.B., Sneegas, E.C., 1967. High-velocity metalworking—a survey, office of technology utilization. National Aeronautics and Space Administration.
Northrup, E.F., 1907. Some newly observed manifestations of forces in the interior of an electric conductor. Physical Review 24, 474–497.
Okagawa, K., Aizawa, T., 2004. Impact seam welding with magnetic pressure for aluminum sheets. Material Science Forum 465–466, 231–236.
Oliveira, D.A., Worswick, M.J., Finn, M., Newman, D., 2005. Electromagnetic forming of aluminum alloy sheet: free-form and cavity fill experiments and model. Journal of Materials Processing Technology 170, 350–362.
Oliveira, D.A., Worswick, M., 2003. Electromagnetic forming of aluminium alloy sheet. Journal de Physique 110, 293–298.
Park, Y., Kim, H., Oh, S., 2005. Design of axial/torque joint made by electromagnetic forming. Thin-Walled Structures 43, 826–844.
Pfestorf, G.K.M., Wiznerowicz, F., 1964. Über elektrische Verfahren zur Hochleistungsumformung. ETZ-A 85 (18), 575–577.
Plum, M., 1988. Electromagnetic forming. ASM Handbook Forming and Forging 14, 644–653.
Poynton, W.A., Travis, F.W., Johnson, W., 1967. The free radial expansion of thin cylindrical tubes using explosive gas mixtures. International Journal of Mechanical Sciences, 385–401.
Psyk, V., 2010. Prozesskette Krümmen – Elektromagnetisch Komprimieren – Innenhochdruckumformen für Rohre und profilförmige Bauteile. Dr.-Ing. Dissertation, Technische Universität Dortmund.
Psyk, V., Beerwald, C., Henselek, A., Homberg, W., Brosius, A., Kleiner, M., 2007. Integration of electromagnetic calibration into a deep drawing process of an industrial demonstrator part. Key Engineering Materials 344, 435–442.
Psyk, V., Beerwald, C., Homberg, W., Kleiner, M., 2004b. Electromagnetic compression as a preforming operation for tubular hydroforming parts. In: Proceedings of the 1st International Conference on High Speed Forming—ICHSF 2004 , Dortmund, pp. 171–180, online available at https://eldorado.tu-dortmund.de/handle/2003/27040.
Psyk, V., Beerwald, C., Homberg, W., Kleiner, M., 2005. Extension of forming limits by using a process combination of electromagnetic forming and hydroforming. In: Proceedings of the 8th International Conference on Technology of Plasticity (ICTP) , Verona.
Psyk, V., Beerwald, C., Homberg, W., Kleiner, M., Beerwald, M., Henselek, A., 2006c. Investigation of the process chain Bending-Electromagnetic compression-Hydroforming on the basis of an industrial demonstrator part. In: Proceedings of the 2nd International Conference on High Speed Forming—ICHSF 2006 , Dortmund, pp. 117–127, online available at https://eldorado.tu-dortmund.de/handle/2003/27067.
Psyk, V., Beerwald, C., Klaus, A., Kleiner, M., 2006a. Characterisation of extruded magnesium profiles for electro-magnetical joining. Journal of Material Processing Technology 177, 266–269.
Psyk, V., Beerwald, C., Kleiner, M., Beerwald, M., Henselek, A., 2004a. Use of electromagnetic forming in process combinations for the production of automotive parts. In: Proceedings of the 2nd European Pulsed Power Symposium—EPPS 2004 , pp. 82–86.
Psyk, V., Brosius, A., Broer, C., Bosse, M., Schaper, M., Kleiner, M., Bach, F., 2006b. Electromagnetic compression of magnesium tubes and process-related improvement of wrought alloys by micro-alloying. In: Proceedings of the 7th International Conference on Magnesium Alloys and their Applications , Dresden, pp. 909–915.
Psyk, V., Gershteyn, G., Demir, O.K., Brosius, A., Tekkaya, A., Schaper, M., Bach, Fr.-W., 2008. Process analysis and physical simulation of electromagnetic joining of thin-walled parts. In: Proceedings of the 3rd International Conference on High Speed Forming ICHSF—2008 , Dortmund, pp. 181–190, online available at https://eldorado.tu-dortmund.de/handle/2003/27091.
Psyk, V., Marré, M., Brosius, A., Tekkaya, A.E., 2009. Umformtechnisches Fügen. Fortschr. Ber. VDI Reihe 2 No. 668, VDI-Verlag Düsseldorf, pp. 133–149.
Psyk, V., Tekkaya, A.E., 2009. Significance of semi-finished part properties regarding the forming result of electromagnetic compression processes. In: Proceedings of the 6th International Conference on Electromagnetic Processing of Materials , Dresden, pp. 715–718.
Rafailoff, L., Schmidt, V., 1975. Fügen von rohrförmigen Werkstücken aus Metall und Porzellan durch Magnetumformung. Industrie-Anzeiger 97 (5), 79–82.
Revuelta, A., Larkiola, L., Korhonen, A.S., Karnevo, K., 2007. High velocity forming of magnesium and titanium sheets. In: Proceedings of the 10th Esaform Conferenence on Material Forming , pp. 157–162.
Risch, D., 2009. Energietransfer und Analyse der Einflussparameter bei der formgebundenen elektromagnetischen Blechumformung. Dr.-Ing. Dissertation, Technische Universität Dortmund.
Risch, D., Beerwald, C., Brosius, A., Kleiner, M., 2004. On the significance of the die design for the electromagnetic sheet metal forming. In: Proceedings of the 1st International Conference on High speed Forming—ICHSF 2004 , Dortmund, pp. 191–200, online available at https://eldorado.tu-dortmund.de/handle/2003/27038.
Risch, D., Brosius, A., Kleiner, M., 2007. Influence of the workpiece stiffness on the electromagnetic sheet metal forming process into a die. Journal of Material Engineering and Performance 16 (3), 327–330.
Risch, D., Brosius, A., Tekkaya, A.E., 2008b. Analysis of different die materials for the electromagnetic sheet metal forming process. In: Proceeding of the 9th, International Conference on the Technology of Plasticity (ICTP) , Gyeongju, pp. 1996–2001.
Risch, D., Gersteyn, G., Dudzinski, W., Beerwald, C., Brosius, A., Schaper, M., Tekkaya, A.E., Bach, F.-W., 2008a. Design and analysis of a deep drawing and inprocess electromagnetic sheet metal forming process. In: Proceedings of the 3rd International Conference on High Speed Forming—ICHSF 2008 , Dortmund, pp. 201–212, online available at https://eldorado.tu-dortmund.de/handle/2003/27089.
Römheld, M., Pohl, F., Hartmann, W., 2008. High-current capability of coaxial cables in magnetoforming applications. In: Proceedings of the 3rd International Conference on High Speed Forming ICHSF—2008 , Dortmund, pp. 265–272, online available at https://eldorado.tu-dortmund.de/handle/2003/27083.
Romanovskiy, V.P., 1971. SPRAVOCHNIK PO XOLODNOY SHTAMPOVKE (Cold Stamping Handbook). Mashinostroyeniye, Moscow.
Rowland, A., 1967. Metal forming by magnetic means. In: Proceedings of the Conference on Electrical Methods of Machining and Forming , pp. 192–197.
Ruge, J., Wohlfahrt, H., 2007. Technologie der Werkstoffe. Viehweg-Verlag.
Rusinek, A., Zaera, R., Klepaczko, J.R., 2005. Advanced thermo-visco-plastic constitutive relations for direct applications in numerical analyses. In: Proceedings of the 21st International Congress of Theoretical and Applied Mechanics.
Sachs, G., 1951. Principles and Methods of Sheet-Metal Fabricating. Reinhold, New York.
Saha, P.K., 2005. Electromagnetic forming of various aircraft components. SAE Technical Papers 114, 999–1009, part 1 S.
Sanderson, L., 1967. Magnetic pulse forming. The Journal of the Gage and Tool Industry 21, 43–46.
Schäfer, R., Pasquale, P., 2009. Die Elektromagnetische Puls Technologie im industriellen Einsatz. Whitepaper PSTproducts GmbH, http://www.pstproducts.com/downloads.htm.
Schäfer, R., Pasquale, P., 2010. Electromagnetic pulse forming technology keys for allocating the industrial market segment. In: Proceedings of the 4th International Conference on High Speed Forming—ICHSF 2010 , Columbus, pp. 16–25, online available at https://eldorado.tu-dortmund.de/handle/2003/27202.
Schinnerl, M., Schoberl, J., Kaltenbacher, M., Lerch, R., 2002. Multigrid methods for the 3D simulation of nonlinear magneto-mechanical systems. IEEE Transaction of Magnetics 38, 1497–1511.
Schmidt, V., 1976. Untersuchung der magnetischen Induktion, Stromdichte und Kraft-wirkung bei der Magnetumformung. Dr.-Ing.-Dissertation, Universität Stuttgart.
Schneider, Horst, 1966. Untersuchungen über das Verhalten von Holzwerkstoff-Platten bei Stoßbeanspruchung sowie über ihren dynamischen Elastizitäts- und Schubmodul. Springer Verlag, Berlin, Heidelberg, New York, Sonderdruck aus Holz als Roh- und Werkstoff Bd. 24, pp. 41–52.
Schwinghammer, R.J., 1966. Shaping metal magnetically. New Scientist, p478.
Seth, M., Vohnout, V.J., Daehn, G.S., 2005. Formability of steel sheet in high velocity impact. Journal of Materials Processing Technology 168, 390–400.
Shang, J., Wilkerson, L., Hatkevich, S., Daehn, G.S., 2010. Commercialization of fuel cell bipolar plate manufacturing by electromagnetic forming. In: Proceedings of the 4th International Conference on High Speed Forming—ICHSF 2010 , Columbus, pp. 47–56, online available at https://eldorado.tu-dortmund.de/handle/2003/27199.
Shribman, V., 2006. Magnetic Pulse Welding of Automotive HVAC Parts. Technical Report. PULSAR Ltd. Magnetic Pulse Solutions.
Shribman, V., 2009. Solid State Welding by Magnetic Pulse. Online at: http://www.pulsar.co.il/FileServer/fbabdc01393bc241f6c05f2aa8d0c011.pdf, shown on 18.08.2010.
Shribman, V., Tomer, Y., 2006. Magnetic pulse technology for improved tube joining and forming. Tube & Pipe Technology, 91–95.
Song, S.C., Duan, Z.P., Tan, D.W., 2001. The application of B-P constitutive equations in finite element analysis of high velocity impact. International Journal of Solids and Structures 38, 5215–5222.
Stiemer, M., Unger, J., Svendsen, B., Blum, H., 2006. Algorithmic formulation and numerical implementation of coupled electromagnetic-inelastic continuum models for electromagnetic metal forming. International Journal for Numerical Methods in Engineering 68, 1301–1328.
Stiemer, M., Unger, J., Svendsen, B., Blum, H., 2009. An arbitrary Lagrangian Eulerian approach to the three-dimensional simulation of electromagnetic forming. Computer Methods in Applied Mechanics and Engineering 198 (17–20), 1535–1547.
Strand, O.T., et al., 2005. In: Paisley, D.L., Snyder, D.R., Thompson, B.J. (Eds.), Proceedings of SPIE. SPIE, Bellingham, WA, p. 593.

Suzuki, H., Murata, M., Negishi, H., 1987. The effect of a field shaper in electromagnetic tube bulging. Journal of Mechanical Working Technology 15, 229–240.
Takatsu, N., Kato, M., Sato, K., Tobe, T., 1988. High-speed forming of metal sheets by electromagnetic force. Japan Society Mechanical Engineering International Journal (JSME) Series III 31 (1), 142–148.
Takeda, N., Kobayshi, A., 1990. High-velocity tensile properties of Ti–15V–3Cr–3Al–3Sn alloys. In: Shock Waves and High Strain Rate Phenomena in Metals, pp. 97–106.
Tekkaya, A.E., Brosius, A., Psyk, V., Demir, K., 2007. Untersuchung der komplexen Wechselwirkungen beim elektromagnetischen Umformen rohrförmiger Werkstücke mittels gekoppelter Simulation. In: Proceedings of the 12. Dresdner WZM-Fachseminar: Simulation von Umformprozessen unter Einbeziehung der Maschinen- und Werkzeugeinflüsse , Dresden.
Tekkaya, A.E., Güzel, A., Jäger, A., 2009. Prediction of the microstructure evolution and mechanical properties of aluminum profiles during the process chain of extrusion. Functionally graded materials in industrial mass production. Verlag Wissenschaftliche Scripten, Auerbach, pp. 53–64.
Thiruvarudchelvan, S., 2002. The potential role of flexible tools in metal forming. Journal of Materials Processing Technology 122, 293–300.
Thomas, J.D., Triantafyllidis, N., 2007. Theory of necking localization in unconstrained electromagnetic expansion of thin sheets. International Journal of Solids and Structures 44, 6744–6767.
Thomas, J.D., Seth, M., Daehn, G.S., Bradley, J.R., Triantafyllidis, N., 2007. Forming limit for electromagnetically expanded aluminum alloy tubes: theory and experiment. Acta Materialia 55, 2863–2873.
Tikhonovich, A., Timofeevich, L., Lvovich, A., 1974. Inductor for magnetic pulse pressure shaping of metals. US Patent 3,823,589.
Tillman, W., Vogli, E., Kleiner, M., Beerwald, C., Risch, D., 2005. Adjusted Thermal Spraying Layers to Enhance the Electromagnetic Forming of Metal Sheets. DVS Verlag.
Tillmann, W., Vogli, E., Nebel, J., Giemsa, T., 2008. Funktionsangepasste Schichten für die Elektromagnetische Blechumformung, Wt-online, vol. 98 (1–2), pp. 102–108.
Timpl, F., Ertelt, D., Fischer, V., 1981. Feldprobleme bei der elektromagnetischen Hochenergie-Implus-Umformung. In: International wissenschaftliches Kolloquium, Technische Universität Illmenau, vol. 2 , pp. 127–130.
Uhlmann, E., Forstmann, U., 1998. Impulsmagnetische Umformung. In: ZWF—Zeitschrift für wirtschaftlichen Fabrikbetrieb, vol. 93 , pp. 286–289.
Uhlmann, E., Forstmann, U., Scholz, M., 1999. Flachumformen mit Impulsmagnetfeldern. Wt-Werkstattstechnik 89 (5), 265–268.
Uhlmann, E., Hahn, R., 2003. Pulsed magnetic hot forming of magnesium profiles. Production Engineering 10 (2), 87–90.
Uhlmann, E., Jurgasch, D., 2004. New impulses in the forming of magnesium sheet metals. In: Proceedings of the 1st International Conference on High speed Forming—ICHSF 2004 , Dortmund, pp. 229–241, online available at https://eldorado.tu-dortmund.de/handle/2003/27034.
Uhlmann, E., Jurgasch, D., Rautenstrauch, A., Damavandi, K., 2007. Wirkung des Magnetimpulsverfahrens auf die Nachhaltigkeit in der Produktentstehungsphase. ZWF—Zeitschrift für wirtschaftlichen Fabrikbetrieb 102 (9), 536–539.
Uhlmann, E., Scholz, M., 2003. Zerteilen von Aluminiumblechen durch Impulsmagnetfelder. In: Proceedings of the 2. Kolloquium Elektromagnetische Umformung , Dortmund, pp. 87–94.
Uhlmann, E., Ziefle, A., 2010. Modelling pulse magnetic welding processes—an empirical approach. In: Proceedings of the 4th International Conference on High Speed Forming—ICHSF 2010 , Columbus, pp. 108–116, online available at https://eldorado.tu-dortmund.de/handle/2003/27193.
Ulacia, I., Hurtado, I., Imbert, J., Salisbury, C.P., Worswick, M., Arroyo, A., 2009. Experimental and numerical study of electromagnetic forming of AZ31B magnesium alloy sheet. Steel Research International 80 (5), 344–350.
Vohnout, V.J., 1998. A Hybrid Quasi-Static/dynamic Process for Forming Large Sheet Metals Parts from Aluminum Alloys. Ph.D. Thesis, The Ohio State University.
Vohnout, V.J., Daehn, G.S., 2002. Effect of quasi-static Prestrain and Eddy currents on limit strains in electromagnetic pulse forming of two aluminum alloy. In: Proceedings of the TMS 2002 Annual Meeting , pp. 19–26.
Vohnout, V.J., Daehn, G.S., Shivpuri, R., 1999. A hybrid quasi-static-dynamic process for increased limiting strains in the forming of large sheet aluminum parts. In: Advanced Technology of Plasticity, Proceedings of the 6th ICTP Conference , Nürnberg, pp. 1359–1364.
Vohnout, V.J., Shang, J., Daehn, G.S., 2004. Improved formability by control of strain distribution in sheet stamping using electromagnetic impulses. In: Proceedings of the 1st International Conference on High speed Forming – ICHSF 2004 , Dortmund, pp. 211–220, online available at https://eldorado.tu-dortmund.de/handle/2003/27036.
vom Ende, A., 1991. Untersuchungen zum Biegeumformen mit elastischer Matrize. Dr. -Ing. Dissertation Universität, Erlangen-Nürnberg.
von Finckenstein, E., 1967. Ein Beitrag zur Hochgeschwindigkeitsumformung rohrförmiger Werkstücke durch magnetische Kräfte. Dr.-Ing.-Dissertation, Technische Hochschule Hannover.
Watanabe, M., Kumai, S., Aizawa, T., 2006. Interfacial microstructure of magnetic pressure seam welded Al–Fe, Al–Ni, and Al–Cu lap joints. Materials Science Forum 519–521, 1145–1150.
Weddeling, C., Woodward, S., Marré, M., Nellesen, J., Psyk, V., Tekkaya, A.E., Tillmann, W., 2011. Influence of Groove Characteristics on Strength of Form-fit Joints 211 (5), 925–935.
Weimar, G., 1963. Hochgeschwindigkeitsbearbeitung III—Umformung von Blechen und Rohren durch magnetische Kräfte. Werkstatt und Betrieb 96 (12), 893–900.
Welleman, A., Fleischmann, W., 2006. High power semiconductor devices and solid state switches for pulsed discharge applications. In: Proceedings of the 2nd International Conference on High Speed Forming—ICHSF 2006 , Dortmund, pp. 239–248, online available at https://eldorado.tu-dortmund.de/handle/2003/27056.
Wilson, F.W., 1964. High-Velocity Forming of Metals. Prentice-Hall Inc.
Wilson, M., Srivastava, K., 1965. Design of efficient flux concentrators for pulsed high magnetic fields. The Review of Scientific Instruments 36 (8), 1096–1100.
Wolf, H., 1974. Magnetumformen ergänzt als wirtschaftliche Fertigungsmethode andere Formverfahren. Maschinenmarkt 80, 1106–1109.
Wolf, H., Meinel, M., 1972. Energie- und kraftübertragende Eigenschaften von Feldformern der Magnetumformung; Teil 1. Umformtechnik 6-6, Zwickau.
Wolf, H., Meinel, M., 1989. Fügen durch Magnetumformung—Erreichbare Effekte. Fertigungstechnik und Betrieb 39 (11), 672–673.
Wood, W.W., 1967. Experimental mechanics at velocity extremes—very high strain rates. Experimental Mechanics 19, 441–446.
Woodward, S., Weddeling, C., Daehn, G.S., Psyk, V., Carson, B., Tekkaya, A.E., 2010. Production of low-volume aviation components using disposable electromagnetic actuators. Journal of Materials Processing Technology 211 (5), 886–895.
Yu, H., Li, C., Zhao, Z., Li, Z., 2005. Effect of fieldshaper on magnetic pressure in electromagnetic forming. Journal of Materials Processing Technology 168, 245–249.
Zener, C., Hollomon, J.H., 1944. Effect of strain rate upon plastic flow of steel. Journal of Applied Physics 15 (1), 22–32.
Zerilli, F.J., Armstrong, R.W., 1987. Dislocation-mechanics-based constitutive relations for material dynamic calculations. Journal of Applied Physics 61 (5), 1816–1825.
Zhang, Y., Babu, S., Daehn, G.S., 2010a. Impact welding in a variety of geometric configurations. In: Proceedings of the 4th International Conference on High Speed Forming—ICHSF 2010 , Columbus, pp. 97–107, online available at https://eldorado.tu-dortmund.de/handle/2003/27194.
Zhang, Y., Babu, S., Prothe, C., Blakely, M., Kwasegroch, J., LaHa, M., Daehn, G.S., 2011. Application of high velocity impact welding at varied different length scales. Journal of Materials Processing Technology 211 (5), 944–952.
Zhang, Y., Daehn, G., L'Eplattenier, P., Babu, S., 2009. Experimental study and numerical simulation on magnetic pulse welding for pre-flanged AA6061-T6 and Cu101 Sheets. In: Trends in Welding Research, Proceedings of the 8th International Conference , pp. 715–720, online available at doi:10.1361/cp2008twr715.
Zittel, G., 1975. Magneform: an accepted production tool. In: Proceedings of the 5th International Conference on High Energy Rate Fabrication , Denver, pp. 3.1.1–3.1.35.
Zittel, G., 1976. Getting the most out electromagnetic forming. Assembly Engineering, 26–29.
Zittel, G., 2010. A historical review of high speed metal forming. In: Proceedings of the 4th International Conference on High Speed Forming—ICHSF 2010 , Columbus, pp. 2–15, online available at https://eldorado.tu-dortmund.de/handle/2003/27203.